Extrinsic and Intrinsic Regulation of Adult Neural Stem Cell Activation

Dissertation
submitted to the
Combined Faculty of Natural Sciences and Mathematics
of the Ruperto Carola University Heidelberg, Germany
for the degree of
Doctor of Natural Sciences

Presented by
MSc. Inmaculada Luque Molina
born in: Cuevas de San Marcos, Spain
Oral examination: July 17th 2019

Dissertation
submitted to the
Combined Faculty of Natural Sciences and Mathematics
of the Ruperto Carola University Heidelberg, Germany
for the degree of
Doctor of Natural Sciences

Presented by
MSc. Inmaculada Luque Molina
born in: Cuevas de San Marcos, Spain
Oral examination: July 17th 2019

Extrinsic and intrinsic regulation of adult neural stem cell activation

Referees: Prof. Dr. G. Elisabeth Pollerberg
Dr. Francesca Ciccolini

Table of content:

Chapter 3. Results

Chapter 4. Discussion

List of figures:

Summary

Adult neural stem cells (NSCs) in the subventricular zone (SVZ) of the lateral ventricles remain largely quiescent. Unravelling the mechanism regulating lineage progression from NSCs to newborn neurons is critical for understanding tissue homeostasis and aging. Extrinsic and intrinsic factors regulate NSC self-renewal and differentiation. In this study, I analyse the effects of one extrinsic and one intrinsic factor in NSC regulation. In both analyses, I investigate the effect of the regulators on the so-called apical NSCs, because they display an apical membrane and apical/basal polarity, and basal NSCs, which lack an apical attachment.

Focusing on the neurotransmitter γ-aminobutyric acid (GABA) as an extrinsic regulator of NSC activation, I show that activation of GABA type A receptors ($GABA_AR$s) on adult NSCs induces cell swelling and cell cycle entry by recruiting the epidermal growth factor receptor (EGFR). Although apical and basal NSCs underwent swelling upon $GABA_AR$ activation, increased EGFR phosphorylation and cell cycle entry was only observed in in the latter, which also displayed higher *Egfr* transcripts than apical NSCs. Underscoring the importance of EGFR signalling in proliferation, pharmacological blockade of EGFR prevented NSC proliferation. In addition, I show that activation of $GABA_AR$s also promotes a decrease in the expression of the cell adhesion receptor β1Integrin, both in basal and apical NSCs and loss of the epithelial marker Prominin1 in apical NSCs.

As an intrinsic regulator of NSC activation, I have studied the role of the orphan nuclear receptor TLX and its interaction with NOTCH signalling. This analysis revealed that lack of *Tlx* leads to the overexpression of *Hes1* and increases NOTCH activation in apical NSCs, suggesting that this may contribute to impaired neurogenesis. Indeed, downregulation of *Hes1* in the apical SVZ restored neurogenesis and increased proliferation. Interestingly, this effect was mostly noted in basal NSCs, highlighting a non-cell autonomous regulatory mechanism mediated by NOTCH signalling.

Thus, altogether my results show that GABA and TLX-HES1 interaction both play an important role in the regulation of adult NSC quiescence, being both essentials for proper NSC activation and apical-basal lineage progression.

Zusammenfassung

Adulte neurale Stammzellen (NSZ) in der subventrikulären Zone (SVZ) der lateralen Ventrikel ruhen hauptsächlich. Um Gewebehomöostase und Altern zu verstehen ist es unumgänglich, den Mechanismus, der die Linienprogression von NSZ zu neugeborenen Neuronen reguliert, zu entschlüsseln. Intrinsische und extrinsische Faktoren steuern Selbsterneuerung und Differenzierung. In dieser Arbeit analysiere ich die Effekte eines intrinsischen und eines extrinsischen Faktors auf die Regulation von NSZ. In beiden Analysen untersuche ich den Effekt der Regulatoren auf die sogenannten apikalen NSZ, die eine apikale Membran sowie apikal-basale Polarität besitzen, und die basalen NSZ, denen eine apikale Verbindung fehlt.

Mit Hauptaugenmerk auf den Neurotransmitter γ-Aminobuttersäure (GABA) als extrinsischer Regulator für Zellzyklusaktivierung zeige ich, dass die Aktivierung von GABA-Typ-A-Rezeptoren ($GABA_AR$) auf adulten NSZ durch die Rekrutierung des epidermalen Wachstumsfaktorrezeptors (EGFR) Schwellung und Eintritt in den Zellzyklus induziert. Obwohl apikale und basale NSZ durch $GABA_AR$-Aktivierung anschwellen, ist erhöhte EGFR-Phosphorylierung und Eintritt in den Zellzyklus nur bei apikalen NSZ feststellbar; diese zeigen auch mehr *Egfr*-Transkripte als die apikalen NSZ. Pharmakologische Blockierung von EGFR verhindert die Proliferation der NSZ, was die Wichtigkeit von EGFR-Signalen in der Proliferation unterstreicht. Zusätzlich zeige ich, dass die Aktivierung von $GABA_AR$ sowohl in apikalen als auch in basalen NSZ zu einer Verringerung des Zelladhäsionsrezeptors β1-Integrin, sowie zum Verlust des epithelialen Markers Prominin-1 in apikalen NSZ führt.

Als einen intrinsischen Regulator für NSZ-Aktivierung untersuche ich die Rolle des "orphan" Kernrezeptors TLX und seine Interaktion mit der NOTCH-Signalkette. Diese Untersuchung ergab, dass Mangel an *Tlx* zur Überexpression von *Hes1* führt und NOTCH-Aktivierung in apikalen NSZ erhöht, was nahelegt, dass dies zur eingeschränkten Neurogenese beitragen könnte. Tatsächlich wird durch das Herunterregeln von *Hes1* in der apikalen SVZ die Neurogenese wiederhergestellt und die Proliferation steigt. Interessanterweise fällt dieser Effekt vor allem in basalen NSZ auf, was einen nicht-zellautonomen Regulationsmechanismus aufzeigt, der durch NOTCH vermittelt wird.

Zusammengenommen zeigen meine Ergebnisse daher, dass sowohl GABA als auch die Interaktion von TLX und HES1 eine wichtige Rolle in der Ruheregulation adulter NSZ spielen, da beide für die ordnungsgemäße NSZ-Aktivierung und apikal-basale Linienprogression essentiell sind.

Articles from this thesis:

The orphan nuclear receptor TLX represses *Hes1* expression thereby affecting NOTCH signalling and lineage progression in the adult SEZ

Inma Luque-Molina, Yan Shi, Yomn Abdullah, Sara Monaco, Gabriele Hölzl-Wenig, Claudia Mandl, Francesca Ciccolini. Stem cell Reports. Accepted on May 06, 2019

Chapter 1. Introduction

1.1 Neural stem cells and adult neurogenesis

A stem cell is a cell with the ability of renewing itself and giving rise to multiple cell types. By definition, neural stem cells (NSCs) have the ability to create cells in the neural lineage, like neurons, oligodendrocytes and astrocytes (Gage, 2000; McKay, 1997). During development, neuroepithelial and radial glial cells are considered the NSCs that give rise to the different cell types forming the central nervous system in vertebrates and mammalians (Kriegstein, 2009). However, for a long time, it was believed that the formation of new neurons only occurred during embryonic stages. This belief continued until the 1960s, when Joseph Altman reported the generation of new neurons in multiple regions of the adult mammalian brain like hippocampus, cortex and olfactory bulbs (Altman, 1962; Altman and Das, 1965). These findings were also confirmed with the studies in songbirds by Fernando Nottebohm, who found newly formed cells in the brain with not only the structure of neurons but also the electrophysiological properties (Burd & Nottebohm, 1985; Paton & Nottebohm, 1981). However, several decades after this discovery, there are still many questions regarding the mechanism of regulation and activation of adult NSCs.

1.1.1 Neurogenesis during development

In early stages of development, neuroepithelial cells derived from ectoderm can give rise the first neurons in the neural system. At the moment when cortical neurogenesis begins, approximately at E9-E10 in the mouse, the neuroepithelial cells start acquiring radial glia (RG) features (Fig.1.1) as they express glial markers, like glial fibrillary acid protein (GFAP) and they transition to become RG cells (Götz & Huttner, 2005). These RG cells display an apical-basal polarity that allows them to be in contact at the same time with the ventricular cavity and with the blood vessels at the apical and basal side respectively (Angevine et al.,

1970). These cells are able to symmetrically divide creating two RG cells, or divide asymmetrically giving rise to an identical cell and, either an intermediate progenitor (IPC) or a differentiated cell (neuron, astrocyte or oligodendrocyte) (Kriegstein, 2009). The resulting neuronal IPC will colonize the embryonic subventricular zone (SVZ) as the newly formed neurons migrate through the RG fibres until reaching their final position (Noctor et al., 2004). These new neurons can differentiate in different neuron subtypes due to intrinsic

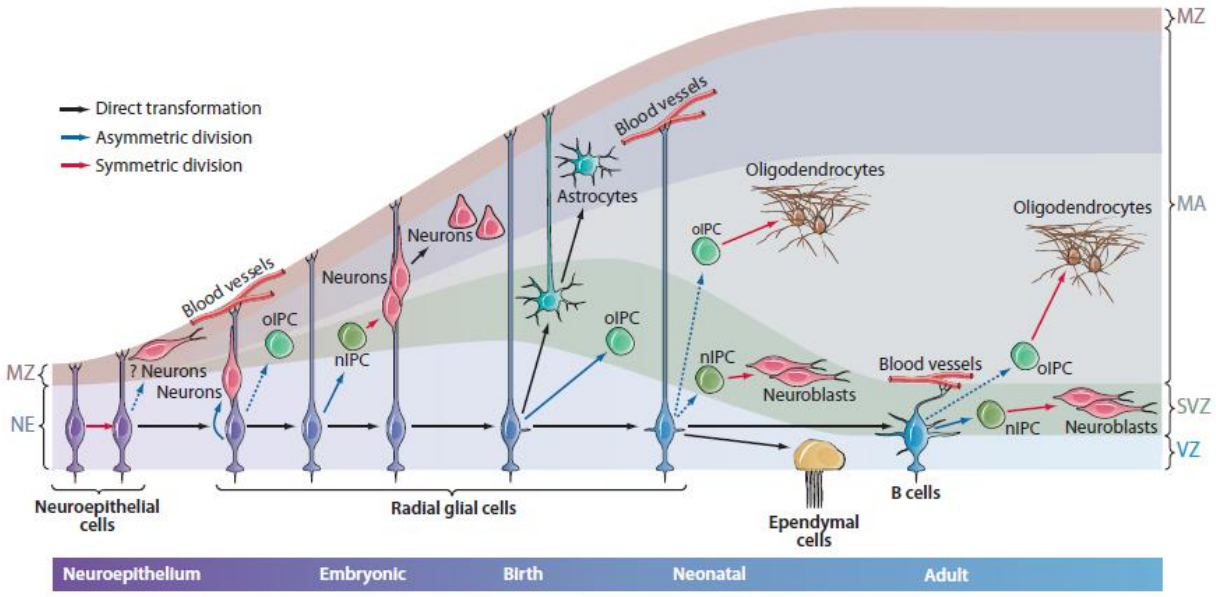

Figure 1.1. Embryonic and adult neurogenesis. Scheme representing the formation of neurons, astrocytes and oligodendrocytes during development and in the adult. Neuroepithelial cells give rise to radial glial cells (RG) which present the ability to differentiate and give rise to intermediate progenitor cells (IPC), neurons, astrocytes and oligodendrocytes during embryonic stages. These RG have apical-basal polarity, and they are the origin of adult NSCs (or B cells). Abbreviations: MZ= marginal zone, NE= neuroephithelium, oIPC= oligodendrocyte intermediate progenitor, nIPC= neuron intermediate progenitor, MA= mantel, SVZ= subventricular zone, VZ= ventricular zone. (Scheme adapted from Kriegstein & Alvarez-Buylla 2009).

cellular mechanisms (transcriptional factors and epigenetic modifications) which are influenced by their original region in the ventricular zone (VZ) and by the moment in the development in which differentiation takes place (Qian et al., 2000; Weinandy et al., 2011).

1.1.2 Postnatal neurogenesis

In the mammalian brain there are two known regions that where postnatal neurogenesis occurs, one is the granular zone of the dentate gyrus in the hippocampus (Cameron et al., 1993; Eriksson et al., 1998), and the other is the SVZ of the lateral ventricles (Doetsch et al., 1999; Lois & Alvarez-Buylla, 1993). In these two niches, NSCs give rise to intermediate progenitors, which ultimately differentiate into neurons, astrocytes and oligodendrocytes. At the end of development, most of RG cells differentiate into astrocytes (Noctor et al. 2008). Some of these cells with astrocytic characteristics derived from RG become indeed the source of NSCs in the adult individual (Merkle et al., 2004).

1.1.2.1 Neurogenesis in the hippocampus

The subgranular zone (SGZ) of hippocampus comprises NSCs and intermediate progenitor cells that give rise to granular neurons involved in pattern separation, learning and memory (Ming & Song, 2011). These NSCs, also called cell type I in the SGZ niche, stay in a quiescent state presenting a very low rate of cell divisions until they become activated. They can give rise to intermediate progenitors type II and III which produce neuroblasts that migrate into the inner granular layer, where they differentiate into adult granular neurons in the hippocampus (Encinas et al., 2011). The process of neurogenesis is regulated by several intrinsic and extrinsic factors in a tightly way, the participation of different transcription factors as well as growth factors is crucial in this regulation (Song et al., 2012).

The final integration of the newly formed neurons within the circuitry depends on the synaptic input/output from the other existing neurons. Several studies have found that the synaptic integration of these cells is depending on a specific sequence in which NSCs get activated by ambient GABA, followed by input-specific GABAergic signalling (Ge et al., 2006; Overstreet-Wadiche & Westbrook, 2006; Song et al., 2012).

1.1.2.2 Neurogenesis in the subventricular zone

The SVZ of the lateral ventricles is the largest adult neurogenic niche in the mammalian brain. NSCs in this niche are maintained in a quiescent state, which far from being a passive state, it comprises the activation of a specific cell program that is strictly regulated and is very important for stem cell renewal, somatic replacement and DNA integrity (Orford & Scadden, 2008). Activation of these cells is controlled by different extrinsic and intrinsic factor. Once activated, NSCs can give rise to transit amplifying progenitors (TAPs) which are actively dividing cells (Doetsch et al., 1999). These TAPs eventually differentiate and

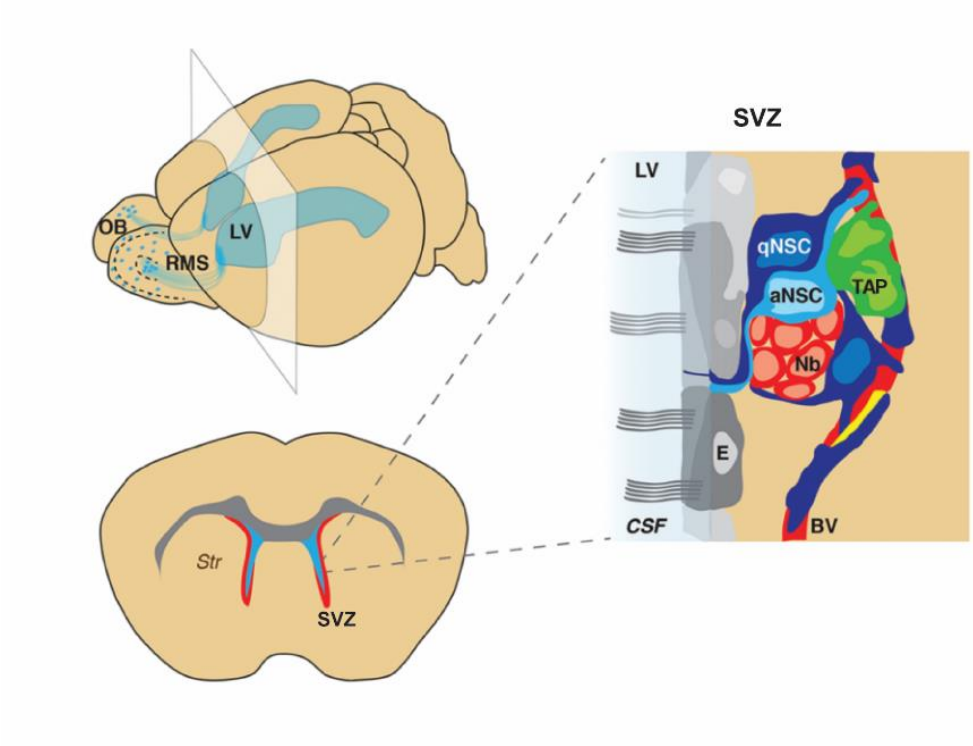

Figure 1.2 Adult neurogenesis in SVZ. Scheme representing adult neurogenesis in the SVZ. NSCs in the SVZ of the lateral ventricles (LV) give rise to transit amplifying progenitors (TAPs). After several cell divisions, TAPs differentiate into neuroblasts which leave the niche and migrate tangentially through the rostral migratory stream (RMS) toward the olfactory bulbs (OBs). Once neuroblasts reach the OB, they migrate radially and differentiate into GABAergic interneurons. Abbreviations: OB= olfactory bulbs, RMS= rostral migratory stream, LV= lateral ventricles, SVZ= subventricular zone, Str= striatum, CSF= cerebral-spinal fluid, E= ependymal cell, qNSC= quiescent neural stem cell, aNSC= activated neural stem cell, Nb= neuroblast, TAP= transit amplifying progenitor, BV= blood vessel. (Scheme adapted from Chaker et al., 2016)

produce neuroblasts, which migrate tangentially through the rostral migratory stream (RMS) towards the olfactory bulbs (OBs) (Fig.1.2). Once they reach the OBs, neuroblasts migrate radially while they differentiate and integrate in the neural circuit as GABAergic interneurons (Chaker et al., 2016). Within the SVZ, NSCs are contained in the centre of the so-called pin-wheel structures, where they are surrounded by ependymal cells (Mirzadeh et al., 2008). These stem cells, also known as type B cells, show astrocytic features in an ultrastructural and molecular level, including the expression of glial fibrillary acidic protein (GFAP) and glutamate aspartate transporter (GLAST) (Doetsch et al., 1999). However, unlike differentiated astrocytes, they present a bi-polar morphology with an apical process that exhibits a primary cilium in contact with the cerebral spinal fluid (CSF), and a basal long process in contact with vascular vessels and the extravascular basal lamina, which is rich in laminin and collagen-1 (Fig.1.2 and 1.3). The primary cilium is involved in signal processing from CSF, and it is characterized for presenting the transmembrane glycoprotein Prominin1, also known as CD133 (Khatri et al., 2014; Mirzadeh et al., 2008) (Fig.1.3).

Over the years, it has been a difficult task to identify specific markers that allow NSCs identification and isolation from the rest of progenitor cells in the niche. As previously described, quiescent neural stem cells (qNSCs) express the glial marker GFAP and Prominin1, although qNSCs can also present negative immunoreactivity for Prominin1 (Codega et al., 2014). When NSCs activate, they exhibit the epidermal growth factor receptor (EGFR) at the cell surface, and they also present immunoreactivity for the intermediate filament protein nestin. TAPs are identified for their immunoreactivity to EGFR and nestin, whereas neuroblasts present immunoreactivity to the cytoplasmic protein doublecortin (DCX) (Fig.1.3) (Codega et al., 2014).

1.2 Extrinsic regulation of NSCs in the SVZ

Among the variety of molecules that create the niche, we can find many different extrinsic signals that regulate self-renew, activation and differentiation of NSCs in adult SVZ. Of note,

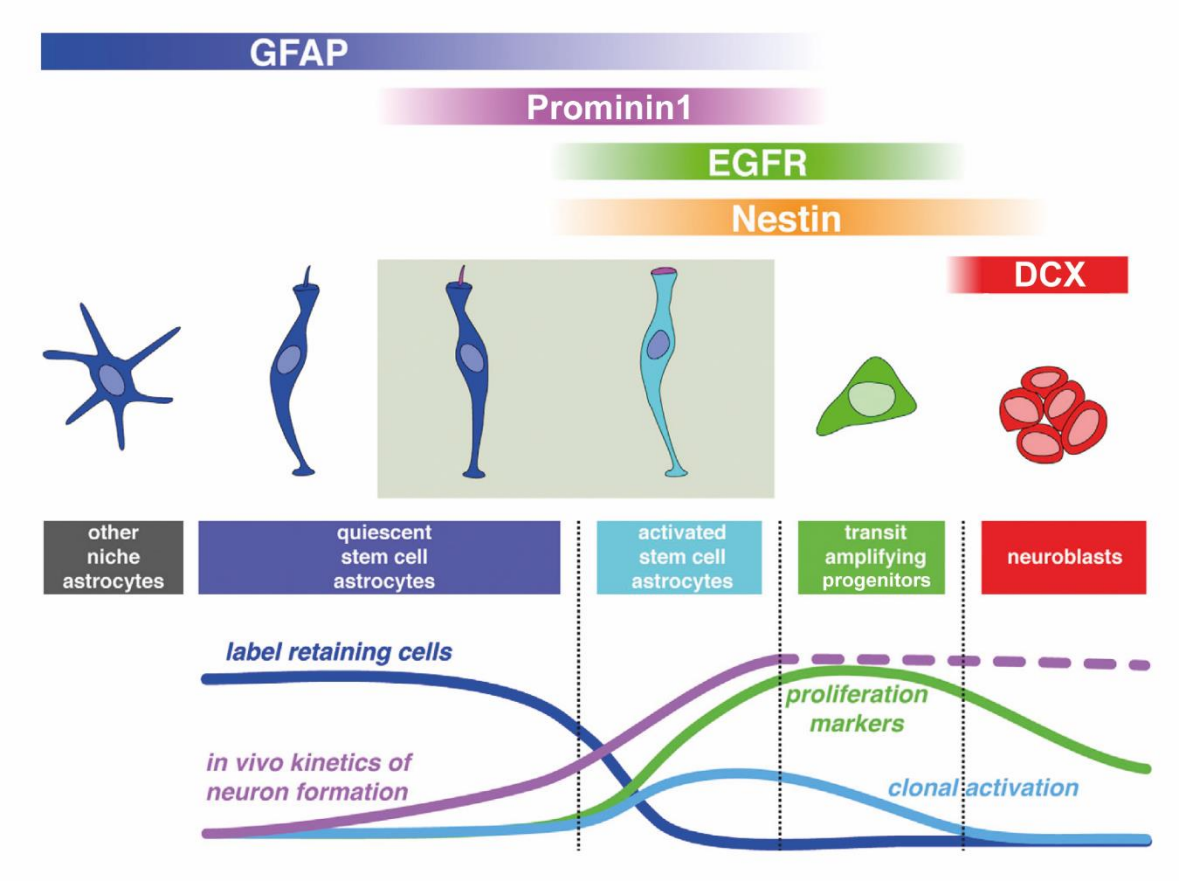

Figure 1.3 NSCs and progenitors in the SVZ niche. Scheme representing the different cell types included in the SVZ. The scheme also shows the different markers used for cell identification and their *in vivo* and *in vitro* properties. Quiescent stem cells are label-retaining cells (dark blue line) that present few cell divisions *in vivo* and *in vitro*. Activated stem cells are highly proliferative (green line), in a same way as transit amplifying progenitors. Abbreviations: GFAP: glial fibrillary acidic protein, EGFR= epidermal growth factor receptor, DCX= doublecortin. (Scheme adapted from Codega et al., 2014)

it is important to mention that in the adult niche, compared with the developing or postnatal brain, NSCs receive signals from a fully formed brain, a brain with complex structures and with all the connections stablished. Therefore, the extrinsic regulation of NSCs in the adult brain is a complex selection of molecules that in combination create the niche. These regulatory molecules include factors from neighbour cells, like ependymal cells, as well as signals from the choroid plexus, the CSF and the vasculature.

As mentioned before, NSCs present an apical non-motile primary cilium that lack the central pair of microtubules. This cilium is implicated in signal transduction, although the mechanism of this regulation is not well known. Even though the function of the primary

cilium is not yet understood, it is interesting that other progenitor cells in the developing and adult brain present this type of primary cilium, like radial glia, embryonic neuroepithelial cells and adult avian neural precursors (Alvarez-Buylla et al., 1998; Sotelo & Trujillo, 1958). The primary cilium is required during the development in the neural tube for the proper sonic hedgehog (SHH) signalling (Wong & Reiter, 2008), and it may be implicated in signalling from other molecules in the CSF. Indeed, there are other signalling molecules in the CSF like insulin growth factor 2 (IGF-2), SHH, retinoic acid, Wnts, and bone morphogenetic protein (BMP) that are implicated in NSC regulation (Huang et al., 2010; Lehtinen et al., 2011). Similarly, microglia and endothelial cells secrete molecules which regulate neuroblast migration (Leventhal et al., 1999) and NSC self-renewal (Shen et al., 2004). Indeed, NSC contact with endothelial cells is involved in the regulation of the quiescent state and cell cycle arrest (Ottone et al., 2014).

Other molecules that act as extrinsic regulators of NSCs are the fibroblast growth factor 2 (FGF-2) and the epidermal growth factor (EGF). It is not clear which cells secrete these mitogens in the SVZ, however, both of them participate in NSC activation, lineage progression and possibly dedifferentiation (Anderson, 2001; Raff, 2003).

Ependymal cells displayed at the apical surface of the SVZ (Fig.1.2) are also involved in secreting substances that regulate NSC. These cells secrete Noggin, an antagonist of the BMP, another growth factor that is expressed in the SVZ and regulates quiescence. Secreted Noggin promotes neurogenesis *in vitro* and *in vivo* (Lim et al., 2000).

Likewise, neurotransmitters play a role in the regulation of adult neurogenesis. For example, serotonin (5-HT) regulates cell proliferation and OB neurogenesis by acting through receptors in the SVZ (Banasr et al., 2004; Brezun & Daszuta, 1999), and dopamine innervations from the mid brain act mainly on TAPs promoting neurogenesis through an EGFR related mechanism (Kim et al., 2010; O'Keeffe et al., 2009).

In this study, I focus in the extrinsic mechanisms involved in NSCs regulation by the neurotransmitter γ-aminobutyric acid (GABA).

1.2.1 GABAergic regulation of NSCs

In the central nervous system, GABA is the major inhibitory neurotransmitter. Its actions are mediated by ionotropic $GABA_A$ and metabotropic $GABA_B$ receptors. The former are implicated in short-term responses, while the latter mediate long-term responses (Owens and Kriegstein, 2002). $GABA_A$ receptors ($GABA_A$Rs) have been thoroughly studied in the context of neurogenesis. These receptors belong to the superfamily of ionotropic receptors (Moss & Smart, 2001). They are chloride channels formed by five subunits, which can differ from 19 different subunits (α_{1-6}, β_{1-3}, γ_{1-3}, δ, θ and π) assembled to form a pentameric structure (Dieriks et al., 2013).

Different studies have shown that GABA is involved in the regulation of multiple aspects of neurogenesis, including proliferation, migration, and neuronal specification in the postnatal neurogenic niche (Aprea & Calegari, 2012; Cesetti et al., 2011). In the SVZ, GABA is mainly released by neuroblasts, creating a GABA ambient which activates $GABA_A$Rs in precursor cells. Another source of GABA in the SVZ may be represented by ependymal cells, meninges, the choroid plexus (Tochitani & Kondo, 2013) and the synaptic output from striatal neurons (Young et al., 2014). Even though many studies have indicated that $GABA_A$Rs are the main receptors implicated in this regulation by GABA in the SVZ, it is not well known the mechanism by which this regulation takes place. During development, activation of $GABA_A$R promotes proliferation of primary precursors in the apical SVZ while it blocks proliferation at the basal side of the niche (Haydar et al., 2000). Besides this, in the postnatal niche, GABA presents an inhibitory effect on the proliferation of intermediate progenitors including TAPs and neuroblasts (Aprea and Calegari, 2012). This inhibitory effect is proposed to be part of a negative feedback by which GABA released by neuroblasts, in a non-synaptic manner, interferes with proliferation of intermediate progenitors, thereby decreasing the number of neuroblasts that are being generated. This feedback would explain a mechanism for controlling the rapid proliferation of TAPs. However, this regulation is less clear when it comes to NSCs, as they remain mostly quiescent, presenting very few cell divisions. Some studies have indicated that $GABA_A$R activation inhibits adult NSC proliferation (Fernando et

al., 2011; Liu et al., 2005), while other reports have shown that $GABA_AR$ activation may in fact increase the proliferation of apical precursors in the pre- and neonatal niche (Cesetti et al., 2011; Young et al., 2012), in a similar way as the GABA effect on proliferation of progenitors in the embryonic SVZ. Thus, many aspects of GABAergic regulation in the SVZ niche are not yet elucidated.

1.3 Intrinsic regulation of NSCs in the SVZ

Besides the distinctive molecules that create the niche and regulate neurogenesis in the adult brain, it is very important to point out that NSCs are regulated by transcription factors and differential gene expression that make them respond in an intrinsic differential way to the external signals (Lim & Alvarez-Buylla, 2016). For instance, NSCs give rise to different OB neurons depending on the region that they occupy within the SVZ (dorsal, lateral, ventral, anterior or posterior) (Merkle et al., 2007). In this sense, ventral NSCs give rise to a different pool of neurons in the OB than dorsal NSCs, suggesting that even though they are exposed to similar niche molecules, their internal program makes them respond in a different way. Several genes, transcription factors and epigenetic marks are involved in this regulation. In this study we focus in the intrinsic regulation by the orphan nuclear receptor TLX and NOTCH1 receptor.

1.3.1 Orphan nuclear receptor TLX in neurogenesis

Tlx gene, also known as Nr2e1 (nuclear receptor subfamily 2, group E, member 1), is the vertebrate homolog of the Drosophila gene tailless (*tll*). This gene, mainly expressed in the developing brain and retina, encodes an orphan nuclear receptor with no identified ligand. *Tlx* expression increases with age, reaching high levels in the adult brain. Adult mice lacking *Tlx* expression ($Tlx^{-/-}$) present extremely reduced hippocampal dentate gyri, besides, they

show enlarged lateral ventricles while OBs present a reduction in size, suggesting a failure in neurogenesis (Monaghan et al., 1995; Shi et al., 2004). Dysregulation of *Tlx* has an effect in the appearance of human neurological disorders. In fact, *Tlx*$^{-/-}$ mice present an aggressive and un-social phenotype (Kumar et al., 2007; Monaghan et al., 1995).

TLX receptor is found in qNSCs and in TAPs in adult brain (Li et al., 2012; Obernier et al., 2011). In fact, the receptor has been shown to be implicated in regulation of NSC maintenance and self-renewal in the adult brain (Shi et al., 2004).

TLX regulates the transcription of multiple genes by activating or repressing their expression, although it mostly acts as a transcriptional repressor. This activity as repressor is carried out by recruiting histone deacetylases (HDAC3 and HDAC5) into the promoter of target genes, like *p21* and *Pten* (Sun et al., 2007), inhibiting these cell cycle regulators. It also activates the expression of proneural genes like *Mash1* (Elmi et al., 2010). TLX has been also described to regulate gene expression through microRNAs (miRNAs), non-coding RNA sequences that function as negative regulator of gene expression. For instance, in the SVZ, miR-9 inhibits the expression of *Tlx* gene, and at the same time, TLX acts as a transcriptional repressor for miR-9, being their expressions inversely correlated during differentiation. This comprises a negative feedback loop that allows a quick transition from NSCs to intermediate progenitor during differentiation (Zhao et al., 2009). TLX can be also regulated by lethal-7b, another miRNA that acts as a regulator for NSCs (Zhao et al., 2010). Another interesting feature of TLX in relation to NSCs regulation is that it activates Wnt7a/Beta-catenin signalling pathway to stimulate NSC proliferation and self-renewal (Qu & Shi, 2009). Besides, TLX interacts with SOX2, a transcription factor necessary for neurogenesis. This interaction is proposed to be necessary for regulating the transcriptional activity in the SVZ (Shimozaki et al., 2012). Thus, TLX is involved in many mechanisms necessary for the regulation of proliferation and differentiation of NSCs.

1.3.2 NOTCH signalling regulation of NSCs

NOTCH is a single-pass transmembrane receptor that, during the canonical signalling, activates through ligands expressed in the neighbour cells. Binding of the ligand with the receptor activates a cellular program, and as a result, the NOTCH intracellular domain (NICD) is released. This activated portion of NOTCH receptor translocates to the nucleus where it binds to the recombining binding protein suppressor of hairless (RBPJ), forming a complex that activates specific gene expression (Ables et al., 2011). In mammals we can find four different NOTCH receptors (NOTCH1, NOTCH2, NOTCH3 and NOTCH4) and five different ligands, the delta like ligands (DLL1, DLL2 and DLL3) and the Jagged proteins (JAG1 and JAG2) (Kageyama et al., 2009). NOTCH signalling is very important during development, given that most of the spatial pattern differentiation depends on its activation. However, NOTCH receptors and ligands are also expressed in different cell types in the adult brain, suggesting the importance of this signal not only in development but also in brain functioning (Berezovska et al., 1998). In the adult SVZ, cells express NOTCH1 and its two ligands JAG1 and DLL1 (Stump et al., 2002). NOTCH signalling in NSCs supresses neuronal differentiation while promoting stem cell maintenance (Aguirre et al., 2010). In fact, Chambers et al. transduced postnatal SVZ cells with an activated form of NOTCH receptor, finding that this alteration prevented cell migration to the OB and supressed differentiation, keeping the cells in a more quiescent state. In a similar way, conditional deletion of *Rbpj* in the adult SVZ forces NSCs differentiation into TAPs and neuroblasts, leading to a complete depletion of NSCs (Imayoshi et al., 2010). These findings show the importance of NOTCH in NSC regulation.

NOTCH signalling activates target genes such as *Hes1* and *Hes5,* two transcription factors belonging to the family of Hairy/enhancer of split (Hes) basic helix-loop-helix (bHLH) (Iso et al., 2003). HES1 represses the transcription of the proneural gene *Mash1* (Sasai et al., 1992). Interestingly, *Mash1*, which is mostly expressed in TAPs, promotes the expression of NOTCH ligands, thereby promoting activation of NOTCH signalling in the neighbour cells and preventing differentiation (Kageyama et al., 2009), which suggests a potential feedback

from progenitors to regulate NSC differentiation. Given the importance of *Hes* genes in regulation of NSCs and in the canonical signalling pathway of NOTCH, many experiments were made in mutant mice to understand this regulation. For instance, overexpression of *Hes1*, *Hes3* and *Hes5* in the embryonic brain leads to inhibition of differentiation and maintenance of the RG phenotype. In a similar way, in mice lacking *Hes1* and *Hes5* expression, RG cell differentiate prematurely into neurons. Interestingly, in mice lacking *Hes* gene expression, the premature differentiation of radial glia is correlated with an increased expression of proneural bHLH transcription factors like *Mash1* (Hatakeyama, 2004; Ishibashi et al., 1994; Ohtsuka et al., 1999). Altogether, these findings indicate that NOTCH signalling and its targets play an important role for NSC regulation.

1.4 Aims of this study

Adult neurogenesis has been studied for many years, however, there is not yet a complete understanding of all the molecules and regulators implicated in the formation of new neurons. The study of NSC regulation is of vital importance given that understanding the signals that control NSC activation and differentiation can help in future treatments like stem cell therapy and in the understanding of tumour dynamics in the brain.

In this study I have investigated the regulation of NSC activation by extrinsic and intrinsic factors. On one side, as an example of extrinsic regulation I have investigated the effect of GABA released in the SVZ on cell cycle activation, focusing on:

The effect of $GABA_AR$ activation on the cycling properties of the neural precursors in the adult SVZ.

1) The response of quiescent NSCs and proliferating NSCs to $GABA_AR$ activation.
2) Implications of epidermal growth factor receptor (EGFR) in the GABAergic regulation of NSC proliferation.
3) Analysis of the involvement of the cell adhesion molecule Integrin in the GABAergic regulation of NSC proliferation.

On the other side, as an example of intrinsic regulator, I investigated the role of TLX and its interaction with NOTCH signalling in regulating NSC activation, using a mouse model where the expression of *Tlx* gene is ablated by LacZ knock in (*Tlx*$^{-/-}$). For this analysis I have focussed on:

1) Analysis of NOTCH signalling activation in cells and brain slices from *Tlx*$^{-/-}$ mice.
2) Viral transduction of apical cells in lateral ventricles to downregulate *Hes1* expression in the mutant SVZ.
3) Analysis of the implications for neurogenesis of *Hes1* downregulation in *Tlx*$^{-/-}$ mice.

Chapter 2. Materials and methods

2.1 Chemicals, reagents and materials used

2.1.1 General reagents

Reagent	Company
Ammonium chloride	Merck
DAPI	Roche
Diazepam	Ratiopharm
Doxycycline	BioChemica AppliChem
Ethanol	Sigma
Fetal bovine serum	Gibco
Glycine	Life Technologies
Isopropanol	Applichem
Low Melting Agarose	Life Technologies
Narcoren	Boehringer Ingelheim
Mowiol	Calbiotech
NP-40	CN Biomedicals Inco.
Paraformaldehyde	Riedel de Häel
Triton- X100	Sigma

Equipments	Company
FACS Aria II	BD
Bench Centrifuge	Eppendorf
Centrifuge (Heraeus)	Thermo scientific
Pro-Flex PCR system	Applied biosystems
StepOnePlus Real-time-qPCR system	Applied biosystems
Spectrophotometer	Denovix
Confocal Microscope SP8	Leica
Fluorescence microscope Axiophot	Zeiss
Vibratome HM 650V	Microm

2.1.2 Reagents and materials for genotyping

Reagent	Company
Agarose	Biozym
dNTPs	VWR
DNA ladder (1Kb)	Thermo scientific
EDTA	Sigma-Aldrich
Loading Buffer	Thermo scientific
NaCl	Fisher scientific
Midori green nucleic acids stain	Nippon genetics
Proteinase K	Merk
SDS	OMNI life science
Taq-DNA Polymerase	PeqLab
Tris	Roth

2.1.3 Reagents and materials for cell culture and FACS

Reagents and materials	Company
B27 supplement	Invitrogen
Chamber slide (8 wells)	Lab-tek, Nunc
DiI	ThermoFisher
D-(+)-glucose 45%	Sigma-Aldrich
DNase	Sigma-Aldrich
Euromed-N (NS-A) medium	Euroclone/Biozol
FCS	Gibco
huFGF-2	Peprotech
huEGF	Peprotech
KCl	Sigma
Leibowitz L15 medium	Gibco
L-glutamine	Gibco
Muscimol	Sigma
Neurobasal-A (NB-A) médium	Euroclone/Biozol
Ovomucoid	Sigma-Aldrich
Papain	Sigma-Aldrich

Reagent	Company
Penicillin/Streptomycin	Gibco
PD 158780	Calbiochem
Sucrose	Sigma

2.1.4 Reagents and materials for RNA extraction, RT-PCR and qPCR

Reagents	Company
dNTPS	VWR
M-MLV enzyme	Promega
Oligo dT(primers)	Promega
PicoPure™ RNA Isolation Kit	Applied Biosystems
qPCR assay	Applied Biosystems
RNAsin	Promega

TaqMan probe (Applied Biosystems)	Reference Number
β-actin	Mm01205647_g1
EGFR	Mm00433023_m1
β1-Integrin	Mm01253227_m1

2.1.5 Reagents and materials for viral production and stereotaxic injections

Reagents and materials	Company
Amicon Ultra-4 Centrifugal Filter	Millipore
Atipamezol	Prodivet pharmaceuticals
Benzonase	Sigma
Buprenorphine	Norbrook
Dulbecco's Modified Eagle Medium (DMEM), high glucose, pyruvate	Gibco
FCS	Gibco
Fentanyl	Piramal
Flumazenil	Fresenius Kabi
HiTrap Heparin Column	Amersham
Iscove's Modified Dulbecco's Medium (IMDM)	Life Technologies
L-glutamine	Gibco

Naloxon	Inresa Arzneimittel
Non-essential amino acids	Gibco
Medetomedin	Alvetra
Midazolam	Hameln
Mini-prep Kit	Quiagen
Maxi-prep Kit	Invitrogen
Penicillin/Streptomycin	Gibco
Sodium Deoxycholate	Sigma

2.1.6 Antibodies

Primary Antibodies	**Dilution**	**Company**
BrdU mouse IgG	1:10	Roche
beta1 Integrin rat IgG2K	1:500	Merk Millipore
DCX (Doublecortin) mouse IgG	1:500	Santa Cruz
EGFR mouse IgG1	1:100	Sigma
phospho-EGFR (Y1068) rabbit IgG	1:500	Abcam
GFAP mouse IgG1	1:1000	Sigma
Hes1 mouse IgG2b	1:50	Santa Cruz biotech.
Ki67 Rabbit IgG	1:100	Abcam
LeX (SSEA1) mouse IgM	1:30	Hybridoma Bank Iowa
Nestin mouse IgG1	1:100	Sigma
NICD (activated Notch 1) rabbit IgG	1:500- 1:2000	Abcam
Prominin1 APC conjugated	1:100	Miltenyi Biotec

Secondary Antibodies	**Dilution**	**Company**
Mouse IgG-488	1:1000	Thermo Fisher
Mouse IgG-cy3	1:200	Jackson Lab (Dianova)
Rabbit IgG-488	1:1000	Thermo Fisher
Rabbit IgG-cy3	1:200	Jackson Lab (Dianova)
Rat IgG-647	1:500	Thermo Fisher

2.1.7 Software

Microsoft Office (Word, Excel, PowerPoint)
GraphPad Prism 5.0
Adobe illustrator CS4
ImageJ/ FIJI software
Mendeley

2.2 Mice lines and genotyping

All animal procedures were carried out with the permission of the local authorities and according to the ethical guidelines for the care and use of laboratory animals (Karlsruhe, Germany). These mice were kept with water and food *ad libitum* during the entire experimental procedure. Adult C57Bl/6, hGFAPtTA;H2B-GFP, and *Tlx*$^{-/-}$ mice were killed by neck dislocation after CO_2 exposure, whereas neonatal C57Bl/6 were killed by decapitation.

2.2.1 Wild type (WT) mice

For *in vivo* experiments and stem cell isolation, 8-week-old wild-type C57Bl/6 mice from both genders were used. For FACS experiments, mice were injected intraperitoneally twice every 12 hours with diazepam (3 µg/g of body weight) to activate GABA type A receptors ($GABA_AR$) or phosphate buffer (PBS) as control, and killed within 24 hours after the first injection. For immunohistochemistry analysis, mice were intraperitoneally injected twice every 12 hours with diazepam (3 µg/g of body weight) or PBS. These mice were also given a single intraperitoneal injection of the thymidine analogue iododeoxyuridine (IdU) (100 mg/kg body weight, dissolved in PBS) at the same time of the first diazepam/PBS injection. Mice were perfused 24 hours or 7 days after the first injection.

2.2.2 GFAP-H2B mice (hGFAPtTA;H2B-GFP)

The hGFAPtTA;H2B-GFP mice (abbreviated as GFAP-H2B) were obtained by crossing two different transgenic mouse lines, one of them containing a transgene expressing the human histone H2B fused to the green fluorescent protein (H2B-GFP) under the control of a tetracycline-responsive regulatory element (Tumbar et al., 2004). The other mouse line contains a genetic insert in which the human glial fibrillary acidic protein (GFAP) promoter drives the expression of a tetracycline-controlled trans-activator protein (tTA) (Wang et al., 2004).

In the resulting selected progeny, we have mice with both inserts, so in order to repress the expression of the reporter fusion protein, 1-month-old animals were given 50 mg doxycycline (doxy) in the drinking water during four weeks. With this treatment, the new production of the reporter protein GFP-H2B was stopped. Therefore, only quiescence neural stem cells (qNSCs) that had not divided more than five times (Waghmare et al., 2008) during the treatment period are GFP positive (GFP^+). In mice without doxy treatment, all stem cells (cells expressing GFAP) are GFP^+.

8-week-old mice treated with doxy and without doxy were injected twice every 12 hours with diazepam (3 μg/g of body weight) or PBS (as control) as shown in table 1. These mice were killed 24 hours after the first injection by either neck dislocation or by perfusion for immunohistochemistry.

Table 1. NSC types labelled in each condition

	Doxycycline treatment	**No doxycycline treatment**
Diazepam injection	**qNSCs** (activated $GABA_AR$)	**Proliferating and qNSCs** (activated $GABA_AR$)
PBS injection	**qNSCs**	**Proliferating and qNSCs**

The genotyping of the mice was performed from tail tissue biopsies. To extract the DNA, tissue was incubated in TESS buffer (Table 1) containing proteinase K (20µg/µl) over night (O/N) on a rocker at 56^0C. Next day, sodium chloride (NaCl) (5M) was added to the solution and mixed by inversion at room temperature (RT). After 15 minutes of full speed centrifugation, supernatant containing the DNA was isolated and mixed with 500µl of isopropanol. The mixture was mixed by inversion and centrifuged at full speed for 15 minutes. The supernatant was carefully removed, and the pellet was let to dry at 37^0C for 30-60 minutes. Last, pellet was resuspended in 100 µl TE buffer (Table 2).

Table 2	
TESS buffer:	**TE buffer:**
50mM Tris pH8	10mM Tris pH8
100mM EDTA	1mM EDTA pH8
100mM NaCl	
1% SDS	

To genotype the mice, polymerase chain reaction (PCR) was performed to amplify the transgenes in the DNA solution extracted from the tail biopsies. The primers used to amplify both transgenes were:

H2B trans Forward: 5'-AAG TTC ATC TGC ACC ACC G-3'

H2B trans Reverse: 5'-TCC TTG AAG AAG ATG GTG CG-3'

GFAP trans Forward: 5'-CGC TGT GGG GCA TTT TAC TTT AG-3'

GFAP trans Reverse: 5'-CAT GTC CAG ATC GAA ATC GTC-3'

DNA solution was mixed with primers, polymerase, polymerase buffers and deoxynucleotides triphosphates (dNTPs) as described in table 3.

Table 3	
PCR mix genotype GFAP-H2B:	**PCR conditions:**
1µl 10x Reaction buffer S	94 °C 1.5 min
2µl 5x Enhancer buffer P	94 °C 30 s*
0.2µl dNTP (10mM)	62 °C 60 s*
0.2µl Primer GFAP transFW (100µM)	72 °C 60 s*
0.2µl Primer GFAP transRW (100µM)	72 °C 2 min
0.2µl Primer H2B transFW (100µM)	4 °C forever
0.2µl Primer H2B transRW (100µM)	
0.1µl peqGOLD Taq-DNAPolymerase	
4.7µl H_2O	
1.2µl DNA solution	
*=35x cycles	

The PCR conditions are described in table 3.

The PCR product was mixed with 6x Loading Buffer and loaded into a 2% Agarose gel in TBE Buffer (Tris-borate 89 mM, EDTA 2 mM pH 8), to which Midori green nucleic acids stain (1:500000) was added to visualize the DNA. 1Kb Plus DNA ladder was used (0,5 µg). The expected bands were:

H2B transgene: 173bp

GFAP transgene: 450bp

2.2.3 *Tlx*$^{-/-}$ mice

Mice lacking the tailless gene homologue (*Tlx*) expression by LacZ knock in (*Tlx*$^{-/-}$) were generated by Taconic Farms Inc., for Dr Paula Monaghan, University of Pittsburgh. This mouse line was maintained by crossing heterozygotes mice. Tissue extracted from tail biopsies was used to genotype them. The same protocols used for GFAP-H2B mice were used to isolate the DNA, PCR of the target gene, and electrophoresis. Amplification of the genomic DNA was done using three primers: 5'- GCCTGCTCTTTACTGAAGGCTCTT-3', 5'ATTGGGTCC AGACATGGCCCTAGTTG-3', and 5'-GTTCATGTTGACT TCCAAACACTTCTTC-3'. The PCR conditions are described in table 4.

Table 4	
PCR conditions *Tlx*$^{-/-}$ genotype:	
95ºC	15 min
95ºC	30 s*
55ºC	1 min*
72ºC	30 s *
72ºC	10 min
4ºC	forever
*= 32 x cycle	

2.3 Stem cell isolation and cell culture procedures

2.3.1 Subventricular zone (SVZ) dissection and flow cytometry analysis by FACS

Subventricular zones from 8-week-old mice were dissected in dissection solution (Table 5). The dissected tissue was digested with papain solution (1.6mg/ml) for 3 min at 37°C. Afterwards, the enzyme was inhibited with ice cold ovomucoid solution (1.4mg/ml) and washed away, and the tissue was dissociated in sort medium (table 5) with a pipette. The cell suspension was then filtered in a 35 µm nylon mesh BD falcon tube to obtain a single cell solution.

The cell suspension was incubated for 30 minutes at 4ºC with an antibody against Prominin1 directly conjugated to an allophycocyanin (APC) fluorophore (1:100). After the incubation time, the non-bound antibody was washed away from the cell suspension by centrifugation for 5 minutes at 1000 rcf. Cells were incubated then with propidium iodide (PI) (1:100) to discard dead cells. After this, cells were analysed and sorted by FACS. The gates used to isolate the different populations are shown in figure 1.

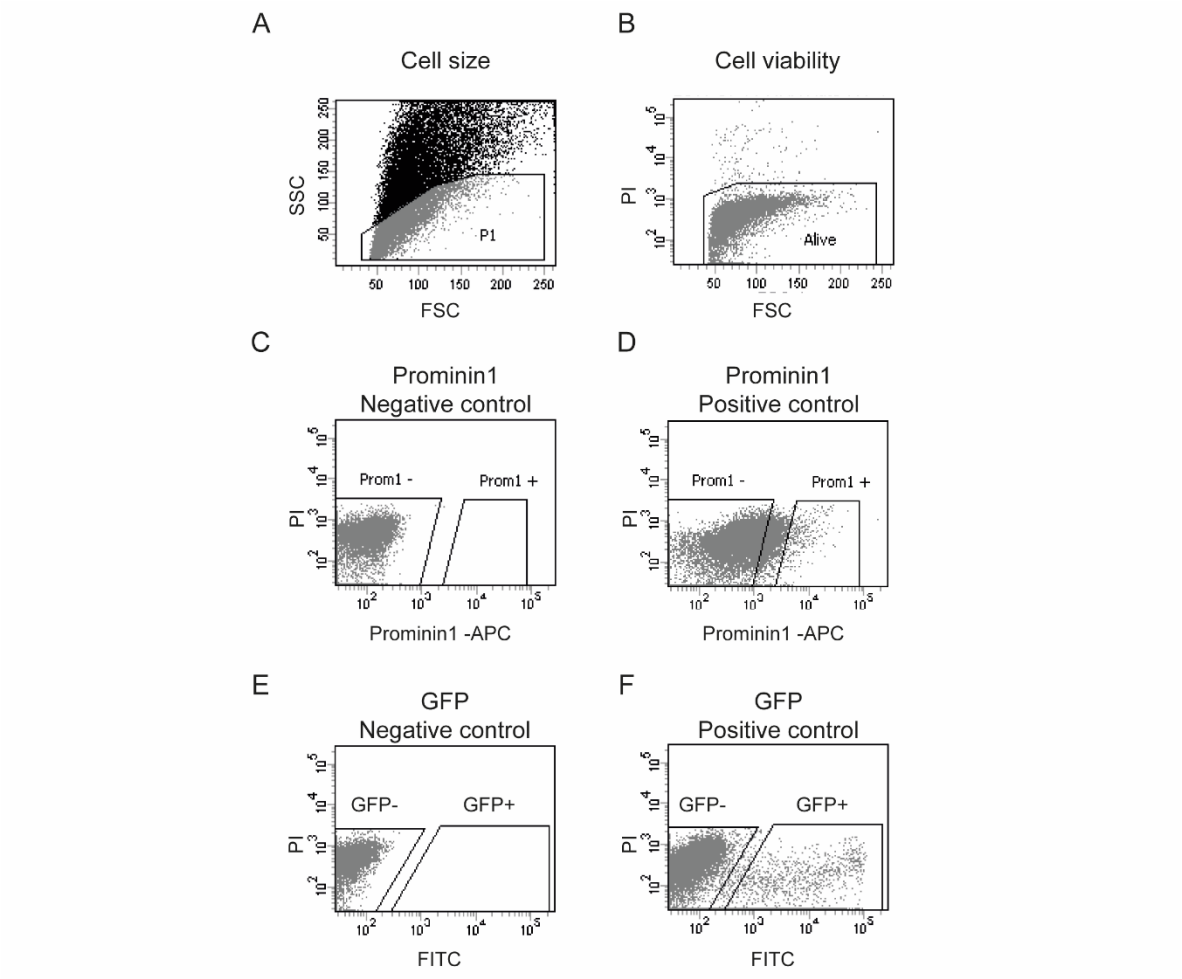

Figure 2.1 Gate settings for florescent activated cell sorting (FACS).
Cell suspension from the dissected SVZ was stained with Prominin1-APC conjugated antibody. Cells were selected according to their size with gate P1 (A). The viability of the cells was analysed using PI (B). Negative controls were used to set the gates for Prominin1 staining (C) and when cells expressing GFP were analysed (E). D and F show a representative example of cells immunopositive for Prominin1 (D) or GFP (F). Abbreviations: SSC: side scatter, FSC: forward scatter, PI: propidium iodide, GFP: green fluorescent protein.

For the experiments meant to label the apical side of the SVZ, brains were dissected, and ventricles were cut open by the medial wall. Then, the apical surface of the lateral wall of the ventricles was exposed to DiI lipophilic dye for 3 minutes at room temperature. The stained tissue was then washed twice with Leibowitz L15 medium, and the SVZ was dissected and dissociated as described above.

Cells were sorted in sort medium and plated in Euromed-N (NS-A) cell medium (Table 5) for overnight experiments and clone analysis. For immunocytochemistry analysis, sorted cells

were plated in an 8 well chamber slide coated with poly-D-lysin in Neurobasal-A (NB-A) cell medium (Table 5).

Table 5			
Dissection solution (pH 6.9):	**Sort medium:**	**NS-A cell medium:**	**NB-A cell medium:**
150 mM Sucrose	1:2 NS-A complete*	NS-A complete*	NB-A complete*
125 mM NaCl	1:2 Leibowitz L15 Medium	1:50 (50X) B27	1:50 B27
3.5 mM KCl	2% B27 supplement	10ng/ml huFGF-2	10ng/ml huFGF-2
1.2 mM NaH2PO4	1%FCS	20ng/ml huEGF	20ng/ml huEGF
2.4 mM CaCl2・2H2O	45% D-(+)- Glucose		
1.3 mM MgCl2・6H2O	10 ng/ml huFGF-2		
0.1%(6.65 mM) Glucose	0.001% DNAse		
2 mM Hepes			
*NS-A/NB-A complete: NS-A/NB-A medium supplemented with L-Glutamine (2mM) and penicillin/streptomycin (100μg/ml).			

2.3.2 Muscimol and PD 158780 treatments

Cells directly isolated from the SVZ were treated with muscimol to activate the $GABA_AR$. These cells were plated either in NS-A (for re-sort experiments) or in NB-A cell medium (for immunocytochemistry analysis) with muscimol (50μM) for 24 hours at 37°C 5% CO_2. After this time, cells were either fixed with 3% paraformaldehyde (PFA) in PBS containing 4% sucrose for immunocytochemistry analysis, or they were incubated with an APC directly conjugated antibody against Prominin1 (1:100) and processed for flow cytometry.

In the experiments meant to block EGFR tyrosin kinase, PD 158780 (20μM) was added to the cells plated in NB-A cell medium for 24 hours at 37°C, 5% CO_2. After this time, cells were fixed with 3% PFA in PBS containing 4% sucrose for 10 minutes and processed for immunocytochemistry analysis.

2.3.3 Immunocytochemistry

Fixed cells were incubated with 10 mM glycine in PBS for 5 minutes. Then, cells were either permeabilized in 0.5% NP-40 in PBS for 5 minutes (when permeabilization was necessary) and rinsed with PBS, or directly incubated with the primary antibody. The incubation with the primary antibodies was performed O/N at 4°C. Next day, after washing twice with PBS, the secondary antibody was applied to the cells for 1 hour at RT. Cells were also incubated with 4',6-diamidino-2-phenylindole (DAPI) (1:100) during this time. Afterwards, cells were washed twice with PBS, and 30µl Mowiol was added to the slide. Finally, a 24 mm X 60 mm glass coverslip was put on top of the slice to cover the cells. Mowiol was let to dry at RT for 24 hours. After this time, cells were analysed by microscopy.

2.4 RNA isolation, retrotranscription and quantitative PCR

2.4.1 RNA isolation

Each selected population of cells was sorted by FACS directly into 100 µl RNA lysis buffer. Then, cells were briefly homogenized by vortexing and kept at -80^{o}C until RNA extraction. RNA was extracted accordingly to the PicoPure™ RNA Isolation Kit (Applied Biosystems). Briefly, the lysate was mixed with same volume of 70% ethanol before transferring into the spin column. To bind the RNA to the column, the column was spin down, and the flow-through was discarded. The column was then washed with 100 µl of W1 buffer. DNAse was added to the column to eliminate non-target DNA. The column was washed twice with 100 µl of W2 buffer, and RNA was eluted in 20 µl of elution buffer. RNA concentration was measured with a Denovix spectrophotometer.

2.4.2 Retrotranscription

The RNA was retro-transcribed into cDNA directly after the extraction. 8 µl RNA were annealed with 2 µl OligodT at 80ºC for 3 minutes. Then, the RNA containing solution was mixed with the rest of components showed in table 6 to a final volume of 20 µl. All the reagents were mixed well and incubated at 42ºC for 60 minutes for retrotranscription in a Pro-Flex PCR system. The reverse transcription was stopped by incubation at 80ºC for 10 minutes. The resulting cDNA was stored at -20 ºC until performance of quantitative PCR.

Table 6
Retrotranscription mixture:
1:5 MLV buffer (5x)
dNTP´s (10mM)
RNAsin (40U/ µl)
M-MLV (200 U/ µl)
10 µl RNA and oligodT
DEPEC water (up to 20 µl)

2.4.3 Quantitative PCR (qPCR)

To analyse the levels of mRNA of the genes of interest in each cell population, the Taqman gene expression assays (Applied Biosystems) were used. The analysis was based on pre-designed probes for the genes of interest, and their expression was quantified respect to the basal expression of β-actin. The cDNA solution was mixed with probes and master mix as showed in table 7. Then, the mixture was incubated at 95ºC for 10 min and followed by 55 cycles of 95ºC for 15 seconds and annealing at 60ºC for 1 minute in a real-time-qPCR instrument (Applied biosystems). The data was collected during the annealing procedure.

Table 7
qPCR mixture:
Taqman Master Mix (2X) 10 µl
Probe 1 µl
RNase-free ddH2O 5 µl
cDNA 4 µl

Cycle threshold (CT) values were obtained from the logarithmic phase of amplification plots for the genes of interest and were normalized to the average CT value of *beta Actin* calculating the delta CT value (ddCT) for each cell population.

2.5 Adeno associated virus (AAV) production and surgeries

2.5.1 Plasmid preparation

Plasmids constructs used to create adeno-associated viral particles (AAV) type 2/1 were created by Dr. Yan Shi (Shi, 2015). These plasmids contain either a short-hairpin sequence to downregulate *Hes*1 gene or a scramble sequence as control, both expressed under the regulation of a U6 promoter. These sequences are followed by the humanized recombinant green fluorescent protein (hrGFP) sequence which is driven by the chicken β-actin promoter (CBA) and follow by the woodchuck hepatitis virus posttranscriptional regulatory element (WPRE) and bovine growth hormone (bGH) polyA signal. Besides these, the following packaging plasmids were used:

pRV1 - Containing the AAV2 Rep and Cap sequences.

pH21 - Containing the AAV1 Rep and Cap sequences.

pFdelta6 - Adenovirus-helper plasmid.

All plasmids were amplified using the bacterial strain Stbl3 (Invitrogen) to avoid recombination and partial deletion. To do so, competent cells were transformed by heat shock at 42^{o}C for 45 seconds using 100ng of DNA. After that, bacteria cells were incubated in LB medium for 1 hour at 37 ^{o}C. These cells were plated in LB agar plates containing 100 µg/ml ampicillin and grown overnight at 37 ^{o}C. Isolated colonies were selected and grown in 5 ml LB medium with 100 µg/ml ampicillin at 37 ^{o}C on a shaking plate overnight. DNA from these cells was isolated following the instructions of the Quiagen Mini prep kit. In order to verify the plasmid sequence, DNA from the different plasmids was digested with restriction enzymes as shown in table 8.

Table 8			
Vector:	**Enzyme:**	**Buffer:**	**Products:**
pFdelta6	HindIII	R	5572bp 3011 bp 2937 bp 2381 bp 1522 bp
pRV1	XbaI	Tango	7505 bp 3867 bp
pH21	SacI	SacI	3953 bp 2827 bp 540 bp
pAAV-U6-shHes1-CBA-GFP	HindIII BamHI	NeBuffer 2.1	70 bp
pAAV-U6-shSC-CBA-GFP	HindIII BamHI	NeBuffer 2.1	70 bp

The different fragments were checked by agarose gel electrophoresis. The correct clones were amplified by growing them in 500 ml of LB medium with 100 μg/ml ampicillin at 37 ^{o}C on a shaking plate overnight. DNA from these cells was isolated according to the instructions of the Invitrogen Maxi-prep kit.

2.5.2 AAV production

The cell line HEK293 was used for viral production. Cells were grown in DMEN high glucose medium supplemented with heat inactivated fetal calf serum (FCS) (1:10), non-essential amino acids (1:100), sodium pyruvate (1mM) and penicillin/streptomycin (100μg/ml). Cells were split when 70% confluence was reached. Two viral particles were prepared, one containing the plasmid with the short hairpin sequence to downregulate Hes1 (AAV shHes1) and one with a scramble sequence as control (AAV SC). For each viral production, 5x 14cm plates of HEK293 cells were plated. All procedures related to virus production were carried out in biosafety Class II laboratory and tissue culture hood. Before transfection, medium from the cells was change to Iscove's Modified Dulbecco's Medium (IMDM). Transfection mixture was prepared as shown in table 9, and after being filter with a 0.2 μm syringe, it was mixed with 13 ml HEBS buffer (table 9) wilst vortexing the solution. 5ml of the final solution were added to each plate drop-wise in a circular motion to transfect the cells.

Table 9	
Transfection mixture:	**HEBS Buffer (pH 7.05):**
12 ml H_2O	50 mM HEPES
1.65 ml 2.5M $CaCl_2$	280 Mm NaCl
62.5 µg AAV plasmid	1.5 mM Na_2HPO_4
125 µg pFdelta6 plasmid	
31.25 µg pRVI plasmid	
31.25 µg pH21 plasmid	

The cells were incubated at 37ºC. After six hours, the medium was replaced with DMEM complete medium, and plates were returned to the incubator for further 60 hours.

After the incubation time, cells were washed with PBS and detached using a cell scraper. The cell suspension was collected and spin down for 5 minutes at 800 g. The pellet was resuspended in 150 mM NaCl/ 20 mM Tris Sodium deoxycholate (0.5%) and benzonase (50U/ml) were added to the viral suspension, and it was incubated for 1 hour at 37ºC in the water bath. Afterwards, the mixture was centrifuged at 3000g for 15 minutes at 4ºC to remove cell debris. The supernatant was collected and kept at -20ºC until the purification procedure.

To purify and concentrate the AAV, the viral suspension was centrifuged at 3000g for 15 minutes at 4ºC. Heparin columns were pre-equilibrated with 10 ml of 150 mM NaCl/ 20 Mm Tris. Supernatant from the viral suspension was loaded in the heparin column with a 60 ml syringe and a pump set at 1 ml/min flow rate. Afterwards, the column was washed with 20 ml 100 mM NaCl/ 20 Mm Tris, continued by with 1 ml 200 mM NaCl/ 20 Mm Tris and 1 ml 300 mM NaCl/ 20 Mm Tris. To elute the virus from the column, column was washed sequentially with 1.5 ml 400 mM NaCl/ 20 Mm Tris, 3.0 ml 450 mM NaCl/ 20 Mm Tris and 1.5 ml 500 mM NaCl/ 20 Mm Tris. The final elution was concentrated using Amicron Ultra-4 concentrators at 2000g for 2 minutes to a final volume of 250 µl. The vector solution was sterilized by filtration through a 13 mm, 0.2 µm syringe filter.

2.5.3 Intracranial viral injections

WT and *Tlx*$^{-/-}$ mice were transferred to the KEB facilities (IBF Heidelberg) two days before the surgical injection for adaptation. Mice were anesthetized with 10 µl/g of body weight of sleeping mix (table 10). Then, they were fixed in a WPI stereotaxic frame and, after removing hair, the head was sterilized with 70% ethanol. A 2 cm long incision was made in the skin and two holes were drilled in the skull (one in each hemisphere) according to the right coordinates to target the lateral ventricles (Table 11). Using a Nanofil 10µl syringe with a 33-gauge needle, 0.5 µl of AAV was injected in each hemisphere at 200 nl/s. Once the AAV was injected, the needle was left 5 minutes inside the ventricle in order to minimise the reflux. After stitching, mice were injected with 300 µl pain killer and 250 µl wake up mix (table 10).

Table 10

Sleeping mix:	**Pain killer mix:**	**Wake up mix:**
4,5 ml 0,9% NaCl	4,75 ml 0,9% NaCl	0,5 ml Atipamezol
0,5 ml Medetomedin	0,25 ml Buprenorphine	5 ml Flumazenil
1,0 ml Midazolam		3 ml Naloxon
1,0 ml Fentanyl		

Table 11

Coordinates from Bregma:	**WT Mice:**	**Tlx$^{-/-}$ mice:**
Anterior-posterior (Y):	0 mm	+1.2 mm
Medium-lateral (X):	+/- 1.2 mm	+/- 0.8 mm
Dorso-ventral (Z):	-2.5 mm	-2.5 mm

2.6 Histology and fluorescence microscopy

2.6.1 Perfusion

To preserve brain tissue for immunohistochemistry, mice were intracardially perfused. First, mice were injected intraperitoneally with 50 µl Narcoren (160 mg/ml) to anesthetize them. After confirming the loss of podal reflexes, mice were immobilized to the table. Then, the

chest was cut open to expose the heart, and PBS solution was pumped into the left ventricle with a butterfly needle. An incision was made in the right atrium to remove the blood from the body. Once the blood was clean out (after pumping around 20 ml PBS), when the liver showed a light brown color, PBS solution was switched to 4% paraformaldehyde (PFA) in PBS. PFA was pumped until the body showed stiffness (around 20 ml). Then, the brain was extracted and kept in 4% PFA at 4^{o}C overnight for post-fixation. Next day, brains were washed twice with PBS and kept in 0.05% Azide in PBS at 4^{o}C.

2.6.2 Vibratome sectioning

Brains were embedded in 4% low melting agarose in a squared plastic scaffold. Once the agarose was solid, brains were glued to the slicing base of a Vibratome HM 650V. Coronal sections of 35 µm were made from the olfactory bulbs until the hippocampus. Slices were collected and kept in 0.05% Sodium Azide in PBS at 4^{o}C until they were processed for immunohistochemistry.

2.6.3 Immunohistochemistry

Brain sections were washed once with PBS to eliminate the azide. If permeabilization was necessary, sections were incubated in 0.5% NP 40. Then, after washing twice to eliminate the detergent, they were incubated in 100 mM glycine for 15 minutes on a rocking plate at RT, and then changed to 50 mM ammonium chloride and incubated on a rocking plate for 15 minutes at RT for quenching. Slices were incubated in 5% FCS blocking solution for 1 hour. Then, primary antibody was added and incubated overnight at 4^{o}C on a rocking plate. Next day, slices were washed twice with PBS to eliminate primary the antibody, after that, the secondary antibody was added and incubated for 1.5 hours at RT on a rocking plate. The slices were afterwards washed twice with PBS and incubated with DAPI 1:500 in PBS for 10 minutes. The sections were then mounted on glass microscope slides using Mowiol and protected with glass coverslips on top.

For the immunostainings against IdU, sections were treated (before the incubation with the primary antibody) with DNAse (300 µg/ml) in DNAse buffer (table 12) for 30 minutes at 37ºC. Then, the above described immunohistochemistry protocol was followed.

Table 12
DNAse buffer 10X:
100 mM Tris
25 mM MgCl2
5 mM CaCl2

Confocal pictures from these slices were taken using either an AR1 Nikon confocal microscope or a Leica SP8 confocal microscope. Pictures from coronal sections were taken from slices in region 20 and 30 (counting the region 1 as the beginning of the lateral ventricles and continue with next region numbered every 35 µm).

2.7 Quantification and statistical analysis

For each immunohistochemistry analysis, three different regions from the SVZ (dorsal, lateral and ventral) from at least three mice were analysed. Positive cells for the different antigens were counted in relation of total number of cells stained with DAPI. In analysis per region of interest (ROI), cells were counted within a fixed rectangular area (15000 μm^2) aligned with the longest side along the apical side of the SVZ. For quantification of the protein levels, all slices or plated cells were incubated with the same antibody mix. Later, pictures of these sections or cells were taken with a Leica SP8 confocal microscope using a HyDTM detector, which allows photon quantification per pixel. The intensity from the protein of interest was measured using ImageJ and normalized to the background. For these analyses, ≥30 cells per condition were measured.

All images were analysed with ImageJ, and analyses were performed either with Microsoft Excel software or with GraphPad Prism 5.0. Plots show the result as the mean ± SEM (Standard Error of the Mean). For statistical analysis, Student's t test was utilized, with

Welch's correction being used where necessary (if the variances were significantly different as measured by the F-test). (n.s.: not significant; *: $p < 0.05$; **: $p < 0.01$; ***: $p < 0.001$).

Chapter 3. Results

3.1 Extrinsic regulation. GABA regulation of NSCs quiescence

3.1.1 Diazepam promotes cell cycle activation in the adult subventricular zone

In order to study whether GABA in the subventricular zone (SVZ) might be regulating activation of adult neural stem cells (NSCs), 8-weeks-old wild type (WT) mice were given an intraperitoneal injection of diazepam, a positive allosteric modulator of $GABA_AR$, or PBS (as control) in combination with the thymidine analogue IdU, and sacrificed 1 or 7 days after the injection. Coronal sections from the SVZ were stained with antibodies against Ki67 and IdU to analyse cell cycle entry and DNA replication, respectively (Fig.3.1).

The analysis showed, that 24 hours after the injection, diazepam treatment significantly increased the number of cells that entered the cell cycle ($Ki67^+$) and of cells that had undergone DNA synthesis (IdU^+) in the SVZ (Fig.3.1A). Seven days after the injection, the number of cycling cells, but not of IdU^+ cells, was still increased in the SVZ of diazepam-treated mice (Fig.3.1B). This suggested that, even though diazepam elicited cell cycle entry and DNA synthesis, the dividing cells were not undergoing through repetitive cycles of cell division, since in this case they would have lost with the IdU label after seven days.

To further understand how diazepam affects the cycling dynamics, I quantified the number of single and double immunopositive cells for Ki67 and IdU in the SVZ of diazepam and control injected animals (Fig.3.2). I found that there was no change in the number of single positive cells for Ki67 neither at 1 day nor at 7 days after diazepam injection (Fig.3.2A). However, when looking at the single positive cells for IdU, I observed a significant decrease seven days after treatment (Fig.3.2B), finding at the same time an increase in double positive cells ($Ki67^+IdU^+$) (Fig.3.2C). These results indicate that IdU^+Ki67^- cells entered cell cycle after diazepam treatment and became IdU^+Ki67^+, suggesting that diazepam is activating a population of slow dividing cells that, even when they are in cell cycle, they are not actively dividing, so after seven days, they still have the IdU label.

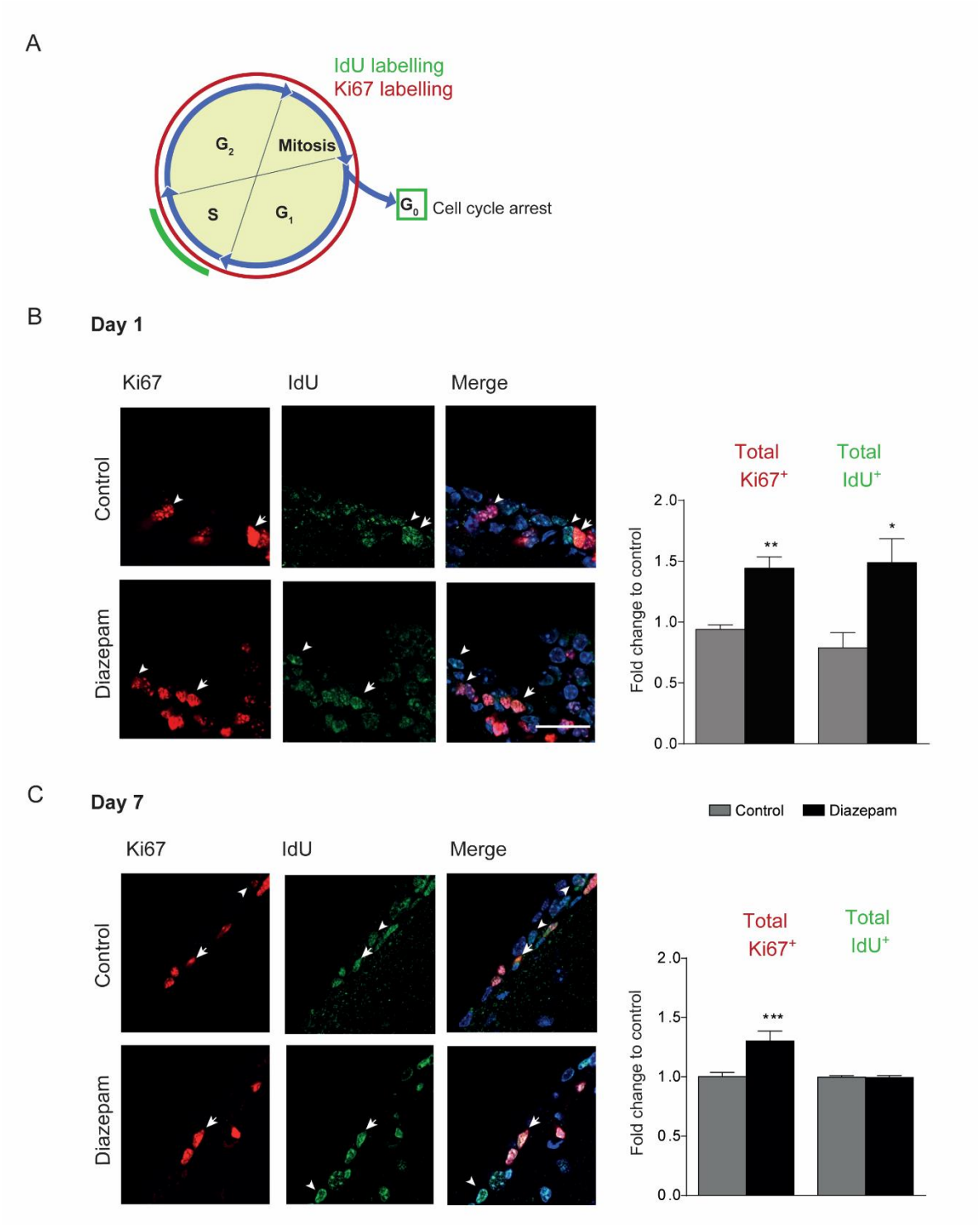
A
IdU labelling
Ki67 labelling
G2
Mitosis
S
G1
G0
Cell cycle arrest
B
Day 1
Ki67
IdU
Merge
Control
Diazepam
Total Ki67+
Total IdU+
Fold change to control
2.0
1.5
1.0
0.5
0.0
**
*
C
Day 7
Control
Diazepam
Ki67
IdU
Merge
Control
Diazepam
Total Ki67+
Total IdU+
Fold change to control
2.0
1.5
1.0
0.5
0.0
***

Figure 3.1 Diazepam promotes cell cycle activation in the SVZ. Analysis of Ki67 expression and IdU incorporation *in vivo*. (A)Scheme of cell cycle phases where Ki67 and IdU are found. (B, C) Confocal photomicrographs of coronal section of the adult SVZ immunostained for Ki67, IdU and DAPI one and seven days after diazepam treatment respectively. (B, C) Second panel: quantification of total Ki67 y and IdU immunoreactivity one and seven days after diazepam treatment respectively. Samples normalized to control. Data is shown as mean+SEM (n≥4, **: p<0.005, ***: p<0.001). Scale bar=50 µm. Arrow head: single immunopositive cell, arrow: double immunopositive cell.

To establish whether diazepam also promoted the proliferation of NSCs, I took advantage of the genetically modified hGFAPtTA:H2B-GFP mice, here after referred to as GFAP-H2B mice. These mice express the tetracycline trans activator (tTA) under the control of the human *Gfap* promoter (a marker for NSCs), and the human histone H2B fused to the green fluorescent protein (H2B-GFP) under the control of a tetracycline-responsive regulatory element (TRE) (Fig. 3.3A). This construct represents a Tet- off system by which the expression of the reporter gene is downregulated by the administration of doxycycline (doxy). Thus, after four weeks of doxy administration in the drinking water, GFP positive cells represent non-dividing label-retaining progenitors, i.e. quiescent NSCs (qNSCs) (Fig.3.3B). However, In the absence of doxy administration, GFP positive cells include proliferating and non-proliferating NSCs (Fig.3.3C). To further investigate the suitability of this mouse model, I performed a thorough characterization of the GFP labelled cells. Upon FACS analysis of the dissociated SVZ (Fig.3.3B, C), I observed that NSCs with very high levels of GFP (GFP^{high}), i.e. cells undergoing mitosis with condensed chromatin (Kanda et al., 1998; Sivakumar et al., 2014) are significantly rarer in mice treated with doxy in the drinking water for four weeks than in the untreated counterpart (Fig.3.3E). Besides, the analysis of the cell cycle marker Ki67 in coronal slices from treated and untreated mice showed a higher number of NSCs in cell cycle in the mice without doxy treatment (Fig.3.3D). Taken together, these data confirmed that administration of doxy to GFAP-H2B mice for four weeks promotes labelling of qNSCs, whereas in the absence of doxy, labelled NSCs are mostly in a proliferative state (pNSCs). Hereafter I will refer to qNSCs and pNSCs, to indicate H2B-GFP-labelled NSCs derived from GFAP-H2B mice treated with doxy in the drinking water for four weeks or left untreated, respectively.

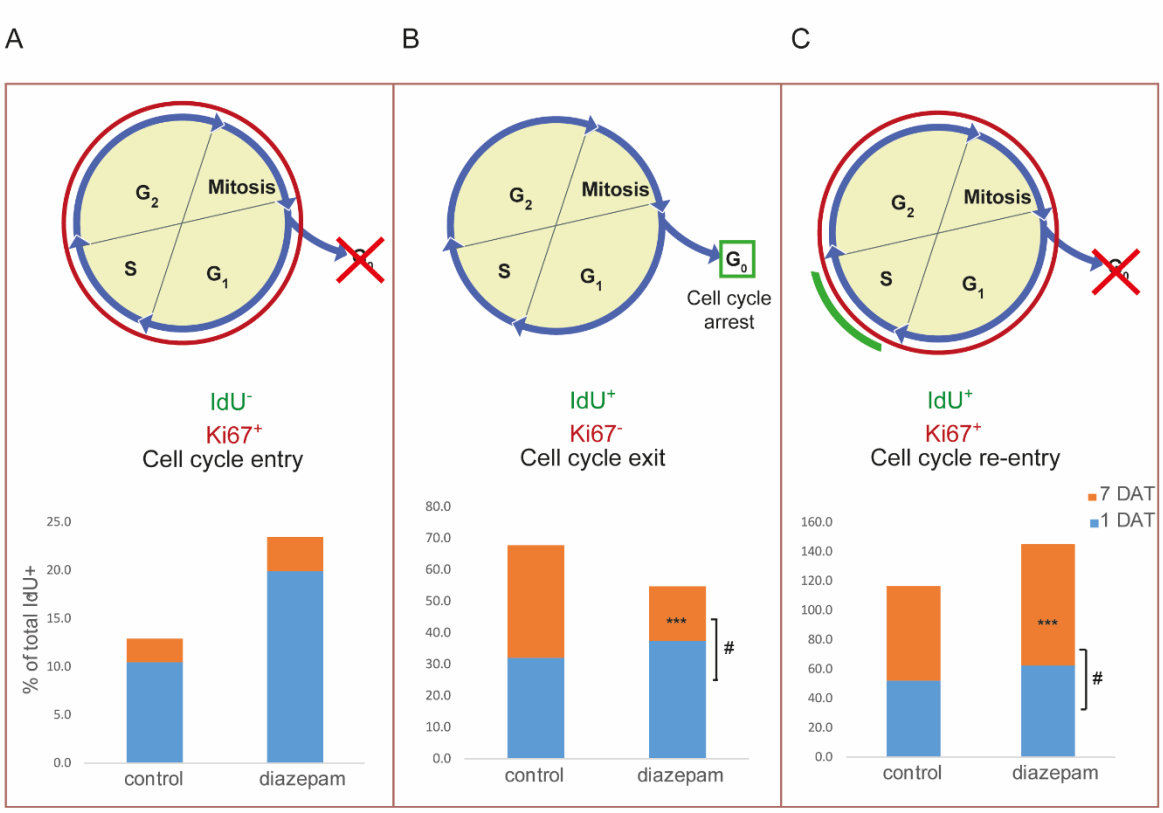

Figure 3.2 Diazepam increases cell cycle activation of a slow dividing population of cells. Analysis of cell cycle dynamic in adult SVZ after diazepam treatment based on Ki67 and IdU immunoreactivity. (A, B, C) Quantification of total Ki67 y and IdU immunoreactivity in coronal sections of adult SVZ one and seven days after diazepam treatment. (A) Representation of cells in cell cycle that have not incorporated IdU (Blue: 1 day after treatment) or cells in cell cycle entry (orange: 7 days after treatment). (B) Representation of cells in S phase that left cell cycle after 24h (blue) or label retaining cells outside the cell cycle (orange). (C) Represent cells in S/G2/mitosis phase (blue) or label retaining cells that were kept in cell cycle during the seven days of treatment (orange). Data is shown as the percentage of the total IdU immunoreactivity. Bars represent the mean of the total populations analysed. (n≥4, #: $p<0.05$ between days of treatment, ***: $p<0.001$ between control and treatment). Abbreviations: DAT= day after treatment.

To investigate whether $GABA_AR$ activation promotes NSC proliferation in the SVZ, I injected intraperitoneally with diazepam or PBS 8 week-old GFAP-H2B mice, which had been either administered doxy for four weeks or left untreated. After further 24 hours mice were sacrificed and processed for immunohistochemistry to investigate Ki67 expression in NSCs (Fig.3.4). This analysis revealed an increased Ki67 expression both in pNSCs (Fig.3.4B) and

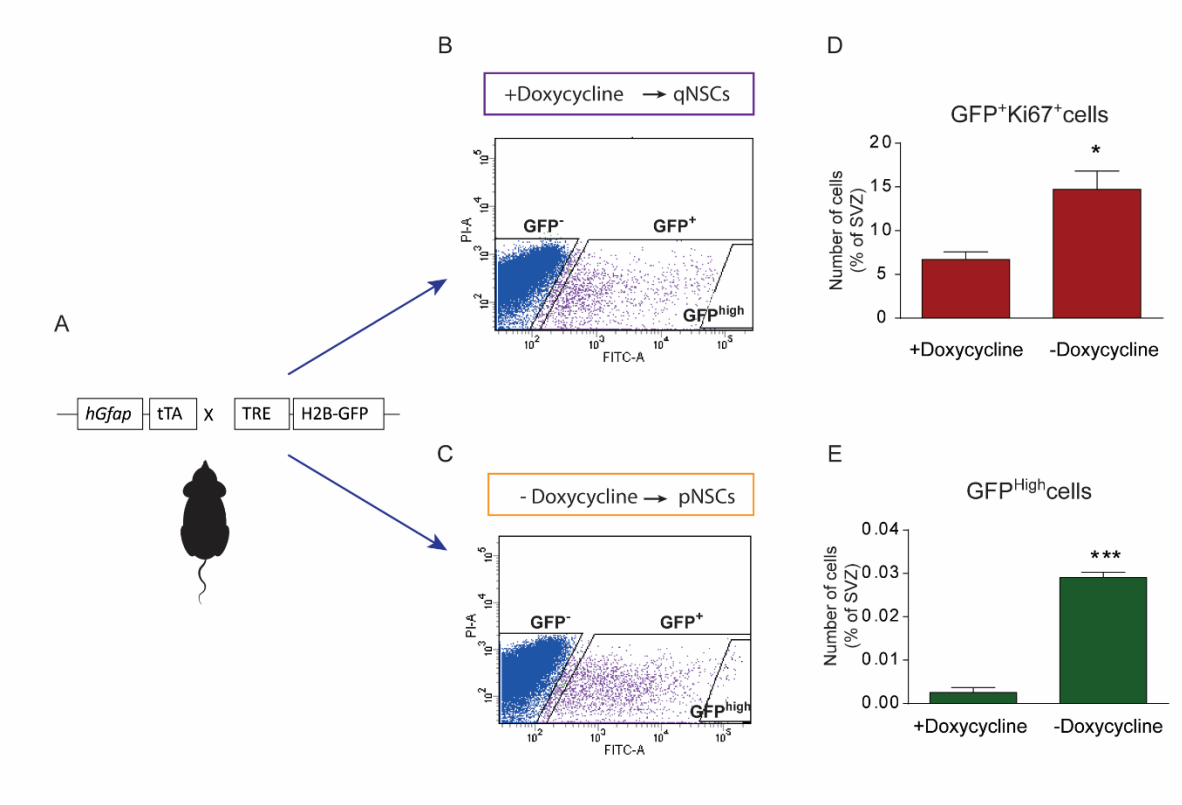

Figure 3.3 Mouse model for the analysis of neural stem cell dynamic. (A) Genetic construct of the *hGfap*-(tTA):(TRE)H2B-GFP genetically modified mice (GFAP-H2B to simplify). This construct presents a Tet off system in which doxycycline (doxy) treatment stops the production of the histone H2B-GFP fusion protein. (B, C) Gates used for FACS analysis of stem cells. Here, the GFP^{+} gate contains all the GFP positive cells while the GFP^{high} contains those cells with high levels of GFP. (D) Number of NSCs in cell cycle ($GFP^{+}Ki67^{+}$) for both conditions (with or without doxy). (E) Number of cells with high GFP levels (highly condensed chromatin). Data shown as mean+SEM (n≥4, *: p<0.05, **: p<0.01, ***: p<0.005). Abbreviations: GFP= green fluorescent protein, FACS= fluorescence-activated cell sorting, SVZ= subventricular zone, pNSC= proliferating neural stem cell, qNSC= quiescent neural stem cell.

qNSCs (Fig.3.4C) upon diazepam injection, indicating that NSCs were indeed affected by diazepam treatment. However, I realized that labelled cells in the SVZ showed different visible intensities of the GFP reporter. I reasoned that in pNSCs GFP intensity positively correlates with the stemness state of the cell, as the expression of GFAP, and therefore of the reported gene, is turned off upon lineage progression (Fig.3.5A, B). Thus, I took advantage of GFP intensity to discriminate between NSCs from more differentiated progenitors. Since the intensity of Ki67 expression also changes according to the phase of the cell cycle, being strong ($Ki67^{++}$) in mitotic cells compared to the remaining cycling cells ($Ki67^{+}$), I analysed the NSCs according to the intensity of both parameters (Fig.3.5A, B). This

analysis showed that diazepam treatment increases the proportion of pNSC, which are $GFP^{++}Ki67^{+}$ (diazepam: 7.91 ± 0.75% vs control: 4.89± 0.42%) (Fig,3.5C), showing that $GABA_AR$ activation promotes cell cycle entry of NSCs.

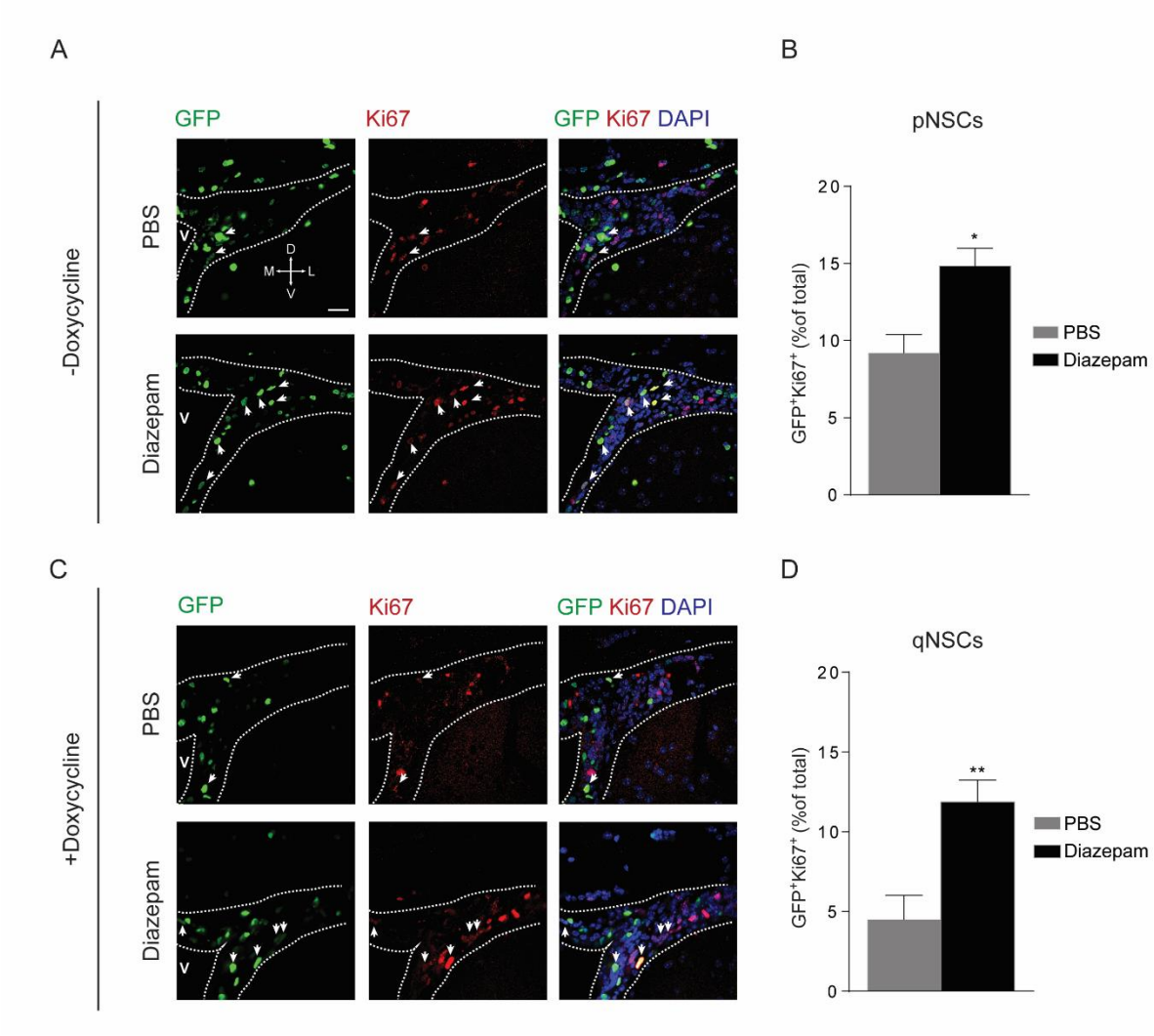

Figure 3.4 Diazepam promotes cell cycle activation in NSCs. Analysis of cell cycle dynamics on proliferating (A-B) and quiescent NSCs (C- D) after diazepam treatment. (A, C) Confocal microphotographs of coronal sections from the SVZ of GFAP-H2B mice with or without doxy treatment. Mice were injected with diazepam or PBS and perfused 24 hours later. (B, D) Quantification of total double positive cells for GFP and Ki67 in mice without doxy treatment (B) or with doxy treatment (D). Data shown as mean+SEM (n≥4, *: p<0.05, **: p<0.01). Scale bar= 50 µm. Arrow: double immunopositive cell. Abbreviations: GFP= green fluorescent protein, SVZ= subventricular zone, qNSC= quiescent neural stem cell, PBS= phosphate buffered saline.

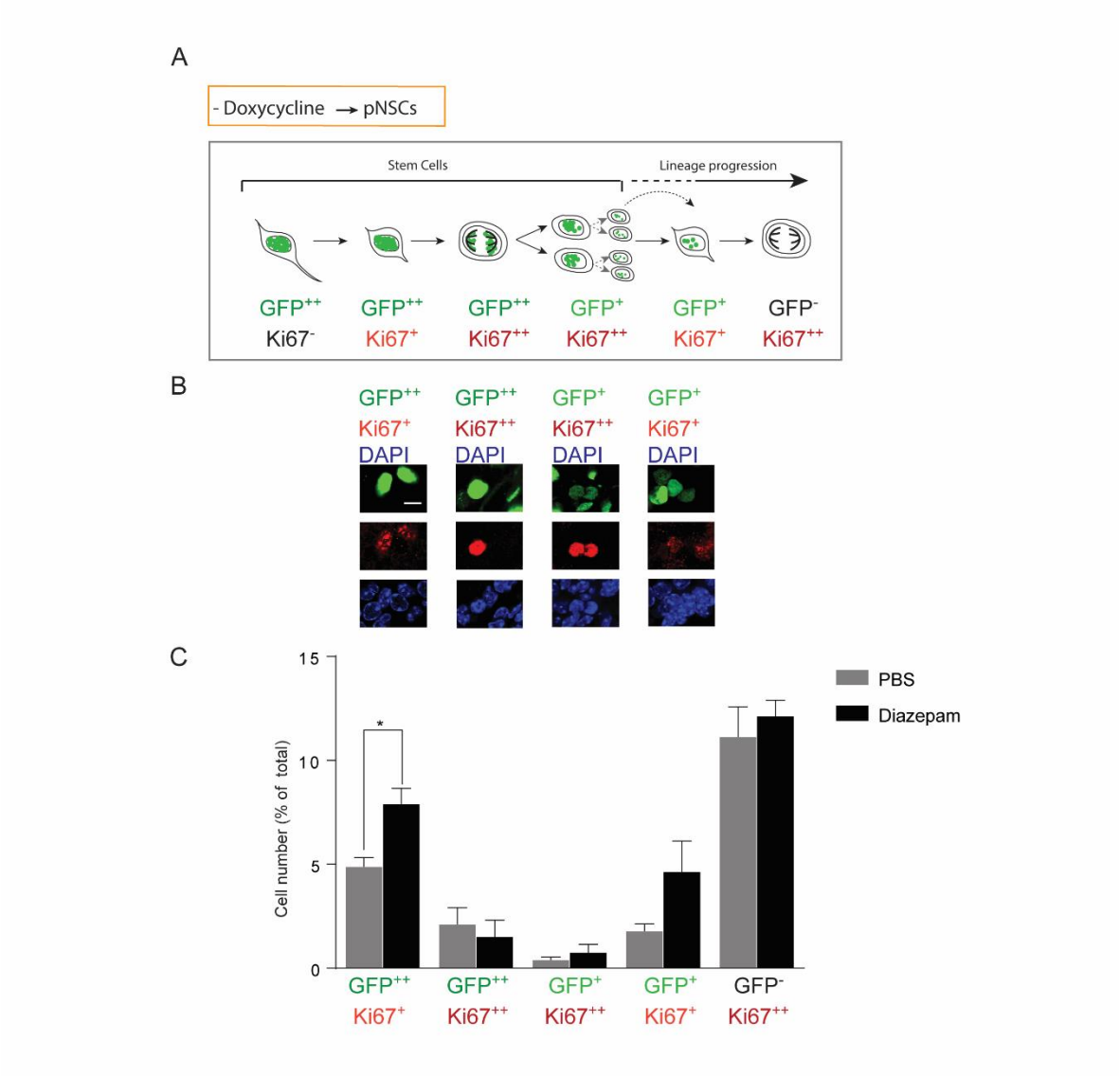

Figure 3.5 NSCs enter cell cycle after $GABA_AR$ activation. Analysis of cell cycle dynamics on proliferating NSCs. (A) Scheme showing the cell dynamics when NSCs (labelled in non-doxy conditions) enter the cell cycle. The scheme shows the different stages according to the intensity of the markers: high or low GFP (GFP^{++} or GFP^{+}) and high or low Ki67 (K^{++} or K^{+}). In this mouse model, all NSCs show high intensity for GFP, however, when they start differentiating, they lose GFP expression. (B) Confocal microphotographs of double immunopositive cells illustrating the different cell cycle stages analysed. (C) Quantification of the different cell groups showed in A in control and diazepam injected mice. Data shown as mean+SEM (n≥4, *: p<0.05, **: p<0.01). Scale bar= 10 µm. Abbreviations: GFP= green fluorescent protein, SVZ= subventricular zone, pNSC= proliferating neural stem cell, PBS= phosphate buffered saline.

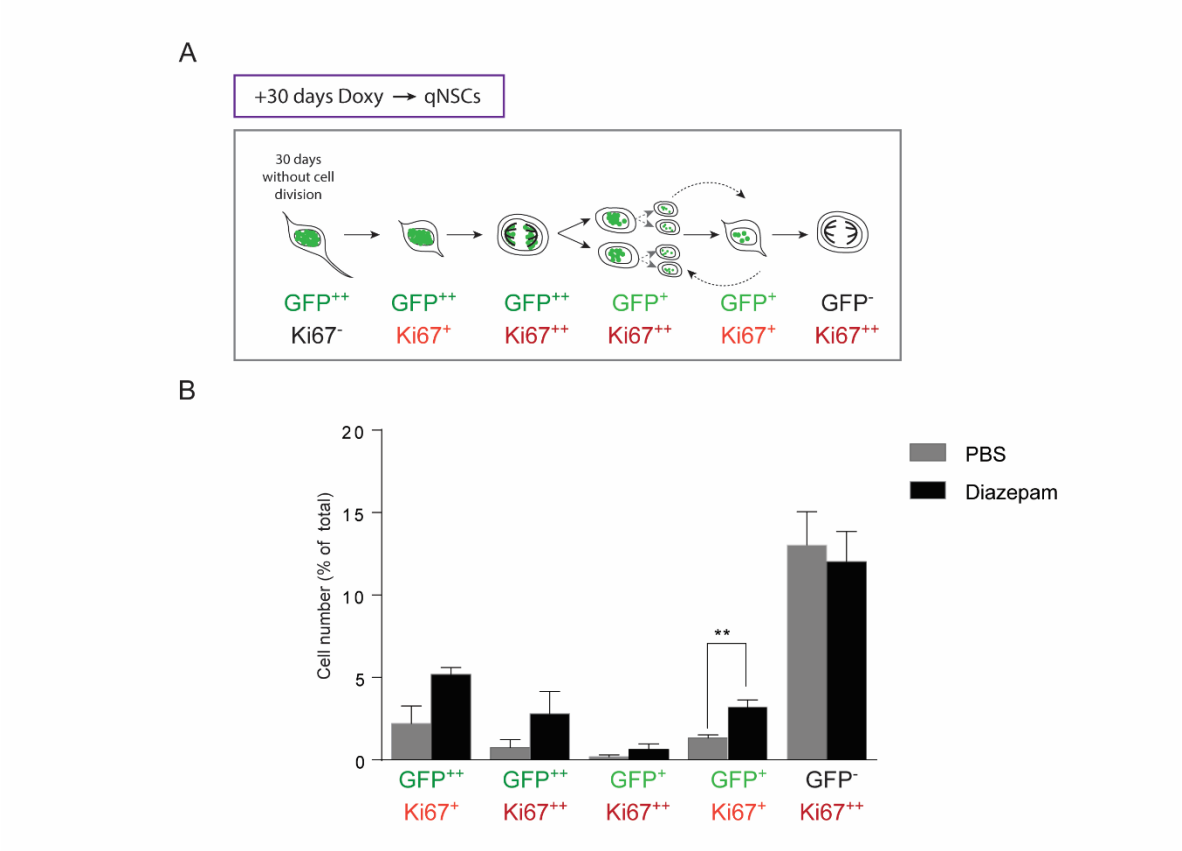

Figure 3.6 Quiescent NSCs activate and enter the cell cycle following $GABA_AR$ activation. Analysis of cell cycle dynamics on quiescent NSCs. (A) Scheme showing the cell dynamics when quiescent NSCs (qNSCs) (labelled in doxy conditions) enter the cell cycle. The scheme shows the different stages according to the intensity of the markers: high or low GFP (GFP^{++} or GFP^{+}) and high or low Ki67 (K^{++} or K^{+}). In mice with 30 days of doxy treatment, qNSCs that have not divided over the treatment period show high intensity for GFP, however, when they start dividing, they lose GFP expression. (B) Quantification of the different cell groups showed in A in control and diazepam injected mice. Data shown as mean+SEM (n≥4, *: p<0.05, **: p<0.01). Abbreviations: Doxy= doxycycline, GFP= green fluorescent protein, SVZ= subventricular zone, qNSC= quiescent neural stem cell, PBS= phosphate buffered saline.

Thereafter, I performed a similar analysis in qNSCs (Fig.3.6). In this situation, GFP intensity is associated with the quiescence state of the cell, as those cells that have not divided during administration of doxy will show greater GFP levels (GFP^{++}), while those that have divided will progressively dilute the expression of the reporter protein (GFP^{+}), until becoming undetectable after 5 rounds of cell division (Waghmare et al., 2008) (Fig.3.6A). In this analysis I observed that diazepam injection led to an increase in the number of $GFP^{+}Ki67^{+}$ cells (Fig.3.6B), whereas cycling GFP^{++} NSCs showed a trend increase, which was not

significant, suggesting that diazepam mostly promotes activation of qNSCs and this effect was stronger in those cells that had already divided.

3.1.2 $GABA_AR$ activation in NSCs leads to lineage progression from Prominin1$^+$ to Prominin1$^-$ NSCs

The previous experiments showed that diazepam promotes cell cycle entry of NSCs in the adult SVZ. To further characterize the effect of $GABA_AR$ activation, I took advantage of flow cytometry to purify qNSCs and pNSCs from the SVZ of GFAP-H2B mice 24 after intraperitoneal injection of diazepam. In these experiments, cells from SVZ were further immunostained with antibodies against Prominin1, which is expressed in cells in contact with the ventricles including ependymal cells and NSCs (Khatri et al., 2014; Mirzadeh et al., 2008)) (Fig.3.7A).

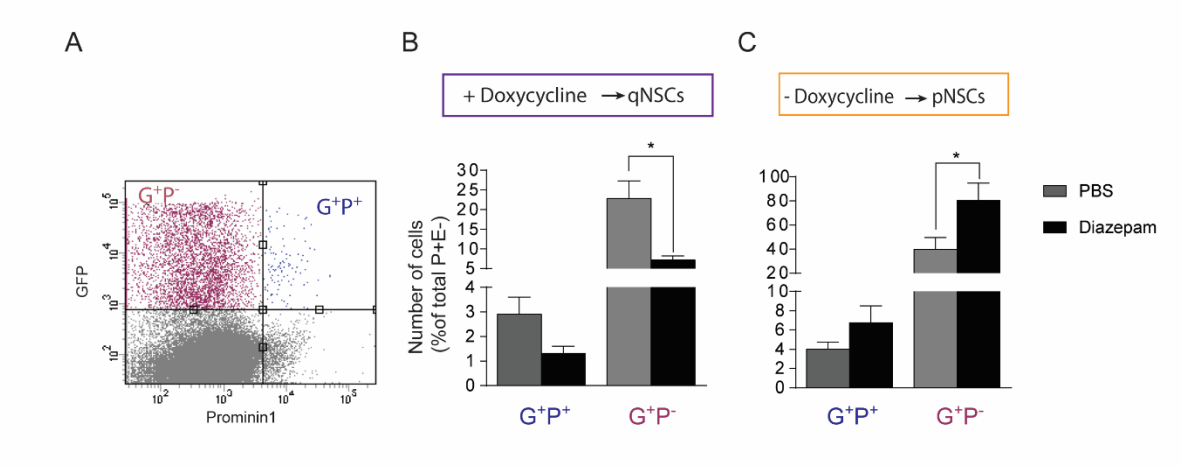

Figure 3.7 Quiescent NSCs become proliferating NSCs after diazepam treatment. FACS sort analysis of the effect of diazepam in GFAP-H2B mice. (A) FACS plot representing the two cell populations analyzed according to prominin1 expression (P^+ or P^-) and to the presence of GFP (G^+ or G^-). (B, C) FACS analysis, 24h after diazepam treatment, of adult SVZ from GFAP:H2B mice after four weeks of treatment with doxycycline and without doxycycline respectively. Data are the mean+SEM of the total cell number normalized to the total Prominin1$^+$EGFR$^-$ cells (P^+E^-) (n≥5, *: p<0.05, **: p<0.01). Abbreviations: P= Prominin1, qNSCs= quiescent neural stem cells, pNSCs= proliferating neural stem cells FACS= Fluorescence-activated cell sorting.

This analysis revealed that both pNSCs and qNSCs were mostly represented by Prominin1$^-$ cells (G^+P^-) and only the minority were Prominin1$^+$ cells (G^+P^+). Consistent with the previous observations in cell cycle analysis, I found that G^+P^+ and especially G^+P^- qNSCs were decreasing 24 hours after diazepam injection (Fig.3.7B), as expected if $GABA_AR$ activation causes qNSCs proliferation and loss of the H2B-GFP labelling. In contrast, in pNSCs, i.e. isolated from mice not exposed to doxy, G^+P^- increased in number upon diazepam injection (Fig.3.7C). However, this change was not obvious in the G^+P^+ stem cell pool, suggesting the possibility that diazepam-induced proliferation is concomitant with the loss of Prominin-1 expression. This could be caused by a lineage progression from P^+ to P^- NSCs, and therefore, this could be the reason why the increase in G^+P^+ cells could not be detected. To test this possibility, apical and basal NSCs were isolated after labelling of the apical SVZ with DiI (Fig.3.8A). These cells were exposed to the $GABA_AR$ agonist muscimol for 24 hours. Thereafter, G^+P^+ and G^+P^- cells were quantified within both apical (DiI^+) and basal (DiI^-) SVZ populations. This analysis revealed that the apical cells were losing Prominin1 expression after $GABA_AR$ activation with a concomitant increase in the number of G^+P^- cells (Fig.3.8B). Moreover, this effect was not observed in the pool of basal SVZ cells. Strangely, the basal pool of cells, which virtually is compounded only by P^- cells, showed high number of G^+P^+ cells 24 hours after being plated. Therefore, in order to understand if this was not the result of an *in vitro* artefact, and to unveil if the NSCs were migrating from an apical to a basal position or just losing the Prominin1 expression, I isolated the whole SVZs and culture them with or without muscimol for 24 hours. Later, DiI was applied and the levels of Prominin1 were measured (Fig.3.8D). This analysis showed again an increase in the number of P^- cells at the expenses of the number of P^+ cells within the apical DiI^+ population (Fig.3.8E). I also found no change in Prominin1 expression among basal DiI^- cells. Taken together these data suggest that after $GABA_AR$ activation a subset of apical NSCs loses Prominin1 expression but not the apical surface. To Further confirm that no migration had taken place after $GABA_AR$

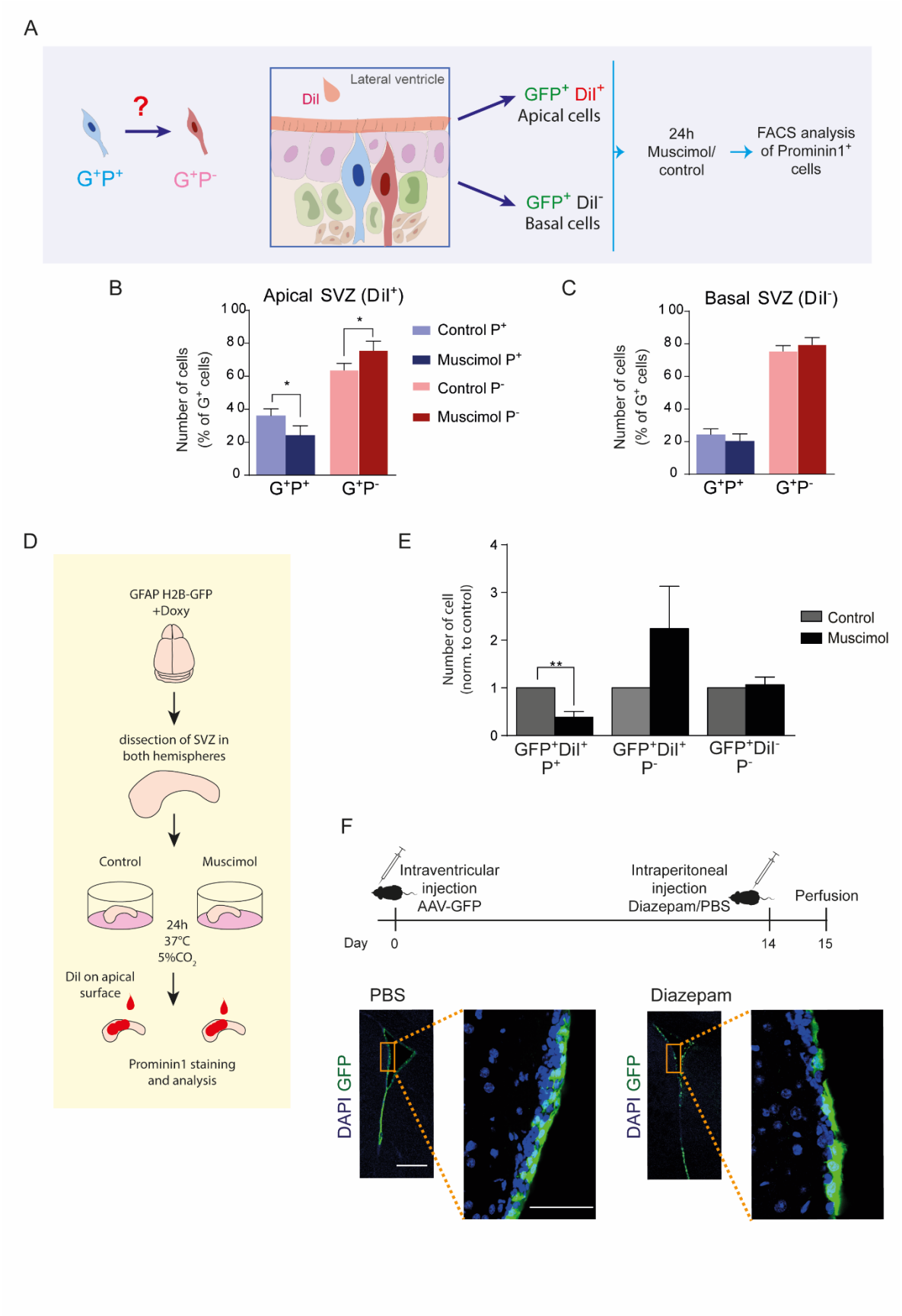
A
G+P+
?
G+P-
Dil
Lateral ventricle
GFP+ DiI+
Apical cells
GFP+ DiI-
Basal cells
24h
Muscimol/
control
FACS analysis
of Prominin1+
cells
B
Apical SVZ (DiI+)
Number of cells
(% of G+ cells)
Control P+
Muscimol P+
Control P-
Muscimol P-
G+P+
G+P-
C
Basal SVZ (DiI-)
Number of cells
(% of G+ cells)
G+P+
G+P-
D
GFAP H2B-GFP
+Doxy
dissection of SVZ in
both hemispheres
Control
Muscimol
24h
37°C
5%CO2
DiI on apical
surface
Prominin1 staining
and analysis
E
Number of cell
(norm. to control)
Control
Muscimol
GFP+DiI+
P+
GFP+DiI+
P-
GFP+DiI-
P-
F
Intraventricular
injection
AAV-GFP
Intraperitoneal
injection
Diazepam/PBS
Perfusion
Day
0
14
15
PBS
Diazepam
DAPI GFP
DAPI GFP

Figure 3.8 $GABA_AR$ activation by muscimol on NSCs promotes lineage progression from P^+ into P^-. (A) Apical and basal NSCs from GFAP-H2B mice are separated using the GFP expression (marker for NSCs) and DiI staining in the apical surface of the ventricles. These cells are treated with muscimol, after 24h, Prominin1 is measured in both cell pools. (B, C) Quantification of total Prominin1 immunopositive cells after muscimol treatment in apical DiI^+ cells (B) and basal DiI^- cells (C). (D) Whole SVZs are dissected and incubated with muscimol. 24 hours later, DiI is applied in the apical surface and cells are analyzed according to GFP expression, DiI incorporation and Prominin1 expression. The quantification of this analysis is shown in E. (F) Mice are intraventricularly injected with AAV expressing GFP under a constitutional promoter to label the apical cells. 14 days after the surgeries, mice are intraperitoneally injected with diazepam/PBS to study cell migration from an apical to basal position. Representative coronal sections from this analysis are shown. Samples are normalized to control. Data is shown as mean+SEM ($n \geq 4$, *: $p<0.05$, **: $p<0.01$). Scale bar= 100 µm and 50 µm in magnifications. Abbreviations: G^+= GFP^+, P= Prominin1, D^+= DiI^+, SVZ= subventricular zone, AAV= adeno associated virus.

activation, wild type (WT) mice were intra-ventricularly injected with adeno associated viral particles (AAV) containing a construct that expresses the humanized *Gfp* gene under the control of the constitutive CBA promoter to label the apical cells. We have previously shown that this approach leads overwhelmingly to the transduction and labelling of apical cells. After 14 days, mice were further injected intraperitoneally with diazepam/PBS and perfused 24 hours later (Fig.3.8F). Coronal slices from these brains were obtained to investigate the position of the GFP^+ cells. These analyses revealed however that virtually all infected cells maintained an apical position, independent of the diazepam treatment, confirming that $GABA_AR$ activation promotes the lineage progression from G^+P^+ to G^+P^- at the apical side of the ventricles.

3.1.3 EGFR is upregulated in NSCs after $GABA_AR$ activation

My results showed that $GABA_AR$ activation promoted an increase in cell cycle activation and lineage progression in NSCs. Since previous studies in our laboratory have shown that $GABA_AR$ activation increases the expression of the epidermal growth factor receptor (EGFR) at the cell surface (Cesetti et al., 2011; Li et al., 2015), I next investigated the involvement of EGFR expression in the GABAergic regulation of NSC proliferation. To do so, I isolated

the RNA from G^+P^+ and G^+P^- qNSCs and pNSCs purified from GFAP-H2B mice 24 hours after intraperitoneal injection of diazepam or PBS as control (Fig.3.9A). In order to study the differential regulation in adults SVZ compared to the postnatal niche, I also performed a similar analysis on G^+P^+ and G^+P^- pNSCs derived from neonatal (P7) mice, as at this age the effect of $GABA_AR$ on EGFR regulation was previously observed (Cesetti et al., 2011; Li et al.,

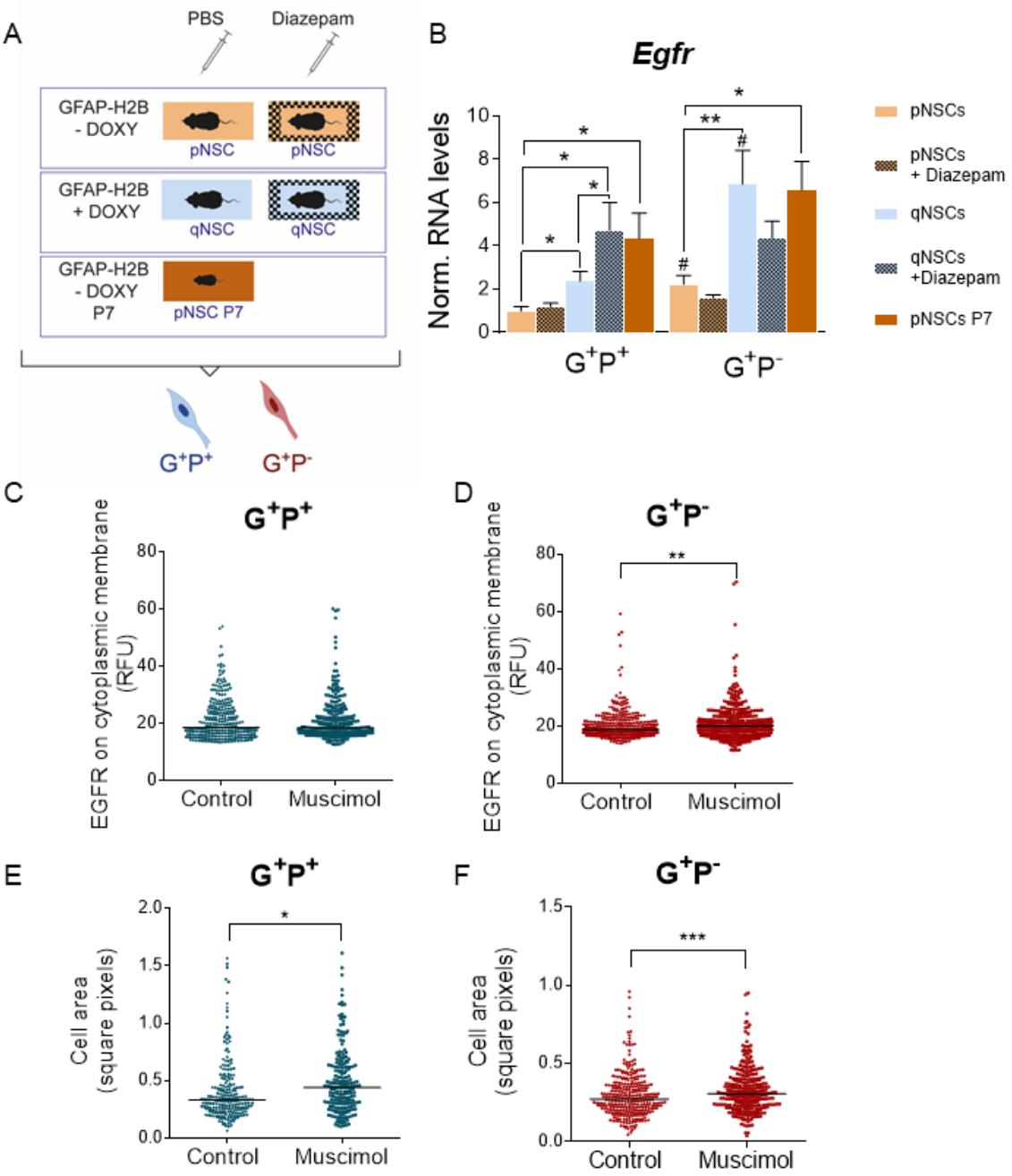

Figure 3.9 $GABA_AR$ activation on NSCs upregulates EGFR, both in RNA and protein levels. (A) G^+P^+ and G^+P^- cells are isolated by FACS from the SVZ of adult mice, with or without doxy treatment, 24h after being intraperitoneally injected with diazepam/PBS. These cells were also isolated from postnatal GFA-H2B mice in the day 7 after birth (P7). (B) RNA levels of *Egfr* in G^+P^+ and G^+P^- from the different treatments explained in A. Values are mean of RQ from ddCT +SEM normalized to proliferating G^+P^+ (n≥7, #: p<0.05 between G^+P^+ and G^+P^- ; *: p<0.05, **: p<0.005 inside the same cell subset (G^+P^+ or G^+P^-). (C-F) G^+P^+ and G^+P^- cells were also isolated from GFA-H2B mice and plated to be stained with antibodies against EGFR in the cell membrane. Fluorescent values are measured for G^+P^+ (C) and G^+P^- (D). Also, cell area was measured for both cell types (E and F respectively). Direct measurements from single cells are plotted, using a n≥100 cells from n≥4 mice per condition (*: p<0.05, **: p<0.01, ***: p<0.005). Abbreviations: G^+= GFP^+, P= Prominin1, RQ= Relative quantification values, ddCT= delta-delta threshold cycle, pNSCs= proliferating neural stem cell, qNSCs= quiescent neural stem cell, RFU= relative fluorescence units.

2015) (Fig.3.9A). This analysis revealed that G^+P^- pNSCs and qNSCs express higher levels of *Egfr* than the G^+P^+ counterpart, suggesting that the latter population proliferates less than the first. Moreover, diazepam only increased *Egfr* transcript levels in G^+P^+ qNSCs, consistent with previous findings that $GABA_AR$ activation increases EGFR protein transportation at the cell membrane (Cesetti et al., 2011a; Li et al., 2015b), but not overall transcript expression. In line with previous observations (Carrillo-García et al., 2014), P7 pNSCs cells showed higher *Egfr* expression levels than the adult counterparts. However, qNSCs also showed high *Egfr* expression, which was unexpected considering their quiescent state. Thus, I next investigated expression of the EGFR protein. To this end, G^+P^+ and G^+P^- pNSCs were isolated from GFAP-H2B mice and afterwards plated in the presence or absence of muscimol for 24 hours. Thereafter, cells were immunostained with antibodies against an extracellular epitope of the EGFR to quantify the protein levels expressed on the cellular membrane. Besides EGFR fluorescent intensity I also measured the cell area. The analysis showed that only G^+P^- cells increased the levels of EGFR at the cell surface (Fig.3.9D). However, both cells types augmented in cell size (Fig.3.9E, D). Altogether these data confirms that both cells types respond to $GABA_AR$ activation, first by increasing cell size, which leads to cell cycle activation as previously observed in the neonatal niche (Li et al., 2015), and second, by upregulating EGFR. To understand whether the increase in EGFR expression reflected an increase in its activation, I looked at the activated form of EGFR by analysing the phosphorylated EGFR at tyrosine 1068 (pEGFR) (Fig.3.10). Coronal slices from mice injected

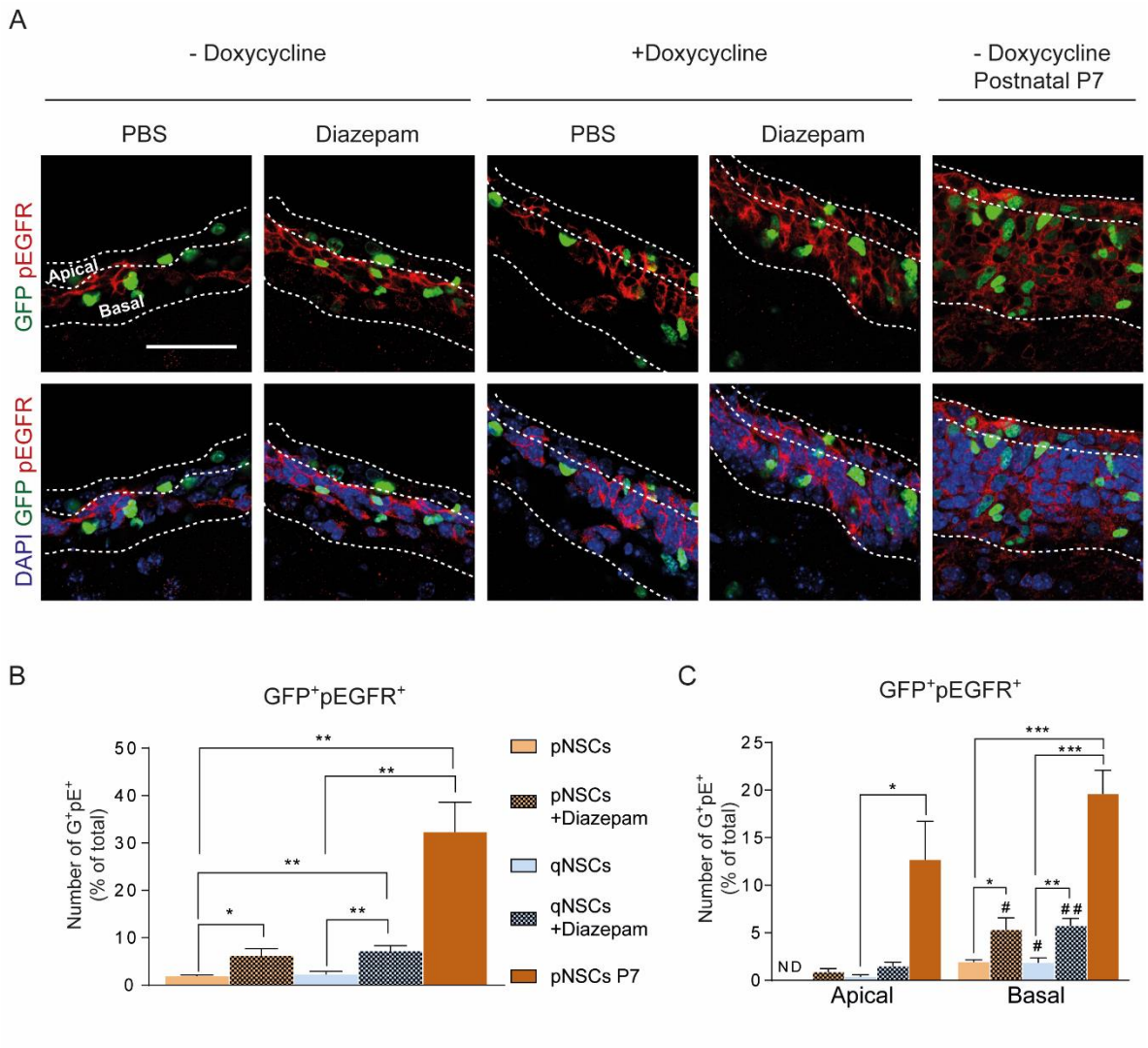

Figure 3.10. Diazepam promotes EGFR activation on NSCs. (A) Representative confocal microphotographs of SVZ stained against phosphorylated EGFR (pEGFR) from adult GFAP-H2B mice, with or without doxy treatment, 24h after being intraperitoneally injected with diazepam/PBS, and from postnatal P7 GFAP-H2B mice. (B) Cell number of total double positive cells for GFP and pEGFR from the mice showed in A. (C) Double immunopositive cells for GFP and pEGFR from the mice showed in A separated according to their position respect to the ventricle cavity (apical= in contact with de ventricle, basal= no physical contact with the ventricle). Data shown as mean +SEM, *= significant difference inside the same cell type, #= significant difference between G^+P^+ and G^+P^- (n=4, *: p<0.05, **: p<0.01, ***: p<0.005, #: p<0.05, ##: p<0.01). Scale bar= 50 µm. Abbreviations: pE= phosphorylated EGFR, ND= non-detected

with diazepam/PBS in doxy and non-doxy conditions, and from P7 mice were analysed for double positive cells (GFP^+ $pEGFR^+$), showing that, as expected, P7 mice displayed the highest number of activated NSCs (Fig.3.10B). But this result was not the consequence of mice at postnatal age having more NSCs than at adult age, but rather an increase in the

proportion of NSCs displaying pEGFR immunoreactivity, because from the total NSCs pool, the EGFR activated fraction represented the 94,6 ± 2,3 % in postnatal mice, while in adult mice it only represented a 8,9 ± 0,7 % of total NSCs. This result explains why NSCs in young mice show a greater increase in proliferation in response to diazepam that NSCs in adult niche. Looking at the adult SVZ, diazepam increased EGFR activation both in pNSCs and qNSCs (Fig.3.10B). To have a better understanding of which subset of cells was being more affected by diazepam treatment, I analysed separately the NSCs in the apical surface of the ventricles (mostly integrated by G^+P^+ cells) from those at the basal side (comprising G^+P^- cells, (unpublished observations)), as shown in figure 3.10 A. This analysis revealed that neonatal SVZs present the highest number of GFP^+pEGFR^+ cells, in both apical and basal subregions of the SVZ compared to adult individuals (Fig.3.10C). Also, independent of the age and doxy treatment, the greatest quantity of $pEGFR^+$ NSCs were found at the basal region, consistent with the RNA data showing that EGFR transcripts in G^+P^- NSCs are greater than in G^+P^+ NSCs. Diazepam significantly increased the number of $pEGFR^+$ pNSCs and qNSCs at the basal side of the niche, however, although comparatively fewer, pNSCs with activated EGFR at the apical side were only detected after diazepam treatment (Fig.3.10C) and never in the control condition.

Altogether, these data show that EGFR signal is up-regulated in NSCs when $GABA_AR$ is activated in the adult niche.

3.1.4 β1Integrin is downregulated in qNSCs after $GABA_AR$ activation

My previous results showed that G^+P^+ and G^+P^- cells increased in cell size after $GABA_AR$ activation. Also, previous analysis in our lab, demonstrated that in the postnatal niche, $GABA_AR$ activation leads to an increase in aquaporin4, cell swelling, and cell activation (Cesetti et al., 2011; Li et al., 2015). Therefore, I thought that activation of NSCs might be as well affecting their interaction with the extracellular matrix (ECM). In order to investigate this, I analysed the expression of the β1Integrin subunit of the integrin receptor, a cell surface receptor implicated in the interaction with the ECM. First, I analysed the transcripts

expression of β*1Integrin* in G^+P^+ and G^+P^- pNSCs and qNSCs 24 hours after diazepam/PBS injection. The analysis revealed that only qNSCs were decreasing β*1Integrin* mRNA levels after diazepam treatment, and this decrease was observed in both, G^+P^+ and G^+P^- cells (Fig.3.11A). Next, I analysed β1Integrin in the intact SVZ of mice with or without doxy after being injected with diazepam/PBS (Fig.3.11B). The quantification of GFP^+β1$Integrin^+$ cells

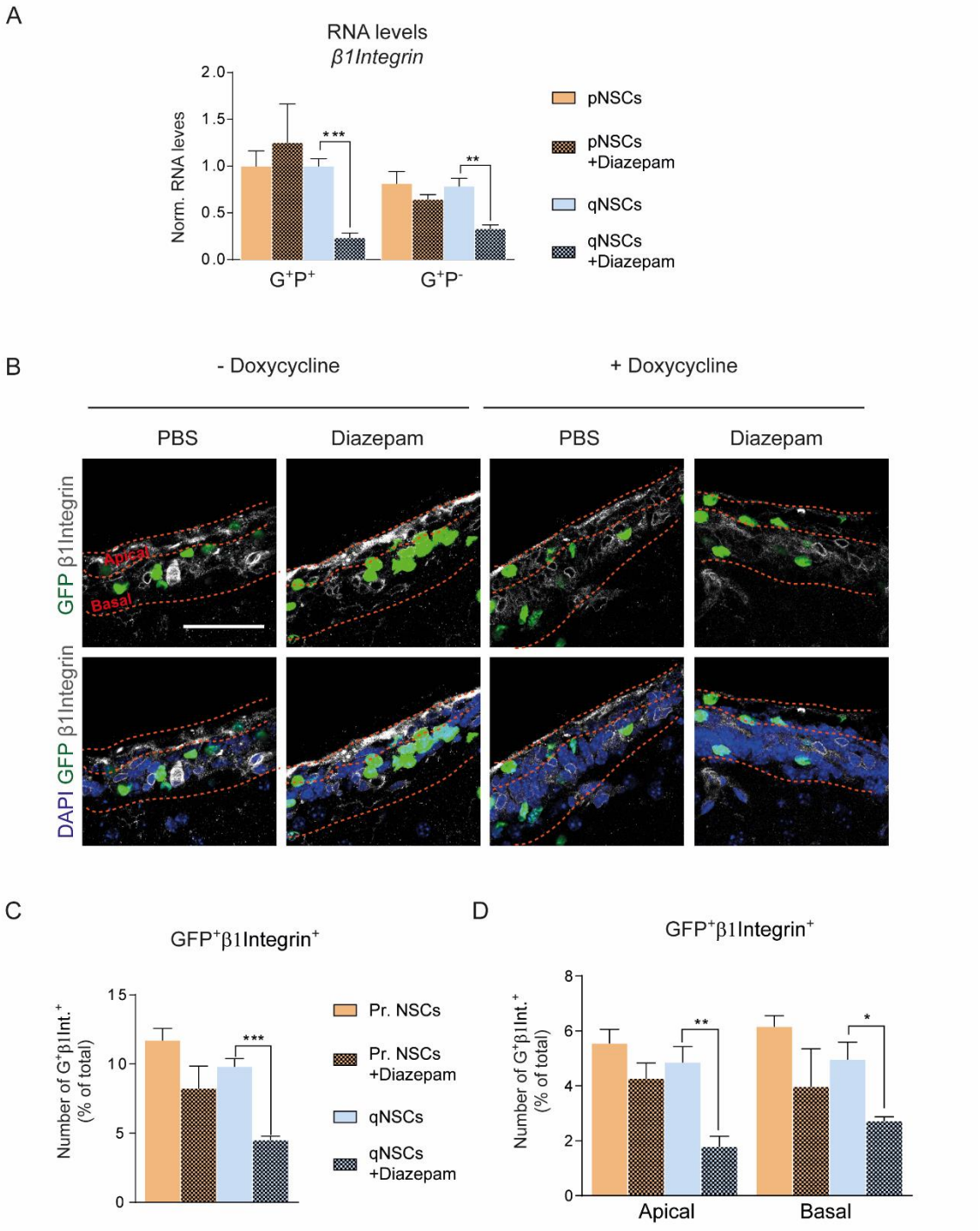

Figure 3.11 Diazepam decreases β1Integrin in RNA and protein levels on NSCs. (A) RNA levels of β*1Integrin* in G^+P^+ and G^+P^- from adult GFAP-H2B mice, with or without doxy treatment, 24h after being intraperitoneally injected with diazepam/PBS. Values are the mean of RQ from ddCT +SEM normalized to proliferating G^+P^+ (n≥7, #: p<0.05 between G^+P^+ and G^+P^- ; *: p<0.05, **: p<0.01 inside the same cell subset (G^+P^+ or G^+P^-). (B) Representative confocal microphotographs of SVZ stained against β1Integrin from adult GFAP-H2B mice in the same treatment conditions as in A. (C) Quantification of total double positive cells for GFP and β1Integrin from the SVZs showed in B. (D) Double immunopositive cells for GFP and β1Integrin from the mice showed in B separated according to their position respect to the ventricle cavity (apical= in contact with the ventricle, basal= no physical contact with the ventricle). Scale bar= 50 µm. Data shown as mean+SEM (n≥4, *: p<0.05, **: p<0.01, ***: p<0.005). Abbreviations: β1Int. = β1Integrin.

showed that, again, only qNSCs were affected by diazepam, and undergoing a reduction in the expression of the receptor (Fig.3.11C). Also in this analysis, I quantified the effect of diazepam in the basal and apical region of the SVZ (Fig.3.11B) to investigate the differences in response between the two NSCs pools. The analysis showed that, in both apical and basal subregions of the niche, only qNSCs reduced β1Integrin expression after diazepam (Fig.3.11D), again suggesting that the change in β1Integrin expression occurred only in qNSCs.

Next, in order to understand the GABAergic regulation of EGFR activation and β1Integrin expression, I analysed β1Integrin (β) together with pEGFR (pE) in qNSCs and pNSCs upon diazepam/PBS injection (Fig.3.12A). The analysis of apical and basal region of the SVZ showed that, compared to the controls and independent of the subregion of the niche, the activation of $GABA_AR$ led to a decrease in the population of NSCs displaying only β1Integrin immunoreactivity ($G^+\beta^+$) (Fig.3.12B, four left panels). A similar and stronger effect of diazepam was observed in qNSCs (Fig.3.12B, four right panels). At the same time, diazepam also led to an increase in the number of pNSCs displaying only pEGFR immunoreactivity (G^+pE^+) in the basal region of the SVZ (Fig.3.12B, four left panels), and, again, this effect was stronger in qNSCs (Fig.3.12B, four right panels). However, double immunopositive NSCs ($G^+pE^+\beta^+$) were not affected by the treatment. Suggesting that $GABA_AR$ activation in NSCs activates a process by which cells with activated EGFR progressively lose the β1Integrin expression, changing from $G^+\beta1^+pE^-$ to $G^+pE^+\beta^-$. Since the increase in EGFR at the cell surface occurs within minutes of $GABA_AR$ activation and does not require a change in EGFR

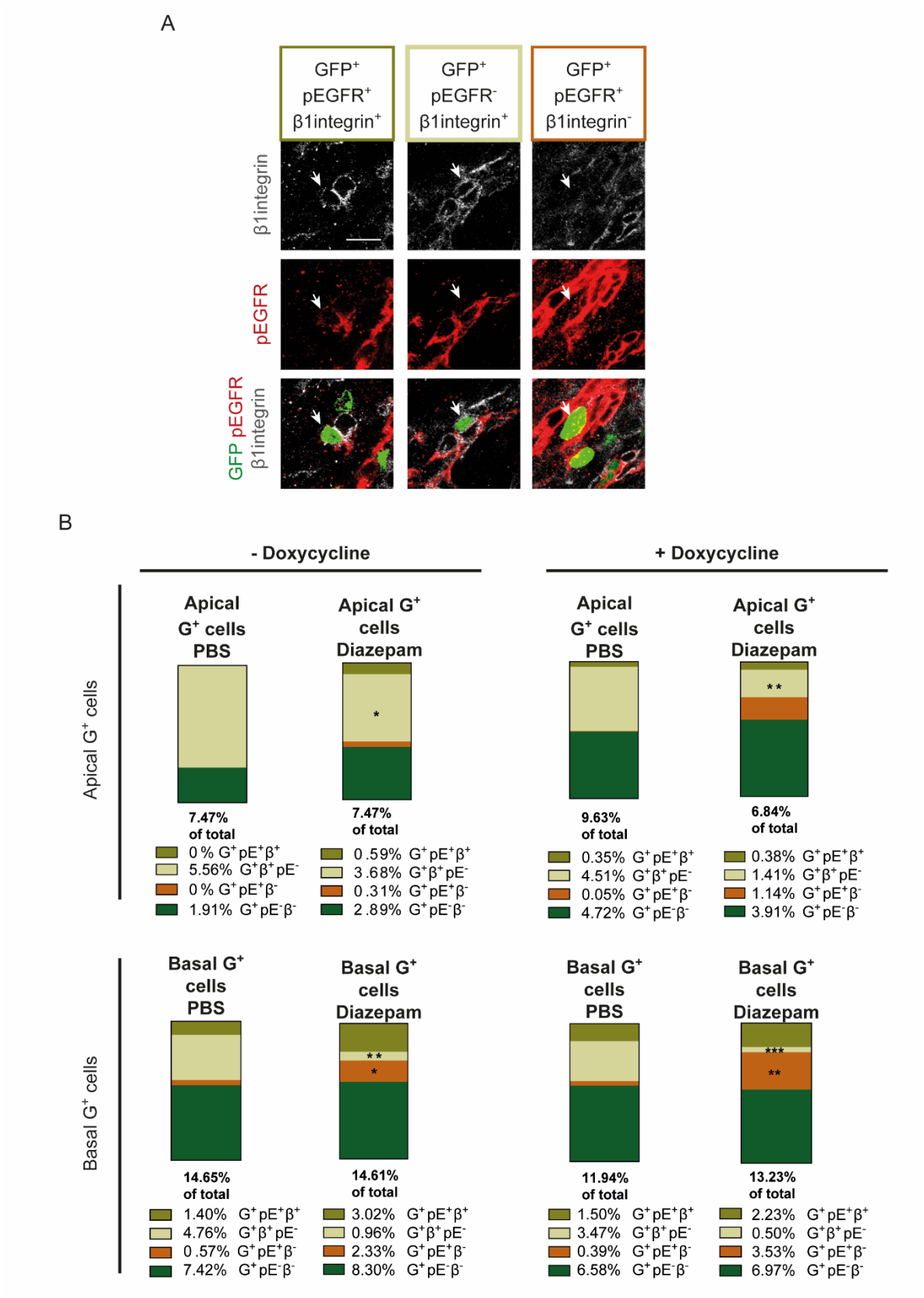
A
GFP+ pEGFR+ β1integrin+
GFP+ pEGFR- β1integrin+
GFP+ pEGFR+ β1integrin-
β1integrin
pEGFR
GFP pEGFR β1integrin
B
- Doxycycline
+ Doxycycline
Apical G+ cells
Basal G+ cells
Apical G+ cells PBS
Apical G+ cells Diazepam
Basal G+ cells PBS
Basal G+ cells Diazepam
7.47% of total
0 % G+pE+β+
5.56% G+β+pE-
0 % G+pE+β-
1.91% G+pE-β-
7.47% of total
0.59% G+pE+β+
3.68% G+β+pE-
0.31% G+pE+β-
2.89% G+pE-β-
9.63% of total
0.35% G+pE+β+
4.51% G+β+pE-
0.05% G+pE+β-
4.72% G+pE-β-
6.84% of total
0.38% G+pE+β+
1.41% G+β+pE-
1.14% G+pE+β-
3.91% G+pE-β-
14.65% of total
1.40% G+pE+β+
4.76% G+β+pE-
0.57% G+pE+β-
7.42% G+pE-β-
14.61% of total
3.02% G+pE+β+
0.96% G+β+pE-
2.33% G+pE+β-
8.30% G+pE-β-
11.94% of total
1.50% G+pE+β+
3.47% G+β+pE-
0.39% G+pE+β-
6.58% G+pE-β-
13.23% of total
2.23% G+pE+β+
0.50% G+β+pE-
3.53% G+pE+β-
6.97% G+pE-β-

Figure 3.12 Diazepam affects mostly a population of qNSCs that upregulate EGFR signalling while decreasing β1Integrin expression. (A) Confocal microphotographs representing examples of the different triple immunopositive cells for GFP, β1Integrin and pEGFR found in the SVZ of adult GFAP-H2B mice with or without doxy treatment, 24h after being intraperitoneally injected with diazepam/PBS. (B) Quantification of the different GFP^+ cells in relation with their expression of phosphorylated EGFR only ($G^+pE^+\beta^-$), β1Integrin only ($G^+\beta^+pE^-$), the expression of both ($G^+pE^+\beta^+$), or only GFP expression (G^+). Cell quantifications are shown according to their position in the SVZ (apical/basal) and according to treatment of the mice (doxy/non-doxy, diazepam/PBS). Data shown as mean+SEM (n≥4, *: p<0.05, **: p<0.01, ***: p<0.005). Scale bar= 10 μm. Abbreviations: β = β1Integrin, pE= phosphorylated EGFR, G=GFP

expression (Cesetti et al., 2011), my data are consistent with a model by which the decrease in β1Integrin is downstream to EGFR activation. Moreover, the fact that the effect on β1Integrin transcript and protein is stronger in qNSCs suggests that $GABA_AR$ activation modulates the EGFR-β1Integrin signalling axis to affect specifically proliferation of NSCs undergoing quiescence, and this effect is greatly noted at basal region of the adult SVZ.

3.1.5 Cell cycle activation of qNSCs after $GABA_AR$ activation is EGFR dependent

My previous results confirmed that $GABA_AR$ activation directs NSCs into cell cycle activation, and they also showed that EGFR plays an important role in this regulation. For this reason, I investigated next whether increase in NSC proliferation requires activation of EGFR. To do so, I isolated G^+P^+ and G^+P^- qNSCs and plated them in the presence or absence of muscimol ($GABA_AR$ agonist) with or without PD158780 (a specific ErbB receptor tyrosine kinase inhibitor) for 24 hours (Fig.3.13). Thereafter, I fixed the cells and immunostained them for Ki67. The analysis showed that the blockage of EGFR activation signal was enough to restore cell cycle entrance to control values, and, this effect was observed in both cell types, G^+P^+ (Fig.3.13B) and G^+P^- (Fig.3.13C). Altogether, these data show that after $GABA_AR$ activation, NSCs need EGFR activation signalling to enter cell cycle.

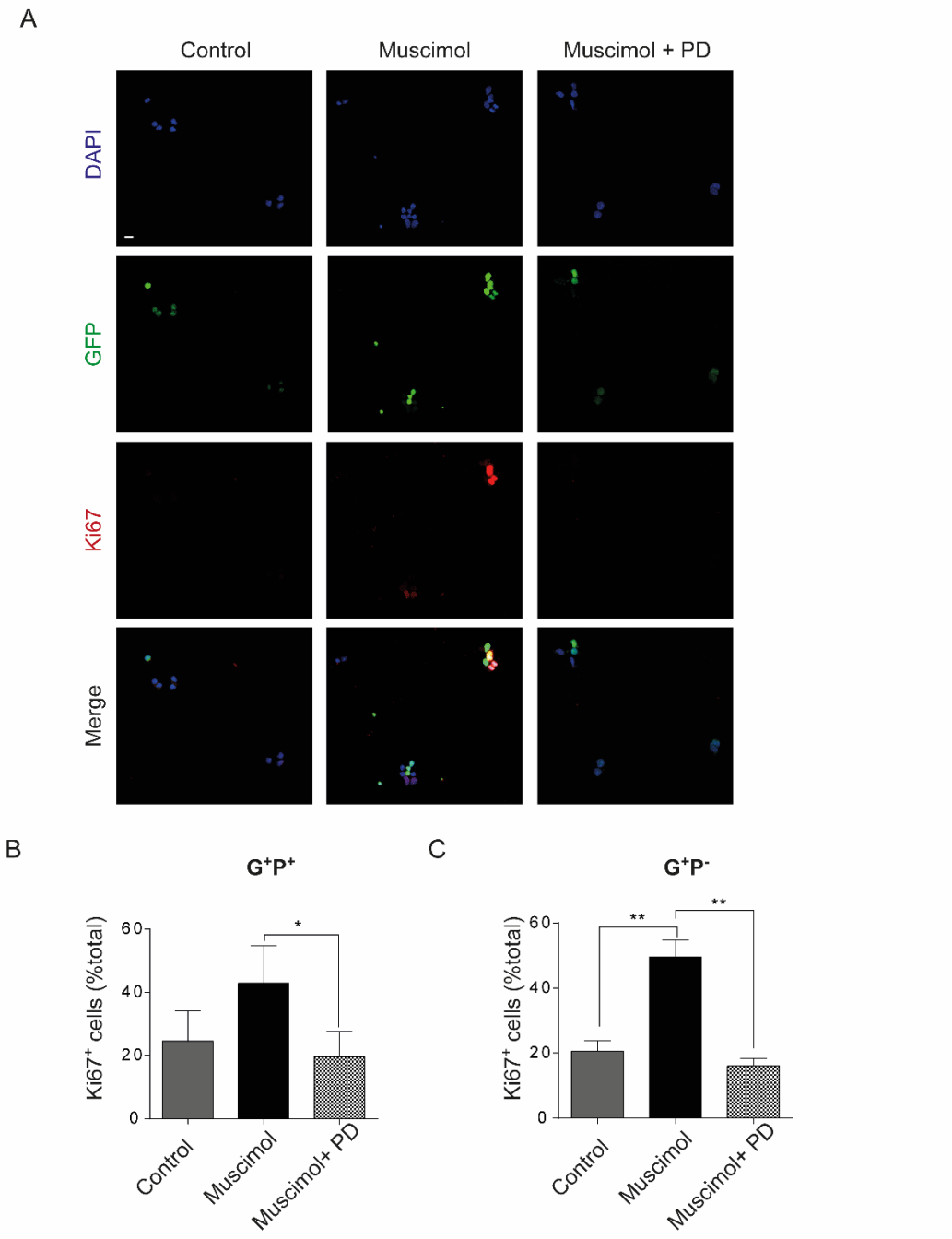

Figure 3.13 Cell cycle entrance of NSCs after $GABA_AR$ activation is EGFR dependent. (A) G^+P^+ and G^+P^- cells from adult GFAP-H2B mice with doxy treatment are plated and treated with muscimol to activate $GABA_AR$ or with muscimol and PD 158780 to block EGFR signaling. Cells are then stained with antibodies against Ki67. The figure shows confocal microphotographs representing examples of the different double immunopositive cells for GFP and Ki67 found in the control, muscimol and muscimol+ PD158780 treatments. (B) Quantification of the cells in cell cycle ($Ki67^+$) in the three experimental settings for G^+P^+ and G^+P^- cells. Data is shown as mean +SEM (n≥3, *: p<0.05, **: p<0.01, ***: p<0.005). Scale bar= 10 µm.

3.2 Intrinsic regulation. TLX regulation of NSCs quiescence

3.2.1 Lack of *Tlx* leads to changes in NOTCH signalling in the SVZ

Previous studies in our group asserted the importance of the orphan nuclear receptor TLX in the activation of NSCs in the SVZ. NSCs lacking *Tlx* expression (*Tlx*$^{-/-}$) showed impaired proliferation and lineage progression (Obernier et al., 2011). Also, recent findings show that TLX interacts in an inhibitory way with *Hes1* and *Hes5* promoters, and lack of *Tlx* exerts an upregulation of NOTCH signalling related genes (Shi, 2015). Therefore, in order to have a better understanding of the relationship between TLX with NOTCH signalling in the regulation of NSCs, I analysed the activated form of NOTCH1 receptor, notch intracellular domain (NICD), in WT and *Tlx*$^{-/-}$ mice. As previously described (Carrillo-García et al., 2014; Cesetti et al., 2011; Khatri et al., 2014), NSCs and progenitors from the SVZ can be isolated based on the expression of Prominin1 (P^+/P^-) and high or low levels of EGFR (E^H/E^L), however E^H cells are almost inexistent in the adult *Tlx*$^{-/-}$ niche. For this reason, only E^L cells could be analysed. In this way, P^+E^L cells, which include qNSCs and ependymal cells, and P^-E^L, i.e. neuroblasts and the majority of cells in the SVZ, were analysed with an antibody against NICD. These results showed that in mice lacking *Tlx*, a higher proportion of P^-E^L cells presented NICD immunoreactivity (Shi, 2015). In order to better characterise this population of $P^-E^LNICD^+$ cells that was increased in the mutant niche, I isolated P^-E^L cells from WT and *Tlx*$^{-/-}$ mice and performed double immunostainings against NICD plus different stem cell and progenitor markers such as doublecortin (DCX), GFAP, LeX-SSEA1 (LeX) and nestin (Fig.3.14A). This analysis revealed that the extra $P^-E^LNICD^+$ cells in *Tlx*$^{-/-}$ were also $GFAP^+$ (Fig.3.14B). Next, I looked at the NICD expression in the intact niche. Since the lack of *Tlx* also causes changes in brain morphology, I analysed the number of cells in the apical and basal region of the SVZ (Fig.3.14C), finding that the mutant niche presents a lower quantity of cells in the basal region compared to WT (Fig.3.14D). The analysis of NICD in the adult SVZ showed that lack of *Tlx* leads to an increase of $NICD^+$ cells in the apical SVZ (Fig.3.14F) which was significant, both in comparison to the cells in the respective basal subregion as well as to the apical WT subregion of the SVZ. Taken together, these data show

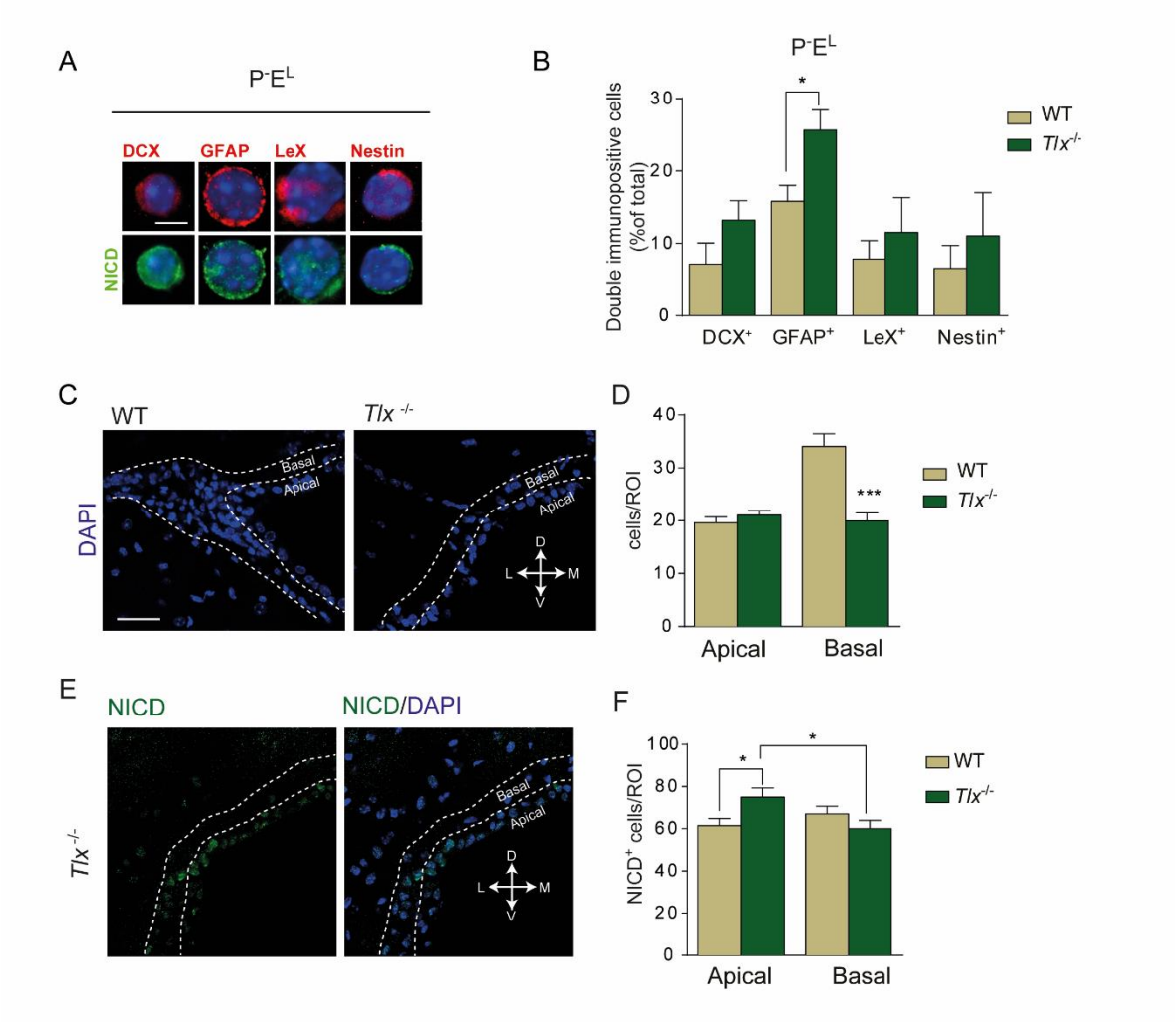

Figure 3.14 NOTCH1 receptor activation increases in NSCs lacking *Tlx* expression. (A) Representative microphotographs of P^-E^L cells isolated from the SVZ of WT and *Tlx*$^{-/-}$ adult mice displaying immunoreactivity to NICD (green) and the indicated antigens (red). (B) Quantitative analysis of the double immunostaining illustrated in A. (C) Confocal microphotographs of SVZ in WT and *Tlx*$^{-/-}$ mice illustrating the different morphology between both adult mice. (D) Quantification of cells in apical/ basal region in WT and *Tlx*$^{-/-}$ mice. (E) Confocal microphotographs of SVZ in *Tlx*$^{-/-}$ mice illustrating the immunoreactivity of NOTCH1 intracellular domain (NICD). (F) Quantification of NICD immunopositive cells in the apical/ basal SVZ of WT and *Tlx*$^{-/-}$ mice. Data is shown as mean +SEM (n≥3, *: p<0.05, ***: p<0.005). Scale bar= 10 µm (in A) and 50 µm (in C- E).

that lack of *Tlx* increases NOTCH activation, and this increase takes place in an apical population of P^- cells.

3.2.2 *Hes1* downregulation in *Tlx*$^{-/-}$ SVZ leads to NOTCH1 inactivation

My previous results showed that NOTCH signalling is upregulated in mice lacking *Tlx*. Besides this, earlier analysis (Shi, 2015) also showed that NSCs in mice lacking *Tlx* showed an increase in the transcript levels of the NICD target gene *Hes1*. This gave us the idea that the impaired proliferation and lineage progression present in these mice could be due to an upregulated *Hes1* expression. Therefore, I next used a viral construct to downregulate *Hes1* by injecting adeno-associated viral particles into the lateral ventricle of *Tlx*$^{-/-}$ adult mice. These viral constructs express *Gfp,* and either a short hairpin to target the *Hes1* mRNAs (AAV sh*Hes1*) or a scrambled sequence (AAV Sc) as control. Mice were sacrificed 14 after the intraventricular injection. The downregulation efficiency of the construct was previously tested by infecting NSC cultures of the cell line O4ANS (Fig.3.15A). The analysis of mice injected with the AAV particles showed that, despite finding the same number of infected cells (GFP^{+}) (Fig.3.15C), the SVZs of mice transduced with AAV sh*Hes1* presented a higher number of cells (Fig.3.15B). To confirm that *Hes1* downregulation also decreases HES1 protein levels, coronal slices from transduced brains where stained with antibodies against HES1 (Fig.3.15D, E). The result showed that, consistent with previous observations, *Tlx*$^{-/-}$ mice present higher levels of HES1 protein compared to WT (Fig.3.15E). Additionally, transduced cells (GFP^{+}) with AAV sh*Hes1* presented significantly lower HES1 levels than the AAV scramble counterpart. Also, and in line with my previous results, transduced cells, which represent only apical cells, showed higher immunofluorescence for HES1 than the non-transduced counterpart (GFP^{-}) in the control situation, confirming again that apical cells in the mutant niche show an upregulated NOTCH-HES1 axis. Indeed, in a similar analysis of NICD immunoreactivity, apical (GFP^{+}) control cells displayed the highest NICD values. This analysis also showed a significant downregulation of NICD expression in GFP^{+} cells upon injection of AAV-sh*Hes1*, but not AAV-Scramble viral particle in the mutant SVZ (Fig.3.15F, G). Thus, *Hes1* downregulation is accompanied by NICD downregulation in the mutant niche.

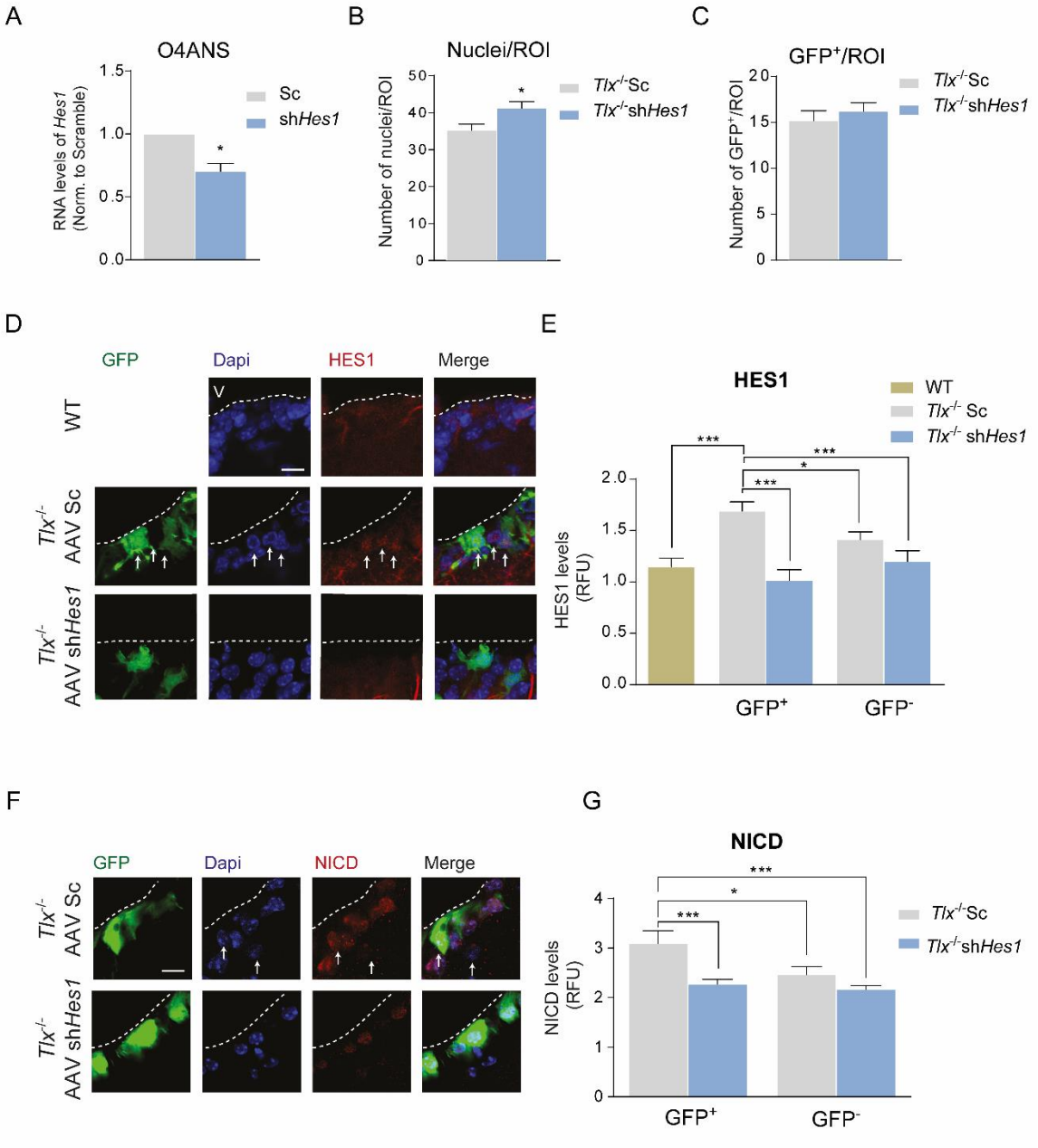
A
O4ANS
RNA levels of Hes1 (Norm. to Scramble)
1.5
1.0
0.5
0.0
*
Sc
shHes1
B
Nuclei/ROI
Number of nuclei/ROI
50
40
30
20
10
0
*
Tlx-/-Sc
Tlx-/-shHes1
C
GFP+/ROI
Number of GFP+/ROI
20
15
10
5
0
Tlx-/-Sc
Tlx-/-shHes1
D
GFP
Dapi
HES1
Merge
WT
Tlx-/- AAV Sc
Tlx-/- AAV shHes1
V
E
HES1
WT
Tlx-/- Sc
Tlx-/- shHes1
HES1 levels (RFU)
2.0
1.5
1.0
0.5
0.0
***
***
*
***
GFP+
GFP-
F
GFP
Dapi
NICD
Merge
Tlx-/- AAV Sc
Tlx-/- AAV shHes1
G
NICD
NICD levels (RFU)
4
3
2
1
0
***
*
***
Tlx-/-Sc
Tlx-/-shHes1
GFP+
GFP-

Figure 3.15 Downregulation of *Hes1* in *Tlx*$^{-/-}$ mice reduces activation of NOTCH1 receptor. (A) RNA levels of *Hes1* in O4ANS cell line after infection with adeno associated viral particles (AAV) containing a construct expressing GFP as reporter gene and either a control scrambled sequence (Sc), or a short hairpin targeting *Hes1* (sh*Hes1*). (B) Number of nuclei per region of interest (ROI) in the SVZ of *Tlx*$^{-/-}$ adult mice 14 days after the intraventricular injection of AAV Sc or AAV sh*Hes1*. (C) Quantification of GFP^{+} infected cells in the SVZ of *Tlx*$^{-/-}$ mice 14 days after the injection with AAV Sc and AAV sh*Hes1*. (D, F) Confocal microphotographs illustrating representative examples of double immunostaining for GFP (green) and HES1/NICD (red) in the SVZ of WT mice (D) and *Tlx*$^{-/-}$ mice 14 days after intraventricular injections with AAV Sc and AAV shHes1. (E, G) Quantification of HES1 (E) and NICD (G) levels (brightness intensity normalized to background). Data for immunohistochemistry quantification is shown as mean ± SEM n≥30 cells per condition. RNA expression data are shown as the mean of RQ from ddCT ± SEM. Quantification data is shown as mean +SEM (n≥3, *: p<0.05, ***: p<0.005). Scale bar= 10 µm. Abbreviations: ROI= region of interest, RFU= relative fluorescence units, NICD= notch1 intracellular domain, Sc= scramble sequence, sh= short hairpin, AAV= adeno associated virus.

3.2.3 *Hes1* downregulation in *Tlx*$^{-/-}$ SVZ leads to proliferation and lineage progression

The previous analysis showed that the SVZ in *Tlx*$^{-/-}$ mice displayed a higher number of cells after downregulation of *Hes1*. For this reason, to investigate a possible increase in proliferation after *Hes1* downregulation, I analysed the cell cycle marker Ki67 together with the lineage markers GFAP and nestin in mice injected with AAV SC and AAV sh*Hes1* (Fig.3.16). Compared to the scramble-injected controls, transduced and non-transduced cells displayed a significantly higher immunoreactivity for Ki67 (Fig.3.16B), GFAP (Fig.3.16C) and nestin (Fig.3.16D). The fact that this effect was taking place in transduced and non-transduced cells suggested a non-cell autonomous mechanism. For this reason, I performed a similar analysis quantifying the changes in marker expression in GFP^{+} and GFP^{-} cells separately (Fig.3.17). As a result, downregulation of *Hes1* changed the expression of the different markers in GFP^{+} and especially in GFP^{-} cells. Cells in cell cycle increased in transduced and non-transduced cells with AAV sh*Hes1* (Fig3.17A-C). However, even though the expression of GFAP (Fig.3.17E, F) and nestin (Fig.3.17H, I) was increased in both populations, the effect was significant only in GFP^{-} cells. Interestingly, most of GFP^{-} cells localized at the basal region of the SVZ, and since they do not express the reporter gene, it

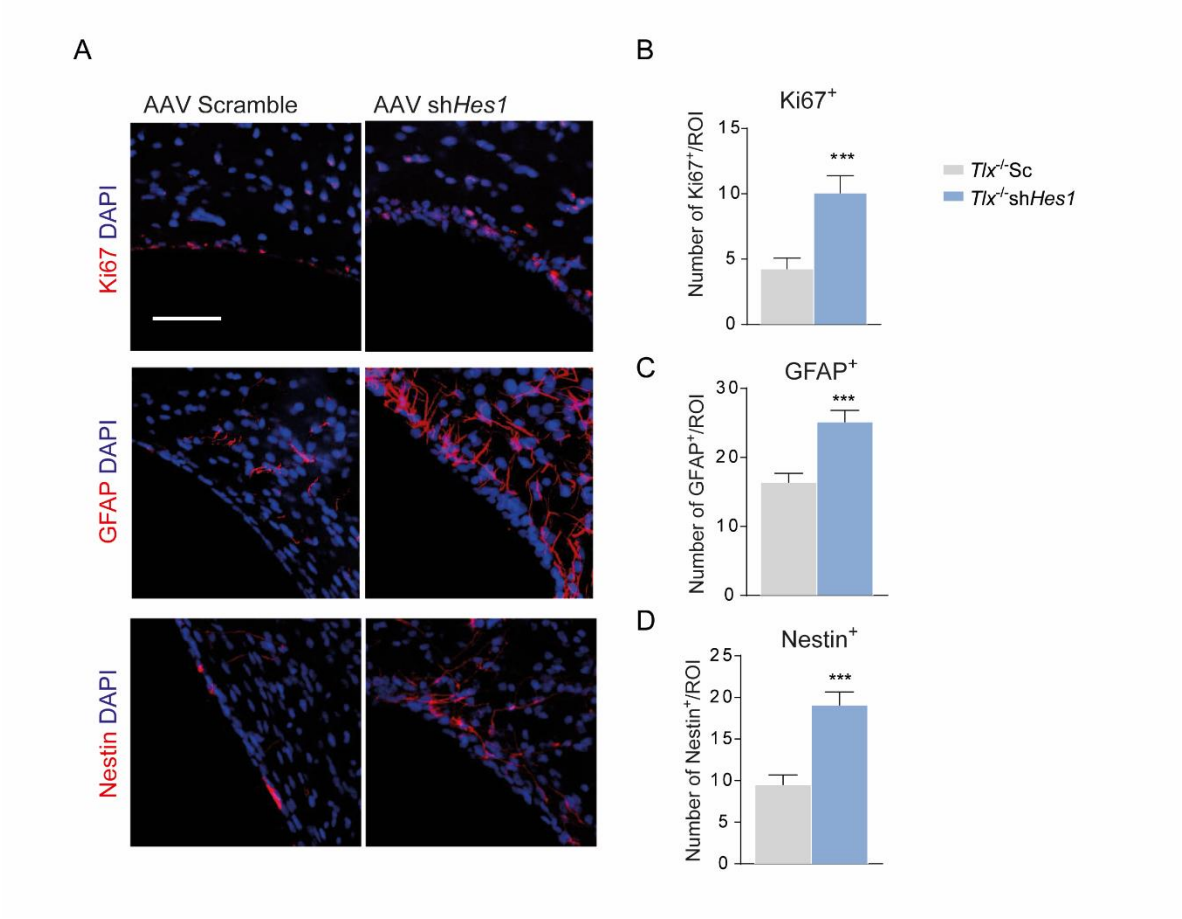

Figure 3.16 Downregulation of *Hes1* in *Tlx*$^{-/-}$ mice increases proliferation and lineage progression. (A) Representative confocal microphotographs of coronal section of *Tlx*$^{-/-}$ SVZ analysed 14 days after intraventricular injection of AAV Sc and AAV sh*Hes1* particles and immunostained against Ki67, GFAP and Nestin. (B- D) Quantification of immunopositive cells for Ki67 (B), GFAP (C) and Nestin (D) in the coronal sections showed in A. Quantification data is shown as mean +SEM (n≥3, *: p<0.05, ***: p<0.005). Scale bar= 10 µm. Initials: GFP = green fluorescent protein, GFAP = Glial fibrillary acidic protein, ROI= region of interest, Sc= scramble sequence, sh= short hairpin.

is reasonable to think that they derived from a basal pool of cells in a quiescent state. I next analysed whether the manipulation with AAV sh*Hes1* affected also neurogenesis. To do so, I look at the expression of DCX (a marker for neuroblasts), finding that, as with the previous makers, there were an increased number of DCX^{+} cells upon *Hes1* downregulation, and most of these cells were also GFP^{-} (Fig.3.17J). Altogether, these findings show that downregulation of *Hes1* expression in *Tlx*$^{-/-}$ mice promotes proliferation and neurogenesis in apical and especially in basal progenitors by a cell autonomous and non-cell autonomous

mechanism respectively. This confirms, that *Hes1* overexpression is a key event in the

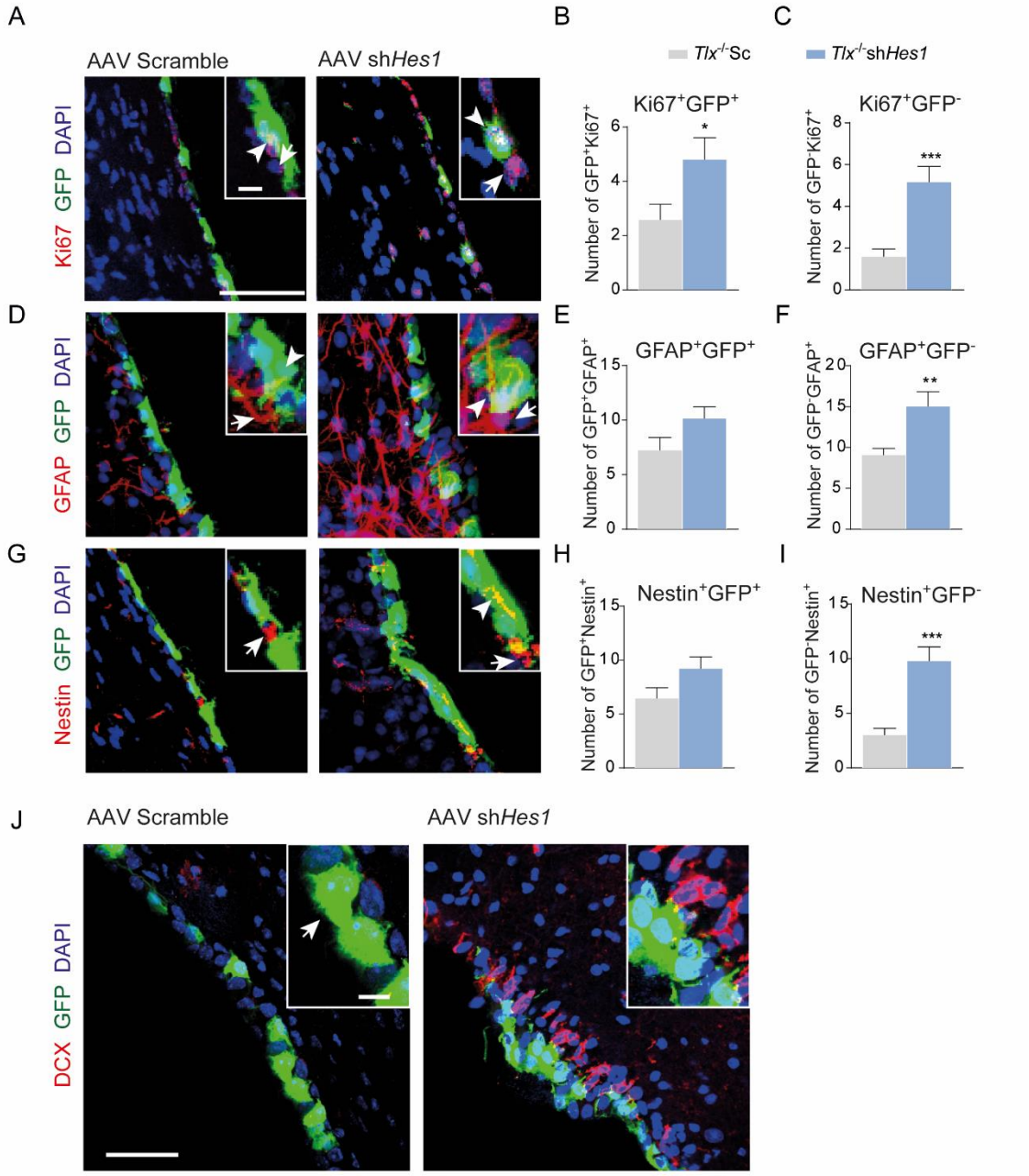

Figure 3.17 Downregulation of *Hes1* in *Tlx*$^{-/-}$ mice promotes differential proliferation and lineage progression in the apical/basal regions of the SVZ. (A, D, G, J) Representative confocal microphotographs of coronal section of *Tlx*$^{-/-}$ SVZ analysed 14 days after intraventricular injection of AAV Sc and AAV sh*Hes1* particles and immunostained against Ki67 (A), GFAP (D), Nestin (G) and DCX (J). (B, E, H) Quantification of double immunopositive cells for GFP (GFP^{+}) and Ki67 (B), GFAP (E) and Nestin (H). (C, F, I) Quantification of GFP^{-} cells immunopositive for Ki67 (C), GFAP (F) and Nestin (I). Data is shown as mean +SEM (n≥3, *: p<0.05, ***: p<0.005). Scale bar= 50 µm (big panels) and 10 µm (in magnifications). Abbreviations: GFP = green fluorescent protein, GFAP = Glial fibrillary, DCX= Doublecortin, Sc= scramble sequence, sh= short

NOTCH-HES1 regulatory axis, which leads to impaired proliferation and neurogenesis in *Tlx*$^{-/-}$ mice.

Chapter 4. Discussion

4.1 Extrinsic regulation of NSC quiescence

4.1.1 $GABA_AR$ activation promotes cell cycle activation of NSCs

In the first part of this thesis I studied the mechanisms by which GABA in the SVZ regulates adult NSC activation. My results show that, by using diazepam *in vivo,* activation of $GABA_AR$ promotes cell cycle entry in the adult SVZ. I also found that a portion of these cells that enter cell cycle after $GABA_AR$ activation remain cycling in the SEZ for up to one week, which suggests that diazepam activates slowly proliferating cells. Furthermore, by using a mouse model to genetically tag qNSC and pNSCs, I could identify that activation of cell cycle affected activation of both NSC pools but not the cell cycle speed. Since in this animal model, also in the absence of doxycycline part of the GFAP-GFP-tagged NSCs are quiescent, it is plausible that the observed increase in cell cycle activation in pNSCs reflects the contaminating qNSCs present in this population.

My differential analysis of G^+P^+ apical and G^+P^- basal NSCs showed that diazepam increased the proliferation especially in the latter, suggesting a differential regulation between the two groups of NSCs. This increase in cell cycle activation is consistent with previous observations in the neonatal niche (Cesetti et al., 2011), however, while in the neonatal brain a single injection of diazepam led to striking increase in NSC proliferation, in the adult, diazepam significantly affects proliferation only of the G^+P^- basal NSCs. Diazepam is a positive allosteric modulator that binds to the interface of α-γ subunits in $GABA_ARs$ (Richter et al., 2012). Both $GABA_ARs$ subunits are present on NSCs, besides, diazepam mediated activation of $GABA_ARs$ in NSCs has already been tested *in vivo* (Cesetti et al., 2011), confirming its utility to study GABAergic regulation of NSCs. Therefore, since diazepam, being an allosteric modulator, cannot by itself activate $GABA_ARs$, responsiveness to diazepam by NSCs reflects an effect directly proportional to endogenous GABA, representing a physiological way to measure the effects of GABA. The effect of $GABA_AR$ activation has also been investigated in the embryonic brain, where GABA promotes cell cycle activation in the VZ, the region where RG cells are found, while it inhibits proliferation

in the embryonic SVZ, suggesting that this inhibitory effect is mostly affecting intermediate progenitors (Haydar et al., 2000). Other studies suggest instead that GABA inhibits NSC proliferation (Fernando et al., 2011; Liu et al., 2005). Interestingly, in these studies the $GABA_AR$ agonist muscimol use the antagonist bicuculline have been used to modulate *in vivo* $GABA_AR$ activation in NSCs. Since, in physiological conditions, $GABA_AR$ activation depends on how much GABA is released in the niche, and given the difficulty of measuring the amount of GABA to which NSCs are exposed, the external tonic activation of $GABA_ARs$ could cause a misreading of the physiological effects that normal GABA levels exert in NSC regulation. In fact, $Prominin1^+$ precursors in the neonatal SVZ showed striking smaller GABAergic current (30 times) compared to neuroblasts (Cesetti et al., 2011), reflecting the differences in the levels of receptor expression and possibly regulation in both cell populations. This supports the notion that a better knowledge of physiological cues is necessary to fully understand GABAergic regulation of NSCs.

4.1.2 GABA induces lineage progression from $Prominin1^+$ to $Prominin1^-$ NSCs

Although Prominin1 is known for being a marker of NSCs, previous reports found NSCs which also display a negative immunoreactivity to Prominin1 (P^-) (Codega et al., 2014). Indeed, my observations highlight how the vast majority of GFAP-GFP-labelled NSCs are P^-. The analysis of these cells has shown that all G^+P^+ cells are located in the apical region of the SVZ, while most of G^+P^- exist in the basal SVZ (unpublished observations). Moreover, by analysing the effect of diazepam separately on G^+P^+ and G^+P^- NSCs, I also observed that $GABA_AR$ activation increased proliferation mostly in the pool of G^+P^- NSCs, whereas G^+P^+ NSCs only showed a trend increase in cell number. This finding led me to formulate the hypothesis that $GABA_AR$ activation might not only induce cell proliferation but also lineage progression from G^+P^+ to G^+P^- NSCs. Investigating this theory, I found that $GABA_AR$ activation induced a loss in Prominin1 expression, leading G^+P^+ to become G^+P^- NSCs (Fig.4.1). Surprisingly, despite losing Prominin1 expression, G^+P^- NSCs did not detached from the apical side of the SVZ but maintained an apical cell surface. This is in keeping with the

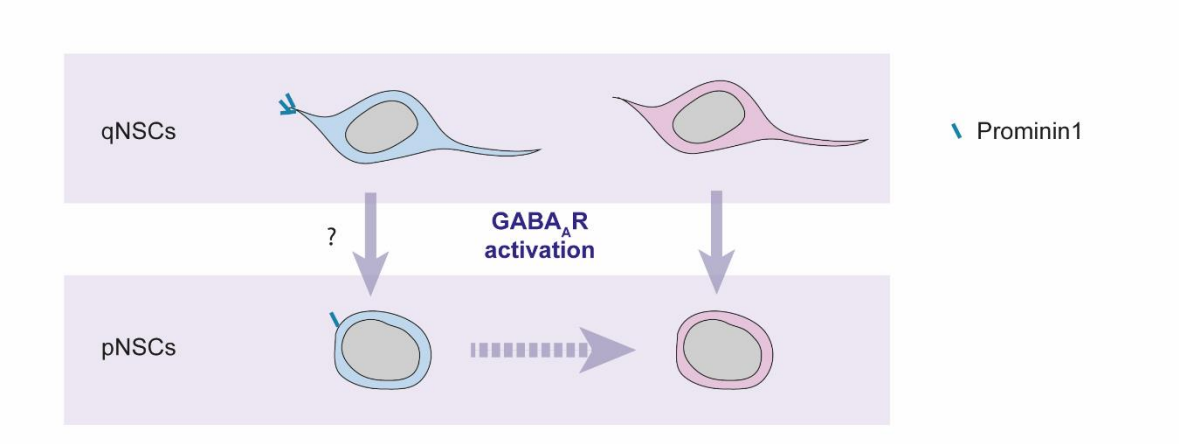

Figure 4.1 Effects of GABA$_A$R activation on P$^+$ and P$^-$ NSCs. Scheme representing the departing hypothesis and the findings on GABA regulation in G$^+$P$^+$ and G$^+$P$^-$ NSCs. GABA$_A$R activation promotes cell cycle entry (arrows), however these effects are mostly seen on G$^+$P$^-$NSCs. Nevertheless, GABA$_A$R activation also induces lineage progression (dashed arrow) from G$^+$P$^+$ into G$^+$P$^-$ pNSCs. This would explain the fact that G$^+$P$^+$ pNSCs do not display a strong increase in number. Suggesting that the increased number of G$^+$P$^-$ pNSCs is due not only to cell cycle activation but also to differentiation. Abbreviations: qNSCs = quiescent neural stem cells, pNSCs= proliferating neural stem cells, P= Prominin1

observation of a recent study where they also identified an apical population of NSC that lack Prominin1 immunoreactivity (Obernier et al., 2018). However, G$^+$P$^-$ NSCs also showed a trend increase in the basal region of the niche, and since the total number of cells in the basal region is greater (almost 100 times more) this suggests that in proportion, a small increased in the basal pool could be difficult to detect. All together, these observations suggest that the lineage progression from qNSCs to neuroblasts implicate different activation states of NSCs, which include a change in Prominin1 expression as well as a delamination from the apical to the basal side of the niche (Fig.4.1). Since TAPs lack GFAP and Prominin1 immunoreactivity (Chaker et al., 2016), a GFAP$^+$ P$^-$ NSC population could represent an intermediate state of differentiation between G$^+$P$^+$ NSCs and TAPs. Interestingly, it has been described that during development, neuroepithelial cells (NE), the primary neural stem cells, release Prominin1-containing vesicular bodies into the CSF. The main source of these vesicular bodies are the midbodies formed during symmetrical divisions with an apical-basal axis (Dubreuil et al., 2007). The authors suggest that this release of Prominin1 could be a way of losing a stem cell marker while losing apical

membrane to proceed into neurogenesis, influencing the balance between proliferation and differentiation. My results indicate that $GABA_AR$ activation reduces Prominin1 expression, which, in a similar way, could be also explained by this mechanism of symmetrical division where Prominin1 is released within the midbodies, therefore decreasing the expression of the marker and decreasing the apical surface while proceeding into lineage progression.

4.1.3 $GABA_AR$ activation involves cell swelling and promotes NSC proliferation by recruiting EGFR

EGFR participates in many aspects of NSC regulation, and several studies have shown its involvement in cell proliferation and migration (Ayuso-Sacido et al., 2010; Suh et al., 2009; Wee and Wang, 2017). For this reason, to study its contribution to the GABAergic regulation of NSC activation, I analysed *Egfr* transcript levels in G^+P^+ and G^+P^- pNSCs and qNSCs. As expected, I found higher *Egfr* transcript levels in the G^+P^- population, suggesting again that this group of NSCs represents a more proliferative and differentiated state than G^+P^+ NSCs. Consistent with previous analyses from our laboratory showing that $GABA_AR$ activation increases EGFR expression by a mechanism which does not involve regulation of transcript levels (Cesetti et al., 2011; Li et al., 2015), I found that diazepam did not increase *Egfr* transcript levels in the pool of G^+P^- qNSCs. Nevertheless, *Egfr* mRNAs was significantly increased in G^+P^+ qNSCs upon diazepam stimulation, which suggest a differential GABAergic regulation of EGFR expression in this group of cells. This differential regulation may reflect the difference in transcript levels for the EGFR between the two groups of NSCs. Since G^+P^+ have a smaller amount of *Egfr* transcript than G^+P^-, it is possible that these cells need to increase transcription to reach the minimal protein levels necessary to promote cell cycle activation. In fact in G^+P^+ EGFR protein levels did not increase upon muscimol treatment, which highlights the need of increasing the transcript levels to promote cell cycle activation. However, G^+P^- have higher levels of *Egfr* transcripts, thus, it is possible that the activation of these cells does not require an increase in transcription, since they already present

enough protein levels to translocate to the cell membrane. In fact, these cells showed an increase of EGFR protein levels upon muscimol, and they also presented higher EGFR activation, which is in keeping with my previous FACS analysis showing that G^+P^- increase proliferation upon $GABA_AR$ activation. Altogether these results confirm a differential GABAergic regulation between adult G^+P^+ and G^+P^-. Interestingly, this difference between G^+P^+ and G^+P^- is not present in postnatal mice, where both *Egfr* transcripts levels and EGFR activation showed similarly high levels in both cell groups. This indicates that in the adult, not only EGFR level decrease in general but there is also a differential regulation between apical and basal NSCs that is not present in neonatal.

Surprisingly, qNSCs showed higher transcript levels than pNSCs, which could also indicate that EGFR levels in these cells are regulated in a post-transcriptional way, as described in previous studies (Katakowski et al., 2010; Seth et al., 1999), where EGFR protein and transcript levels present sometimes inverse patterns, due to posttranscriptional regulatory mechanisms. Indeed, I found that pNSCs and qNSCs present similar number of cells displaying phosphorylated EGFR, which represents a functional reading of EGFR activation. Previous analysis in the neonatal niche, showed that activation of $GABA_AR$ in NSCs from the SVZ leads to Cl^- influx thereby promoting osmotic swelling and trafficking of EGFR to the cell membrane. In the presence of EGF, this event promotes a change in the expression of the cell cycle regulators PTEN (phosphatase and tensin homolog deleted on chromosome 10) and Cyclin D1, promoting cell cycle entry (Cesetti et al., 2011). The fact that both apical G^+P^+ and basal G^+P^- NSCs increase in size in response to muscimol, shows that in both groups of adult NSCs activation, like in the neonatal counterpart, $GABA_AR$ activation leads to Cl^- entry and cell swelling. However, as discussed above, redirection of EGFR to the cell membrane and activation of the receptor occur only in basal NSCs, as G^+P^+ , unlike the neonatal counterpart, display low EGFR expression.

4.1.4 GABA regulates NSC activation via EGFR and β1Integrin

Since the activation of $GABA_AR$ affected cell size, it was logical to think that it would also affect the cell interaction with ECM, and therefore, the molecules implicated in this interaction. The integrin family of surface receptors is involved in interaction between cells and ECM, and this interaction is responsible not only for anchoring the cell surface to ECM but also for initiating the proper response to extracellular signals (Chen et al., 2007; Flanagan et al., 2006). The vast majority of NSCs and progenitor cells express the β1Integrin subunit family of integrins (Hall et al., 2006; Pruszak et al., 2009), which highlights its importance in regulating these cells. For these reasons, I analysed the participation of β1Integrin in the GABAergic regulation of NSCs. My observations showed that transcript levels of β1Integrin were downregulated in G^+P^+ and G^+P^- qNSCs following diazepam injection. Similarly, the proportion of cells displaying β1Integrin immunoreactivity was reduced in apical and basal qNSCs. This indicated that $GABA_AR$ activation signalling cascade affects the expression of β1Integrin in qNSCs. Recently, it has been shown that in NSCs β1Integrin interacts with laminin present in a specialized ECM structure called fractone bulbs. It was also shown that this interaction keeps the NSCs anchored in the pinwheel structure (Nascimento et al., 2018). Besides, studies in the developing brain suggest that anchorage of NSCs to the VZ surface through β1Integrin may be critical for NSC maintenance (Campos et al., 2004). Interestingly, Leone et al. showed that lack of β1Integrin leads to a decrease in $Nestin^+$ precursors, suggesting a role in NSCs differentiation. Supporting this, it has been shown that neuronal differentiation is also accompanied with a decrease in α5β9 Integrin (Yoshida et al., 2003). Thus, the fact that $GABA_AR$ activation decreases β1Integrin expression in NSCs indicates a possible mechanism of detachment of NSCs from pinwheel structures, suggesting again cell cycle activation of these cells and possibly differentiation.
My combined analysis of β1Integrin and pEGFR expression showed that following $GABA_AR$ activation, basal qNSCs decrease β1Integrin expression, both at a transcript and a protein level, while increasing at the same time the activation of EGFR (Fig.4.2). A similar effect was observed in apical qNSCs with respect to β1Integrin but not to EGFR activation, which again

points out that low levels of EGFR in these cells are a limiting factor that prevent their proliferation. Analysis of pNSCs also depicted a similar response in terms of β1Integrin and pEGFR expression, albeit to a lower extent than in qNSCs. However, as discussed in chapter 4.1.1, in light of the fact that GFAP-GFP-labelled pNSCs also include a subset of qNSCs, the change of β1Integrin and pEGFR expression likely reflects the activation of this subset of qNSCs by $GABA_AR$. Previous studies have also demonstrated a negative correlation between EGFR and β1Integrin activation. Xu et al. showed that conditional deletion of *β1Integrin* expression in the murine intestine led to overexpression of EGFR protein levels and aberrant proliferation of intestinal epithelial cells. A1β1Integrin was also found to function as a negative regulator of EGFR through activation of a protein tyrosine phosphatase (Mattila et al., 2005). Interestingly, β1Integrin signalling promotes proliferation and self-renewal of neuroepithelial cells in chick (Long et al., 2016), which would suggest a positive correlation between β1Integrin expression and proliferation. In fact, several studies found that ECM adhesion through Integrins can activate EGFR in a growth factor independent manner (Cabodi et al., 2004). Consistent with these observation, Moro et al. found that in early stages of cell adhesion, Integrins are associated with EGFR in macromolecular complexes, and Integrin response promotes phosphorylation of several tyrosine residues in EGFR, leading to cell survival or actin-cytoskeletal reorganization. However, a crosstalk between β1Integrin and EGFR signalling has also been described in epithelial (Bill et al., 2004) and tumour cells (Adelsman et al., 1999; Wang et al., 1998) which points out their complex mechanism of regulation, and suggests a complementary control of proliferation between the two receptors. In fact, in embryonic stem cells (ESCs), interaction of β1Integrin with laminin α inhibits differentiation, keeping cells in a low proliferative early progenitor state (Domogatskaya et al., 2008; Rodin et al., 2010). Consistent with this effect of β1Integrin-laminin interaction on the maintenance of qNSCs, in the adult SVZ, several ECM-binding receptors, including α6β1Integrins, are downregulated upon activation of NSCs (Codega et al., 2014). In addition, blocking of α6β1Integrins *in vivo* affects cell adhesion and promotes proliferation in the adult SVZ (Shen et al., 2008). This inverse correlation between the integrin signalling and EGFR and activation is in keeping with my observation that *β1Integrin*

is downregulated following $GABA_AR$ activation whereas EGFR activation increases, indicating again that GABA promotes NSCs activation in the adult SVZ (Fig.4.2). My results also indicated that cell cycle activation in these cells is dependent on EGFR, since selective blocking of the receptor kinase led to a reduction of cell cycle activation. However, it is unlikely that the activation of EGFR receptor is ligand independent, as it was previously shown that the presence of exogenous EGF is necessary to obtain increased clone formation upon $GABA_AR$ activation (Cesetti et al., 2011). Altogether, these findings demonstrate that GABA exerts a regulatory effect on NSCs in the adult niche, inciting activation of qNSCs through an EGFR dependant mechanism that involves the signalling mechanisms of β1Integrin with ECM.

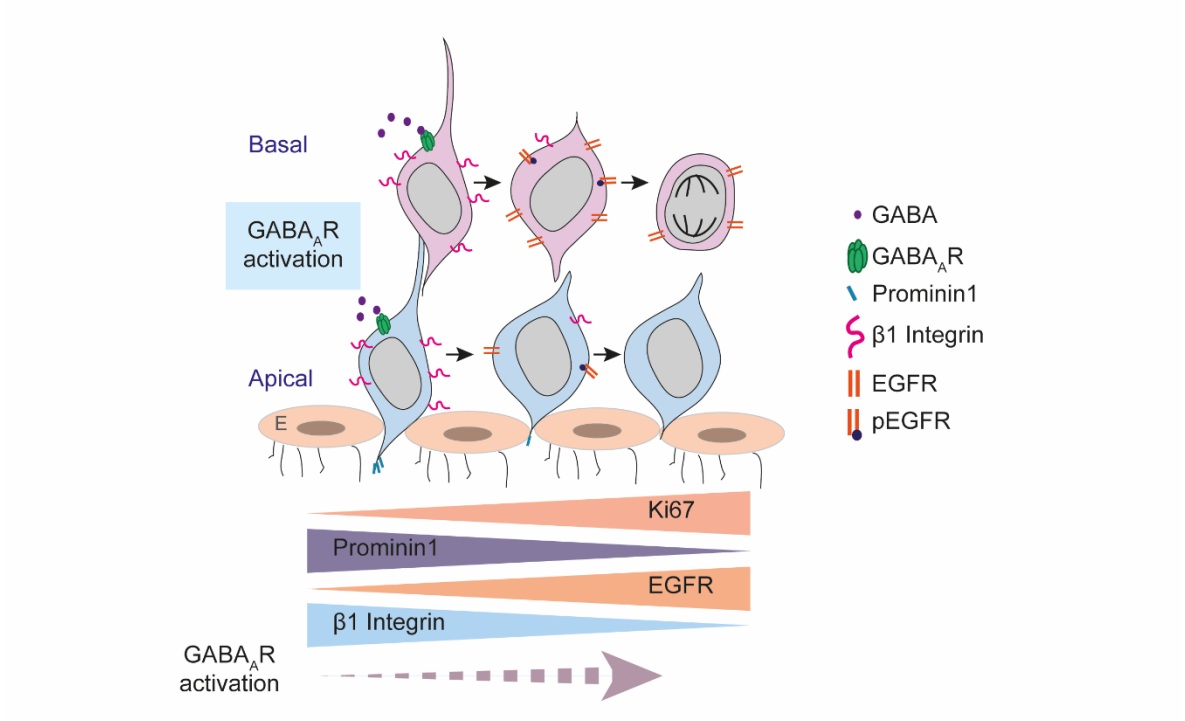

Figure 4.2 Summary of effects of $GABA_AR$ activation found in NSCs. Scheme representing a summary of the findings on GABA regulation in NSCs. $GABA_AR$ activation promotes cell cycle entry in NSCs, given by the increase in Ki67. It also promotes a reduction in Prominin1 expression. $GABA_AR$ activation also promotes proliferation of basal NSCs. The mechanism of regulation implicates cell-swelling, phosphorylation of EGFR and cell detachment from the ECM, by downregulating β1Intengrin expression. Abbreviations: GABA= gamma aminobutyric acid, $GABA_AR$= GABA A Receptor, EGFR= epidermal growth factor receptor, pEGFR= phosphorylated EGFR, E= ependymal cell.

4.2 Intrinsic regulation of NSCs

4.2.1 NOTCH signalling is up-regulated in *Tlx*$^{-/-}$ SVZ

Previous reports have already shown the importance of TLX during development and for stem cell activation (Monaghan et al., 1995; Obernier et al., 2011; Wang et al., 2013). In fact, mice lacking *Tlx* expression show a phenotype with enlarged ventricles and thinner cortex and OB, which already suggested an absence of neurogenesis. However, little is known about the mechanism by which TLX regulates neurogenesis.

Previous experiments in our lab demonstrated that in NSCs cultures, TLX binds the promoter of *Hes1* and *Hes5* genes, inhibiting their transcription (Shi, 2015). This inhibition of genes involved in NSCs maintenance causes an increase in expression of the pro-neural gene *Mash1*, facilitating the differentiation and lineage progression. These results showed that mice lacking *Tlx* expression present an up-regulation of *Hes1* transcripts and other genes related in NOTCH signalling. Following up on these observations, I found that in fact, NOTCH1 activated domain (NICD) is up-regulated in the apical region of the SVZ in *Tlx*$^{-/-}$ mice, specifically in a population of GFAP^{+}P^{-}E^{-} cells. This upregulation is accompanied by an increased levels of HES1 protein also in the apical region, confirming that NOTCH signalling is affected in the mutant niche and this effect is stronger in the apical cells. Similarly, an apical-basal NOTCH gradient was also found in the neuroepithelium of the zebrafish retina, showing higher levels of NOTCH in the apical side (Del Bene et al., 2008). In fact, consistent with my findings in the *Tlx* mutant mice and in the zebrafish retina, it was recently observed in our lab the presence of an apical-basal HES1 gradient also in the SVZ of WT mice, albeit with overall lower HES1 levels than in the SVZ of *Tlx*$^{-/-}$ mice. The fact that the mutant SVZ shows increased levels of HES1 could be the cause of impaired neurogenesis. Consistent with this hypothesis, it has been shown that *Hes1* displays an oscillatory expression that allows proliferation and lineage progression, however, persistent expression of the gene leads to cell cycle exit (Andersen et al., 2014; Baek et al., 2006; Imayoshi et al., 2013). Indeed, the levels of pro-neural genes are proposed to be one of the regulating factors of NSC status of quiescence, activation or differentiation. And these genes are under the

control of NOTCH signalling target *Hes* genes. Also, given that NOTCH signalling is necessary for NSC maintenance (Imayoshi et al., 2010), my results indicate that the aberrant elevated Notch-Hes1 signalling in the apical region of mutant SVZ prevents NSCs from activating, thereby inhibiting adult neurogenesis.

4.2.2 *Hes1* downregulation in *Tlx*$^{-/-}$ SVZ leads to cell cycle activation and lineage progression

NSCs in mice lacking *Tlx* expression present impaired cell cycle activation, consequently, neurogenesis is virtually absent in adult mice (Obernier et al., 2011). Previously I discussed that impairment in neurogenesis in *Tlx*$^{-/-}$ mice is likely due to elevated HES1 levels. Therefore, I tried to rescue proliferation and lineage progression by downregulating Hes1 levels using a viral transduction of shHes1 *in vivo*. My analysis showed that this downregulation promoted cell cycle activation, and this was accompanied by an increase in GFAP^{+} and Nestin^{+} precursors, and more importantly, *Hes1* downregulation restored neurogenesis, given by the increase in DCX^{+} neuroblasts. Interestingly, this effect was mostly found in the non-transduced cells, indicating that *Hes1* downregulation in apical cells, by a non-cell-autonomous mechanism, modified cell cycle activation and lineage progression in the basal pool of cells. Since counteracting NOTCH signalling elicited a similar effect on the proliferation of basal cells, this cell-cell communication is likely to be mediated by interaction of NOTCH receptors with their ligands. Indeed, I also observed that downregulation of *Hes1* causes a decrease in NICD protein levels, pointing out a regulating crosstalk between HES1 and NICD (Fig.4.3). A similar example of cell-cell communication was found in the work of Aguirre and colleagues, where overexpression of EGFR in TAPs led to decreased NOTCH signalling in NSCs via a cell-cell communication mechanism (Aguirre et al., 2010). Also, a similar mechanism of cell-cell regulation was described in the adult zebrafish (Chapouton et al., 2010). Here, the authors suggested a Notch lateral-inhibition mechanism regulating the balance between NSCs and proliferating progenitors after

observing that proliferative progenitors were located close to high-*Notch*-expressing RG cells and that after blocking NOTCH signalling, proliferation increased in the first rather than in the latter, suggesting a NOTCH regulating mechanism by which progenitors, expressing the Delta ligand, induce quiescence in neighbour NSCs by activation of NOTCH. Once progenitors migrate to differentiate, NOTCH activation decreases in RG cells, allowing proliferation of these cells. These observations highlight the dynamic NOTCH interaction between apical and basal precursors which is very important for neurogenesis not only during development (Nelson et al., 2013) but also in the adult niche. Altogether, these data represent a new found role of TLX in regulation of NSC self-maintenance and differentiation through HES1-NOTCH signalling, where TLX inhibition of *Hes1* in apical cells counteracts quiescence and NOTCH activation (Fig.4.3). This decrease in NOTCH activation in apical cells interferes with the Notch-mediated lateral inhibition of basal progenitors, increasing their proliferation.

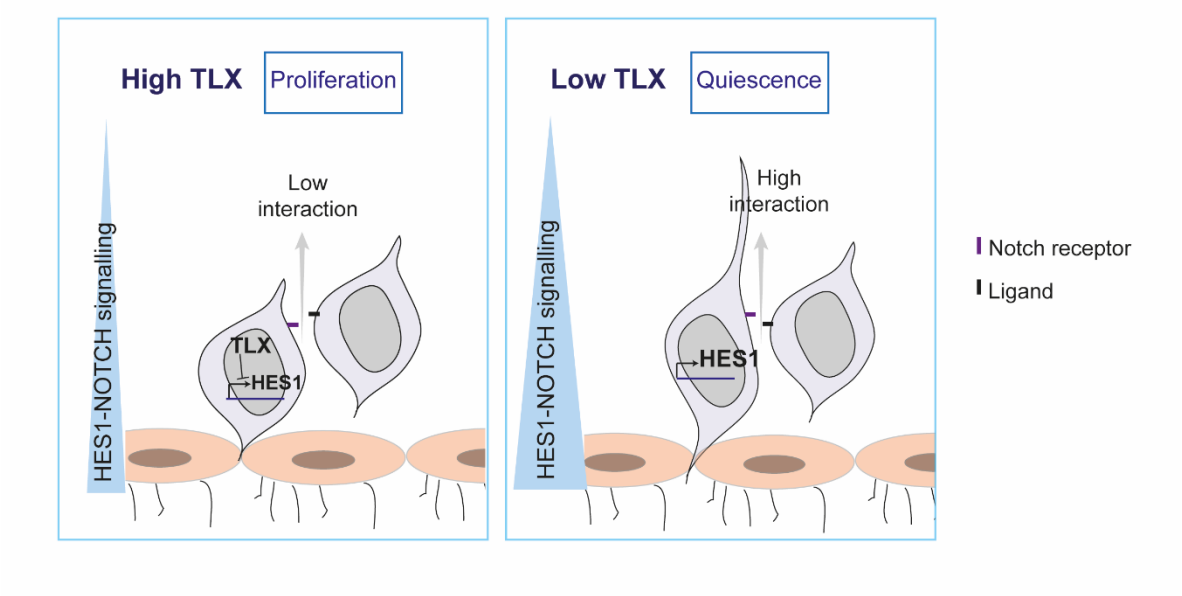

Figure 4.3 Summary of effects seen in TLX-NOTCH signalling in NSCs. Scheme representing a summary of the findings on TLX regulation in NSCs. When TLX is presented in high levels, its interaction with *Hes1* promoter blocks *Hes1* expression, which turns out in a decrease of NOTCH activation, promoting cell proliferation and decreasing the lateral inhibition from basal cells. When cells display low levels of TLX, HES1 increases in an apical-basal gradient, keeping the cells in a quiescent state and promoting lateral inhibition from the basal cells.

4.3 Final notes about extrinsic and intrinsic regulation of NSCs

Understanding the mechanisms by which NSCs are regulated can be an important tool for future progress in stem cell therapy. Also, given the similarities between NSCs and cancer stem cells in brain tumours, a better understanding of this regulation can shed light into new targets for future treatments.

In this thesis, I have investigated the regulation of adult NSCs by extrinsic and intrinsic factors, focusing on GABA regulation and TLX-NOTCH signalling respectively. Both analyses have highlighted the presence of two pools of NSCs, i.e. so called apical and basal NSCs., which differ in terms of cytoarchitecture and gene expression. Although both groups of NSCs respond to intrinsic and extrinsic clues, my analyses have highlighted differences in the responses, which depend on the differential expression of the molecules EGFR and HES1 between the two NSC groups. Whereas the expression of first increases along the apical-basal axis, levels of HES1 protein decrease. Since both molecules have opposite effects on NOTCH signalling, it is tempting to speculate that both factors affect NSC activation by modulation of NOTCH signalling along the apical-basal axis of the niche. With respect of the effect of the extrinsic modulator GABA, my results showed that $GABA_AR$-dependent activation of qNSCs involves cell swelling, EGFR activation and downregulation of β1Integrins. At the same time, I showed that TLX by downregulating *Hes1* expression and NOTCH signalling in apical NSCs, allows the expression of pro-neural genes, leading to lineage progression and neurogenesis. Interestingly, I also observed that NOTCH-mediated lateral inhibition in the apical niche affects proliferation of basal progenitors. Indeed, consisting with my observation, it has been shown before that the cell adhesion receptor β1Integrin co-localizes with NOTCH1 in the developing VZ, and the interaction of both molecules is necessary for NSC maintenance (Campos et al., 2006). Interestingly, in our laboratory it was recently found that another cell-cell adhesion molecule, LeX-SSEA, is associated with NSCs quiescence, and disruption of its interactions promotes cell cycle activation (Luque-Molina et al., 2017). Since LeX-SSEA1 promotes notch signalling in neural precursors (Yagi et al., 2012) it is possible that the antigen affect NSC quiescence by

promoting NOTCH signalling. Consistent with this premise that NOTCH signalling and interaction with the ECM are key points in the regulation of NSC proliferation, it was found that endothelial cell contact with NSCs, which is mostly mediated via Integrin interaction, promotes cell-cell interaction and activation of NOTCH and HES1 which stimulates self-renewal and inhibits proliferation of NSCs (Shen et al., 2004). Taken together, my results and the data of the literature suggest that the effect of GABA and TLX on NSC activation may impinge in both cases on the regulation of NOTCH signalling across the niche, indicating that NOTCH signalling may represent a convergence pathway for the integration of extrinsic and intrinsic cues that keep the balance between NSC maintenance and adult neurogenesis.

References:

Ables, J.L., Breunig, J.J., Eisch, A.J., Rakic, P., 2011. Not(ch) just development: Notch signalling in the adult brain. Nat. Rev. Neurosci. 12, 269–283. https://doi.org/10.1038/nrn3024

Adelsman, M.A., McCarthy, J.B., Shimizu, Y., 1999. Stimulation of β1-Integrin Function by Epidermal Growth Factor and Heregulin-β Has Distinct Requirements for erbB2 but a Similar Dependence on Phosphoinositide 3-OH Kinase. Mol. Biol. Cell 10, 2861–2878. https://doi.org/10.1091/mbc.10.9.2861

Aguirre, A, Rubio, M.E., Gallo, V., 2010. Notch and EGFR pathway interaction regulates neural stem cell number and self-renewal. Nature 467, 323–327. https://doi.org/10.1038/nature09347

Aguirre, Adan, Rubio, M.E., Gallo, V., 2010. Notch and EGFR pathway interaction regulates neural stem cell number and self-renewal. Nature 467, 323–327. https://doi.org/10.1038/nature09347

Altman, J., 1962. Some fiber projections to the superior colliculus in the cat. J. Comp. Neurol. 119, 77–95. https://doi.org/10.1002/cne.901190107

Altman, J., Das, G.D., 1965. Autoradiographic and histological evidence of postnatal hippocampal neurogenesis in rats. J. Comp. Neurol. 124, 319–335. https://doi.org/10.1002/cne.901240303

Alvarez-Buylla, A., García-Verdugo, J.M., Mateo, A.S., Merchant-Larios, H., 1998. Primary neural precursors and intermitotic nuclear migration in the ventricular zone of adult canaries. J. Neurosci. 18, 1020–37.

Andersen, J., Urbán, N., Achimastou, A., Ito, A., Simic, M., Ullom, K., Martynoga, B., Lebel, M., Göritz, C., Frisén, J., Nakafuku, M., Guillemot, F., 2014. A Transcriptional Mechanism Integrating Inputs from Extracellular Signals to Activate Hippocampal Stem Cells. Neuron 83, 1085–1097. https://doi.org/10.1016/J.NEURON.2014.08.004

Anderson, D.J., 2001. Stem cells and pattern formation in the nervous system: the possible versus the actual. Neuron 30, 19–35.

Angevine, J.B., Bodian, D., Coulombre, A.J., Edds, M. V., Hamburger, V., Jacobson, M., Lyser, K.M., Prestige, M.C., Sidman, R.L., Varon, S., Weiss, P.A., 1970. Embryonic vertebrate central nervous system: Revised terminology. Anat. Rec. 166, 257–261. https://doi.org/10.1002/ar.1091660214

Aprea, J., Calegari, F., 2012. Bioelectric state and cell cycle control of mammalian neural stem cells. Stem Cells Int. https://doi.org/10.1155/2012/816049

Ayuso-Sacido, A., Moliterno, J.A., Kratovac, S., Kapoor, G.S., O'Rourke, D.M., Holland, E.C., Garci'a-Verdugo, J.M., Roy, N.S., Boockvar, J.A., 2010. Activated EGFR signaling increases proliferation, survival,and migration and blocks neuronal differentiation in post-natal neural stem cells. J. Neurooncol. 97, 323–337. https://doi.org/10.1007/s11060-009-0035-x

Baek, J.H., Hatakeyama, J., Sakamoto, S., Ohtsuka, T., Kageyama, R., 2006. Persistent and high levels of Hes1 expression regulate boundary formation in the developing central nervous system. Development 133, 2467–2476. https://doi.org/10.1242/dev.02403

Banasr, M., Hery, M., Printemps, R., Daszuta, A., 2004. Serotonin-Induced Increases in Adult Cell Proliferation and Neurogenesis are Mediated Through Different and Common 5-HT Receptor Subtypes in the Dentate Gyrus and the Subventricular Zone.

Neuropsychopharmacology 29, 450–460. https://doi.org/10.1038/sj.npp.1300320
Berezovska, O., Xia, M.Q., Hyman, B.T., 1998. Notch is expressed in adult brain, is coexpressed with presenilin-1, and is altered in Alzheimer disease. J. Neuropathol. Exp. Neurol. 57, 738–45.
Bill, H.M., Knudsen, B., Moores, S.L., Muthuswamy, S.K., Rao, V.R., Brugge, J.S., Miranti, C.K., 2004. Epidermal Growth Factor Receptor-Dependent Regulation of Integrin-Mediated Signaling and Cell Cycle Entry in Epithelial Cells. Mol. Cell. Biol. 24, 8586–8599. https://doi.org/10.1128/MCB.24.19.8586-8599.2004
Birger V. Dieriks, Henry J. Waldvogel, Hector J. Monzo, Richard L.M. Faull, M.A.C., 2013. GABAAreceptor characterization and subunit localization in the human sub ventricular zone. J. Chem. Neuroanat. 52, 58–68. https://doi.org/10.1016/j.jchemneu.2013.06.001
Brezun, J.M., Daszuta, A., 1999. Depletion in serotonin decreases neurogenesis in the dentate gyrus and the subventricular zone of adult rats. Neuroscience 89, 999–1002.
Burd, G.D., Nottebohm, F., 1985. Ultrastructural characterization of synaptic terminals formed on newly generated neurons in a song control nucleus of the adult canary forebrain. J. Comp. Neurol. 240, 143–152. https://doi.org/10.1002/cne.902400204
Cabodi, S., Moro, L., Bergatto, E., Erba, E.B., Stefano, P. Di, Turco, E., Tarone, G., Defilippi, P., 2004. Integrin regulation of epidermal growth factor (EGF) receptor and of EGF-dependent responses 32, 438–442.
Cameron, H.A., Woolley, C.S., McEwen, B.S., Gould, E., 1993. Differentiation of newly born neurons and glia in the dentate gyrus of the adult rat. Neuroscience 56, 337–44.
Campos, L.S., Decker, L., Taylor, V., Skarnes, W., 2006. Notch, epidermal growth factor receptor, and β1-integrin pathways are coordinated in neural stem cells. J. Biol. Chem. 281, 5300–5309. https://doi.org/10.1074/jbc.M511886200
Campos, L.S., Leone, D.P., Relvas, J.B., Brakebusch, C., Fassler, R., Suter, U., ffrench-Constant, C., 2004. 1 integrins activate a MAPK signalling pathway in neural stem cellsthat contributes to their maintenance. Development 131, 3433–3444. https://doi.org/10.1242/dev.01199
Carrillo-García, C., Prochnow, S., Simeonova, I.K., Strelau, J., Hölzl-Wenig, G., Mandl, C., Unsicker, K., von Bohlen Und Halbach, O., Ciccolini, F., 2014. Growth/differentiation factor 15 promotes EGFR signalling, and regulates proliferation and migration in the hippocampus of neonatal and young adult mice. Development 141, 773–83. https://doi.org/10.1242/dev.096131
Cesetti, T., Fila, T., Obernier, K., Bengtson, C.P., Li, Y., Mandl, C., Hölzl-Wenig, G., Ciccolini, F., 2011a. GABA A receptor signaling induces osmotic swelling and cell cycle activation of neonatal prominin + precursors. Stem Cells 29, 307–319. https://doi.org/10.1002/stem.573
Cesetti, T., Fila, T., Obernier, K., Bengtson, C.P., Li, Y., Mandl, C., Hölzl-Wenig, G., Ciccolini, F., 2011b. GABA A receptor signaling induces osmotic swelling and cell cycle activation of neonatal prominin + precursors. Stem Cells 29, 307–319. https://doi.org/10.1002/stem.573
Chaker, Z., Codega, P., Doetsch, F., 2016. A mosaic world: puzzles revealed by adult neural stem cell heterogeneity. Wiley Interdiscip. Rev. Dev. Biol. https://doi.org/10.1002/wdev.248
Chambers, C.B., Peng, Y., Nguyen, H., Gaiano, N., Fishell, G., Nye, J.S., 2001. Spatiotemporal selectivity of response to Notch1 signals in mammalian forebrain

precursors. Development 128, 689–702.
Chapouton, P., Skupien, P., Hesl, B., Coolen, M., Moore, J.C., Madelaine, R., Kremmer, E., Faus-Kessler, T., Blader, P., Lawson, N.D., Bally-Cuif, L., 2010. Notch activity levels control the balance between quiescence and recruitment of adult neural stem cells. J. Neurosci. 30, 7961–74. https://doi.org/10.1523/JNEUROSCI.6170-09.2010
Chen, S.S., Fitzgerald, W., Zimmerberg, J., Kleinman, H.K., Margolis, L., 2007. Cell-Cell and Cell-Extracellular Matrix Interactions Regulate Embryonic Stem Cell Differentiation. Stem Cells 25, 553–561. https://doi.org/10.1634/stemcells.2006-0419
Codega, P., Silva-Vargas, V., Paul, A., Maldonado-Soto, A.R., DeLeo, A.M., Pastrana, E., Doetsch, F., 2014. Prospective Identification and Purification of Quiescent Adult Neural Stem Cells from Their In Vivo Niche. Neuron 82, 545–559. https://doi.org/10.1016/j.neuron.2014.02.039
Del Bene, F., Wehman, A.M., Link, B.A., Baier, H., 2008. Regulation of Neurogenesis by Interkinetic Nuclear Migration through an Apical-Basal Notch Gradient. Cell 134, 1055–1065. https://doi.org/10.1016/j.cell.2008.07.017
Doetsch, F., Caillé, I., Lim, D.A., García-Verdugo, J.M., Alvarez-Buylla, A., 1999. Subventricular zone astrocytes are neural stem cells in the adult mammalian brain. Cell 97, 703–16.
Domogatskaya, A., Rodin, S., Boutaud, A., Tryggvason, K., 2008. Laminin-511 but Not -332, -111, or -411 Enables Mouse Embryonic Stem Cell Self-Renewal In Vitro. Stem Cells 26, 2800–2809. https://doi.org/10.1634/stemcells.2007-0389
Dubreuil, V., Marzesco, A.-M., Corbeil, D., Huttner, W.B., Wilsch-Bräuninger, M., 2007. Midbody and primary cilium of neural progenitors release extracellular membrane particles enriched in the stem cell marker prominin-1. J. Cell Biol. 176, 483–95. https://doi.org/10.1083/jcb.200608137
Elmi, M., Matsumoto, Y., Zeng, Z. jun, Lakshminarasimhan, P., Yang, W., Uemura, A., Nishikawa, S. ichi, Moshiri, A., Tajima, N., Ågren, H., Funa, K., 2010. TLX activates MASH1 for induction of neuronal lineage commitment of adult hippocampal neuroprogenitors. Mol. Cell. Neurosci. 45, 121–131. https://doi.org/10.1016/j.mcn.2010.06.003
Encinas, J.M., Michurina, T.V., Peunova, N., Park, J.-H., Tordo, J., Peterson, D.A., Fishell, G., Koulakov, A., Enikolopov, G., 2011. Division-Coupled Astrocytic Differentiation and Age-Related Depletion of Neural Stem Cells in the Adult Hippocampus. Cell Stem Cell 8, 566–579. https://doi.org/10.1016/j.stem.2011.03.010
Eriksson, P.S., Perfilieva, E., Björk-Eriksson, T., Alborn, A.-M., Nordborg, C., Peterson, D.A., Gage, F.H., 1998. Neurogenesis in the adult human hippocampus. Nat. Med. 4, 1313–1317. https://doi.org/10.1038/3305
Fernando, R.N., Eleuteri, B., Abdelhady, S., Nussenzweig, A., Andäng, M., Ernfors, P., 2011. Cell cycle restriction by histone H2AX limits proliferation of adult neural stem cells. Proc. Natl. Acad. Sci. U. S. A. 108, 5837–42. https://doi.org/10.1073/pnas.1014993108
Gage, F.H., 2000. Mammalian neural stem cells. Science 287, 1433–8.
Ge, S., Pradhan, D.A., Ming, G., Song, H., 2006. GABA sets the tempo for activity-dependent adult neurogenesis 30, 1–8. https://doi.org/10.1016/j.tins.2006.11.001
Götz, M., Huttner, W.B., 2005. The cell biology of neurogenesis. Nat. Rev. Mol. Cell Biol. 6, 777–88. https://doi.org/10.1038/nrm1739
Hall, P.E., Lathia, J.D., Miller, N.G.A., Caldwell, M.A., Ffrench-Constant, C., 2006.

Integrins Are Markers of Human Neural Stem Cells. Stem Cells 24, 2078–2084. https://doi.org/10.1634/stemcells.2005-0595

Hatakeyama, J., 2004. Hes genes regulate size, shape and histogenesis of the nervous system by control of the timing of neural stem cell differentiation. Development 131, 5539–5550. https://doi.org/10.1242/dev.01436

Haydar, Tarik F, Wang, F., Schwartz, M.L., Rakic, P., 2000. Differential Modulation of Proliferation in the Neocortical Ventricular and Subventricular Zones. J. Neurosci. 20, 5764–5774. https://doi.org/https://doi.org/10.1523/JNEUROSCI.20-15-05764.2000

Haydar, Tarik F., Wang, F., Schwartz, M.L., Rakic, P., 2000. Differential Modulation of Proliferation in the Neocortical Ventricular and Subventricular Zones. J. Neurosci. 20, 5764–5774. https://doi.org/10.1523/JNEUROSCI.20-15-05764.2000

Huang, X., Liu, J., Ketova, T., Fleming, J.T., Grover, V.K., Cooper, M.K., Litingtung, Y., Chiang, C., 2010. Transventricular delivery of Sonic hedgehog is essential to cerebellar ventricular zone development. Proc. Natl. Acad. Sci. 107, 8422–8427. https://doi.org/10.1073/pnas.0911838107

Imayoshi, I., Isomura, A., Harima, Y., Kawaguchi, K., Kori, H., Miyachi, H., Fujiwara, T., Ishidate, F., Kageyama, R., 2013. Oscillatory Control of Factors Determining Multipotency and Fate in Mouse Neural Progenitors. Science (80-.). 342, 1203–1208. https://doi.org/10.1126/science.1242366

Imayoshi, I., Sakamoto, M., Yamaguchi, M., Mori, K., Kageyama, R., 2010. Essential Roles of Notch Signaling in Maintenance of Neural Stem Cells in Developing and Adult Brains. J. Neurosci. 30, 3489–3498. https://doi.org/10.1523/JNEUROSCI.4987-09.2010

Ishibashi, M., Moriyoshi, K., Sasai, Y., Shiota, K., Nakanishi, S., Kageyama, R., 1994. Persistent expression of helix-loop-helix factor HES-1 prevents mammalian neural differentiation in the central nervous system. EMBO J. 13, 1799–805.

Iso, T., Kedes, L., Hamamori, Y., 2003. HES and HERP families: Multiple effectors of the notch signaling pathway. J. Cell. Physiol. 194, 237–255. https://doi.org/10.1002/jcp.10208

Kageyama, R., Ohtsuka, T., Shimojo, H., Imayoshi, I., 2009. Dynamic regulation of Notch signaling in neural progenitor cells. Curr. Opin. Cell Biol. 21, 733–740. https://doi.org/10.1016/j.ceb.2009.08.009

Kanda, T., Sullivan, K.F., Wahl, G.M., 1998. Histone-GFP fusion protein enables sensitive analysis of chromosome dynamics in living mammalian cells. Curr. Biol. 8, 377–85.

Katakowski, M., Zheng, X., Jiang, F., Rogers, T., Szalad, A., Chopp, M., 2010. MiR-146b-5p Suppresses EGFR Expression and Reduces *In Vitro* Migration and Invasion of Glioma. Cancer Invest. 28, 1024–1030. https://doi.org/10.3109/07357907.2010.512596

Khatri, P., Obernier, K., Simeonova, I.K., Hellwig, A., Hölzl-Wenig, G., Mandl, C., Scholl, C., Wölfl, S., Winkler, J., Gaspar, J. a, Sachinidis, A., Ciccolini, F., 2014a. Proliferation and cilia dynamics in neural stem cells prospectively isolated from the SEZ. Sci. Rep. 4, 3803. https://doi.org/10.1038/srep03803

Khatri, P., Obernier, K., Simeonova, I.K., Hellwig, A., Hölzl-Wenig, G., Mandl, C., Scholl, C., Wölfl, S., Winkler, J., Gaspar, J.A., Sachinidis, A., Ciccolini, F., 2014b. Proliferation and cilia dynamics in neural stem cells prospectively isolated from the SEZ. Sci. Rep. 4, 3803. https://doi.org/10.1038/srep03803

Kim, Y., Wang, W.-Z., Comte, I., Pastrana, E., Tran, P.B., Brown, J., Miller, R.J., Doetsch,

F., Molnár, Z., Szele, F.G., 2010. Dopamine stimulation of postnatal murine subventricular zone neurogenesis via the D3 receptor. J. Neurochem. 114, 750–760. https://doi.org/10.1111/j.1471-4159.2010.06799.x

Kriegstein, A., 2009. The Glial Nature of Embryonic and Adult Neural Stem Cells. Annu. Rev. Neurosci. 149–184. https://doi.org/10.1146/annurev.neuro.051508.135600

Kumar, R.A., Leach, S., Bonaguro, R., Chen, J., Yokom, D.W., Abrahams, B.S., Seaver, L., Schwartz, C.E., Dobyns, W., Brooks-Wilson, A., Simpson, E.M., 2007. Mutation and evolutionary analyses identify NR2E1-candidate-regulatory mutations in humans with severe cortical malformations. Genes, Brain Behav. 6, 503–516. https://doi.org/10.1111/j.1601-183X.2006.00277.x

Lehtinen, M.K., Walsh, C.A., 2011. Neurogenesis at the Brain–Cerebrospinal Fluid Interface. Annu. Rev. Cell Dev. Biol. 27, 653–679. https://doi.org/10.1146/annurev-cellbio-092910-154026

Leone, D.P., Relvas, J.B., Campos, L.S., Hemmi, S., Brakebusch, C., Fässler, R., Ffrench-Constant, C., Suter, U., 2005. Regulation of neural progenitor proliferation and survival by beta1 integrins. J. Cell Sci. 118, 2589–99. https://doi.org/10.1242/jcs.02396

Leventhal, C., Rafii, S., Rafii, D., Shahar, A., Goldman, S.A., 1999. Endothelial Trophic Support of Neuronal Production and Recruitment from the Adult Mammalian Subependyma. Mol. Cell. Neurosci. 13, 450–464. https://doi.org/10.1006/mcne.1999.0762

Li, S., Sun, G., Murai, K., Ye, P., Shi, Y., 2012. Characterization of TLX Expression in Neural Stem Cells and Progenitor Cells in Adult Brains. PLoS One 7, e43324. https://doi.org/10.1371/journal.pone.0043324

Li, Y., Schmidt-Edelkraut, U., Poetz, F., Oliva, I., Mandl, C., Hölzl-Wenig, G., Schönig, K., Bartsch, D., Ciccolini, F., 2015a. γ-aminobutyric A receptor (GABAAR) regulates aquaporin 4 expression in the subependymal zone: Relevance to neural precursors and water exchange. J. Biol. Chem. 290, 4343–4355. https://doi.org/10.1074/jbc.M114.618686

Li, Y., Schmidt-Edelkraut, U., Poetz, F., Oliva, I., Mandl, C., Hölzl-Wenig, G., Schönig, K., Bartsch, D., Ciccolini, F., 2015b. ??-aminobutyric A receptor (GABAAR) regulates aquaporin 4 expression in the subependymal zone: Relevance to neural precursors and water exchange. J. Biol. Chem. 290, 4343–4355. https://doi.org/10.1074/jbc.M114.618686

Lim, D.A., Alvarez-Buylla, A., 2016. The adult ventricular–subventricular zone (V-SVZ) and olfactory bulb (OB) neurogenesis. Cold Spring Harb. Perspect. Biol. 8. https://doi.org/10.1101/cshperspect.a018820

Lim, D.A., Tramontin, A.D., Trevejo, J.M., Herrera, D.G., García-Verdugo, J.M., Alvarez-Buylla, A., 2000. Noggin antagonizes BMP signaling to create a niche for adult neurogenesis. Neuron 28, 713–26.

Lisa A. Flanagan, Liza M. Rebaza, Stanislava Derzic, Philip H. Schwartz, E.S.M., 2006. Regulation of Human Neural Precursor Cells by Laminin and Integrins. J. Neurosci. Res. 83, 845–856. https://doi.org/10.1002/jnr.20778

Liu, X., Wang, Q., Haydar, T.F., Bordey, A., 2005. Nonsynaptic GABA signaling in postnatal subventricular zone controls proliferation of GFAP-expressing progenitors. Nat. Neurosci. 8, 1179–1187. https://doi.org/10.1038/nn1522

Lois, C., Alvarez-Buylla, A., 1993. Proliferating subventricular zone cells in the adult

mammalian forebrain can differentiate into neurons and glia. Proc. Natl. Acad. Sci. U. S. A. 90, 2074–7.

Long, K., Moss, L., Laursen, L., Boulter, L., ffrench-Constant, C., 2016. Integrin signalling regulates the expansion of neuroepithelial progenitors and neurogenesis via Wnt7a and Decorin. Nat. Commun. 7, 10354. https://doi.org/10.1038/ncomms10354

Luque-Molina, I., Khatri, P., Schmidt-Edelkraut, U., Simeonova, I.K., Hölzl-Wenig, G., Mandl, C., Ciccolini, F., 2017. Bone Morphogenetic Protein Promotes Lewis X Stage-Specific Embryonic Antigen 1 Expression Thereby Interfering with Neural Precursor and Stem Cell Proliferation. Stem Cells 2417–2429. https://doi.org/10.1002/stem.2701

Mattila, E., Pellinen, T., Nevo, J., Vuoriluoto, K., Arjonen, A., Ivaska, J., 2005. Negative regulation of EGFR signalling through integrin-α1β1-mediated activation of protein tyrosine phosphatase TCPTP. Nat. Cell Biol. 7, 78–85. https://doi.org/10.1038/ncb1209

McKay, R., 1997. Stem cells in the central nervous system. Science 276, 66–71.

Merkle, F.T., Mirzadeh, Z., Alvarez-buylla, A., 2007. Mosaic organization of neural stem cells in the adult brain. Science 317, 381–4. https://doi.org/10.1126/science.1144914

Merkle, F.T., Tramontin, A.D., Garcia-Verdugo, J., Alvarez-buylla, A., 2004. Radial glia give rise to adult neural stem cells in the subventricular zone. Proc. Natl. Acad. Sci.

Ming, G. li, Song, H., 2011. Adult Neurogenesis in the Mammalian Brain: Significant Answers and Significant Questions. Neuron 70, 687–702. https://doi.org/10.1016/j.neuron.2011.05.001

Mirzadeh, Z., Merkle, F.T., Soriano-Navarro, M., Garcia-Verdugo, J.M., Alvarez-Buylla, A., 2008. Neural Stem Cells Confer Unique Pinwheel Architecture to the Ventricular Surface in Neurogenic Regions of the Adult Brain. Cell Stem Cell 3, 265–278. https://doi.org/10.1016/j.stem.2008.07.004

Monaghan, A.P., Grau, E., Bock, D., Schütz, G., 1995. The mouse homolog of the orphan nuclear receptor tailless is expressed in the developing forebrain. Development 121, 839–53.

Moro, L., Dolce, L., Cabodi, S., Bergatto, E., Boeri Erba, E., Smeriglio, M., Turco, E., Retta, S.F., Giuffrida, M.G., Venturino, M., Godovac-Zimmermann, J., Conti, A., Schaefer, E., Beguinot, L., Tacchetti, C., Gaggini, P., Silengo, L., Tarone, G., Defilippi, P., 2002. Integrin-induced epidermal growth factor (EGF) receptor activation requires c-Src and p130Cas and leads to phosphorylation of specific EGF receptor tyrosines. J. Biol. Chem. 277, 9405–14. https://doi.org/10.1074/jbc.M109101200

Moss, S.J., Smart, T.G., 2001. Constructing inhibitory synapses. Nat. Rev. Neurosci. 2, 240–250. https://doi.org/10.1038/35067500

Nascimento, M.A., Sorokin, L., Coelho-Sampaio, T., 2018. Fractone bulbs derive from ependymal cells and their laminin composition influence the stem cell niche in the subventricular zone. J. Neurosci. 38, 3064–17. https://doi.org/10.1523/JNEUROSCI.3064-17.2018

Nelson, B.R., Hodge, R.D., Bedogni, F., Hevner, R.F., 2013. Dynamic Interactions between Intermediate Neurogenic Progenitors and Radial Glia in Embryonic Mouse Neocortex: Potential Role in Dll1-Notch Signaling. J. Neurosci. 33, 9122–9139. https://doi.org/10.1523/JNEUROSCI.0791-13.2013

Noctor, S.C., Martínez-Cerdeño, V., Ivic, L., Kriegstein, A.R., 2004. Cortical neurons arise in symmetric and asymmetric division zones and migrate through specific phases. Nat.

Neurosci. 7, 136–44. https://doi.org/10.1038/nn1172
Noctor, S.C., Martínez-Cerdeño, V., Kriegstein, A.R., 2008. Distinct behaviors of neural stem and progenitor cells underlie cortical neurogenesis. J. Comp. Neurol. 508, 28–44. https://doi.org/10.1002/cne.21669
O'Keeffe, G.C., Tyers, P., Aarsland, D., Dalley, J.W., Barker, R.A., Caldwell, M.A., 2009. Dopamine-induced proliferation of adult neural precursor cells in the mammalian subventricular zone is mediated through EGF. Proc. Natl. Acad. Sci. 106, 8754–8759. https://doi.org/10.1073/pnas.0803955106
Obernier, K., Cebrian-silla, A., Thomson, M., Parraguez, J.I., Anderson, R., Guinto, C., Rodas Rodriguez, J., Garcia-Verdugo, J.M., Alvarez-buylla, A., Rodriguez, R., Alvarez-buylla, A., Alvarez-buylla, A., 2018. Adult Neurogenesis Is Sustained by Symmetric Self- Renewal and Differentiation Article Adult Neurogenesis Is Sustained by Symmetric Self-Renewal and Differentiation. Cell Stem Cell 22, 221–234. https://doi.org/10.1016/j.stem.2018.01.003
Obernier, K., Simeonova, I., Fila, T., Mandl, C., Hölzl-Wenig, G., Monaghan-Nichols, P., Ciccolini, F., 2011. Expression of Tlx in both stem cells and transit amplifying progenitors regulates stem cell activation and differentiation in the neonatal lateral subependymal zone. Stem Cells 29, 1415–1426. https://doi.org/10.1002/stem.682
Ohtsuka, T., Ishibashi, M., Gradwohl, G., Nakanishi, S., Guillemot, F., Kageyama, R., 1999. Hes1 and Hes5 as Notch effectors in mammalian neuronal differentiation. EMBO J. 18, 2196–2207. https://doi.org/10.1093/emboj/18.8.2196
Orford, K.W., Scadden, D.T., 2008. Deconstructing stem cell self-renewal: genetic insights into cell-cycle regulation. Nat. Rev. Genet. 9, 115–128. https://doi.org/10.1038/nrg2269
Ottone, C., Krusche, B., Whitby, A., Clements, M., Quadrato, G., Pitulescu, M.E., Adams, R.H., Parrinello, S., 2014. Direct cell-cell contact with the vascular niche maintains quiescent neural stem cells. Nat. Cell Biol. 16, 1045–56. https://doi.org/10.1038/ncb3045
Overstreet-Wadiche, L.S., Westbrook, G.L., 2006. Functional maturation of adult-generated granule cells. Hippocampus 16, 208–215. https://doi.org/10.1002/hipo.20152
Owens, D.F., Kriegstein, A.R., 2002. Is there more to GABA than synaptic inhibition? Nat Rev Neurosci 3, 715–727. https://doi.org/10.1038/nrn919
Paton, JM; Nottebohm, F., 1981. A brain for all seasons: Cyclical anatomical changes in song control nuclei of the canary brain. Science (80-.). 214, 1368–1370. https://doi.org/10.1126/science.7313697
Pruszak, J., Ludwig, W., Blak, A., Alavian, K., Isacson, O., 2009. CD15, CD24 and CD29 Define a Surface Biomarker Code for Neural Lineage Differentiation of Stem Cells. Stem Cells N/A-N/A. https://doi.org/10.1002/stem.211
Qian, X., Shen, Q., Goderie, S.K., He, W., Capela, A., Davis, A.A., Temple, S., 2000. Timing of CNS cell generation: a programmed sequence of neuron and glial cell production from isolated murine cortical stem cells. Neuron 28, 69–80.
Qu, Q., Shi, Y., 2009. Neural stem cells in the developing and adult brains. J. Cell. Physiol. 221, 5–9. https://doi.org/10.1002/jcp.21862
Raff, M., 2003. Adult Stem Cell Plasticity: Fact or Artifact? Annu. Rev. Cell Dev. Biol. 19, 1–22. https://doi.org/10.1146/annurev.cellbio.19.111301.143037
Richter, L., Graaf, C. De, Sieghart, W., Varagic, Z., Mörzinger, M., Esch, I.J.P. De, Ecker,

G.F., Ernst, M., 2012. Diazepam-bound GABAA receptor models identify new benzodiazepine binding-site ligands 8, 455–464. https://doi.org/10.1038/nchembio.917

Rodin, S., Domogatskaya, A., Ström, S., Hansson, E.M., Chien, K.R., Inzunza, J., Hovatta, O., Tryggvason, K., 2010. Long-term self-renewal of human pluripotent stem cells on human recombinant laminin-511. Nat. Biotechnol. 28, 611–615. https://doi.org/10.1038/nbt.1620

Sasai, Y., Kageyama, R., Tagawa, Y., Shigemoto, R., Nakanishi, S., 1992. Two mammalian helix-loop-helix factors structurally related to Drosophila hairy and Enhancer of split. Genes Dev. 6, 2620–34.

Seth, D., Shaw, K., Jazayeri, J., Leedman, P.J., 1999. Complex post-transcriptional regulation of EGF-receptor expression by EGF and TGF-α in human prostate cancer cells. Br. J. Cancer 80, 657–669. https://doi.org/10.1038/sj.bjc.6690407

Shen, Q., 2004. Endothelial Cells Stimulate Self-Renewal and Expand Neurogenesis of Neural Stem Cells. Science (80-.). 304, 1338–1340. https://doi.org/10.1126/science.1095505

Shen, Q., Goderie, S.K., Jin, L., Karanth, N., Sun, Y., Abramova, N., Vincent, P., Pumiglia, K., Temple, S., 2004. Endothelial cells stimulate self-renewal and expand neurogenesis of neural stem cells. Science 304, 1338–40. https://doi.org/10.1126/science.1095505

Shen, Q., Wang, Y., Kokovay, E., Lin, G., Chuang, S.M., Goderie, S.K., Roysam, B., Temple, S., 2008. Adult SVZ Stem Cells Lie in a Vascular Niche: A Quantitative Analysis of Niche Cell-Cell Interactions. Cell Stem Cell 3, 289–300. https://doi.org/10.1016/j.stem.2008.07.026

Shi, Y., 2015. Regulation of Adult Neural Stem Cell Activation by Orphan Nuclear Receptor TLX (NR2E1) and Notch Signaling. Heidelberg University. https://doi.org/10.11588/heidok.00018941

Shi, Y., Chichung Lie, D., Taupin, P., Nakashima, K., Ray, J., Yu, R.T., Gage, F.H., Evans, R.M., 2004. Expression and function of orphan nuclear receptor TLX in adult neural stem cells. Nature 427, 78–83. https://doi.org/10.1038/nature02211

Shimozaki, K., Zhang, C.-L., Suh, H., Denli, A.M., Evans, R.M., Gage, F.H., 2012. SRY-box-containing Gene *2* Regulation of Nuclear Receptor Tailless (*Tlx*) Transcription in Adult Neural Stem Cells. J. Biol. Chem. 287, 5969–5978. https://doi.org/10.1074/jbc.M111.290403

Sivakumar, S., Daum, J.R., Gorbsky, G.J., 2014. Live-Cell Fluorescence Imaging for Phenotypic Analysis of Mitosis, in: Methods in Molecular Biology (Clifton, N.J.). pp. 549–562. https://doi.org/10.1007/978-1-4939-0888-2_31

Song, J., M. Christian, K., Ming, G., Song, H., 2012. Modification of hippocampal circuitry by adult neurogenesis. Dev. Neurobiol. 72, 1032–1043. https://doi.org/10.1002/dneu.22014

Sotelo, J.R., Trujillo-Cenoz, O., 1958. Electron microscope study on the development of ciliary components of the neural epithelium of the chick embryo. Z. Zellforsch. Mikrosk. Anat. 49, 1–12.

Stump, G., Durrer, A., Klein, A.-L., Lütolf, S., Suter, U., Taylor, V., 2002. Notch1 and its ligands Delta-like and Jagged are expressed and active in distinct cell populations in the postnatal mouse brain. Mech. Dev. 114, 153–9.

Suh, Y., Obernier, K., Hölzl-Wenig, G., Mandl, C., Herrmann, A., Wörner, K., Eckstein, V., Ciccolini, F., 2009. Interaction between DLX2 and EGFR regulates proliferation

and neurogenesis of SVZ precursors. Mol. Cell. Neurosci. 42, 308–314. https://doi.org/10.1016/j.mcn.2009.08.003

Sun, G., Yu, R.T., Evans, R.M., Shi, Y., 2007. Orphan nuclear receptor TLX recruits histone deacetylases to repress transcription and regulate neural stem cell proliferation. Proc. Natl. Acad. Sci. U. S. A. 104, 15282–7. https://doi.org/10.1073/pnas.0704089104

Tochitani, S., Kondo, S., 2013. Immunoreactivity for GABA, GAD65, GAD67 and Bestrophin-1 in the Meninges and the Choroid Plexus: Implications for Non-Neuronal Sources for GABA in the Developing Mouse Brain. PLoS One 8, e56901. https://doi.org/10.1371/journal.pone.0056901

Tumbar, T., Guasch, G., Greco, V., Blanpain, C., Lowry, W.E., Rendl, M., Fuchs, E., 2004. Defining the epithelial stem cell niche in skin. Science 303, 359–63. https://doi.org/10.1126/science.1092436

Waghmare, S.K., Bansal, R., Lee, J., Zhang, Y. V, McDermitt, D.J., Tumbar, T., 2008. Quantitative proliferation dynamics and random chromosome segregation of hair follicle stem cells. EMBO J. 27, 1309–20. https://doi.org/10.1038/emboj.2008.72

Wang, F., Weaver, V.M., Petersen, O.W., Larabell, C.A., Dedhar, S., Briand, P., Lupu, R., Bissell, M.J., 1998. Reciprocal interactions between beta1-integrin and epidermal growth factor receptor in three-dimensional basement membrane breast cultures: a different perspective in epithelial biology. Proc. Natl. Acad. Sci. U. S. A. 95, 14821–6.

Wang, J., Lin, W., Popko, B., Campbell, I.L., 2004. Inducible production of interferon-γ in the developing brain causes cerebellar dysplasia with activation of the Sonic hedgehog pathway. Mol. Cell. Neurosci. 27, 489–496. https://doi.org/10.1016/j.mcn.2004.08.004

Wang, Y., Liu, H.-K., Nther, G., Tz, S., 2013. Role of the nuclear receptor Tailless in adult neural stem cells. Mech. Dev. 130, 388–390. https://doi.org/10.1016/j.mod.2013.02.001

Wee, P., Wang, Z., 2017. Epidermal growth factor receptor cell proliferation signaling pathways. Cancers (Basel). 9, 1–45. https://doi.org/10.3390/cancers9050052

Weinandy, F., Ninkovic, J., Götz, M., 2011. Restrictions in time and space--new insights into generation of specific neuronal subtypes in the adult mammalian brain. Eur. J. Neurosci. 33, 1045–54. https://doi.org/10.1111/j.1460-9568.2011.07602.x

Wong, S.Y., Reiter, J.F., 2008. Chapter 9 The Primary Cilium, in: Current Topics in Developmental Biology. pp. 225–260. https://doi.org/10.1016/S0070-2153(08)00809-0

Xu, C., Li, X., Topham, M.K., Kuwada, S.K., 2014. Regulation of sonic hedgehog expression by integrin β1 and epidermal growth factor receptor in intestinal epithelium. IUBMB Life 66, 694–703. https://doi.org/10.1002/iub.1319

Yagi, H., Saito, T., Yanagisawa, M., Yu, R.K., Kato, K., 2012. Lewis X-carrying N-glycans regulate the proliferation of mouse embryonic neural stem cells via the Notch signaling pathway. J. Biol. Chem. 287, 24356–64. https://doi.org/10.1074/jbc.M112.365643

Yoshida, N., Hishiyama, S., Yamaguchi, M., Hashiguchi, M., Miyamoto, Y., Kaminogawa, S., Hisatsune, T., 2003. Decrease in expression of alpha 5 beta 1 integrin during neuronal differentiation of cortical progenitor cells. Exp. Cell Res. 287, 262–71.

Young, S.Z., Lafourcade, C.A., Platel, J.-C., Lin, T. V, Bordey, A., 2014. GABAergic striatal neurons project dendrites and axons into the postnatal subventricular zone leading to calcium activity. Front. Cell. Neurosci. 8, 10.

https://doi.org/10.3389/fncel.2014.00010
Young, S.Z., Taylor, M.M., Wu, S., Ikeda-Matsuo, Y., Kubera, C., Bordey, A., 2012. NKCC1 knockdown decreases neuron production through GABA(A)-regulated neural progenitor proliferation and delays dendrite development. J. Neurosci. 32, 13630–8. https://doi.org/10.1523/JNEUROSCI.2864-12.2012
Zhao, C., Sun, G., Li, S., Lang, M.-F., Yang, S., Li, W., Shi, Y., 2010. MicroRNA let-7b regulates neural stem cell proliferation and differentiation by targeting nuclear receptor TLX signaling. Proc. Natl. Acad. Sci. 107, 1876–1881. https://doi.org/10.1073/pnas.0908750107
Zhao, C., Sun, G., Li, S., Shi, Y., 2009. A feedback regulatory loop involving microRNA-9 and nuclear receptor TLX in neural stem cell fate determination. Nat. Struct. Mol. Biol. 16, 365–71. https://doi.org/10.1038/nsmb.1576

Abbreviations:

APC: allophycocyanin.

AAV: adeno associated virus.

bHLH: basic helix-loop-helix.

BMP: bone morphogenetic protein.

CBA: β-actin promoter.

CT: cycle threshold.

CSF: cerebral-spinal fluid.

DCX: doublecortin.

DNA: Deoxyribonucleic acid.

Doxy: doxycycline.

ddCT: delta cycle threshold.

ECM: extracellular matrix.

EGF: epidermal growth factor

EGFR: epidermal growth factor receptor.

FACS: fluorescence activated cell sorter.

FGF: fibroblast growth factor.

GABA: gamma amino butyric acid.

$GABA_A$Rs: GABA type A receptors.

GFAP: glial fibrillary acidic protein.

GFP: green fluorescent protein.

GLAST: glutamate aspartate transporter.

hrGFP: human recombinant GFP.

IdU: iododeoxyuridine.

IMDM: Iscove's Modified Dulbecco's Medium.

IPC: intermediate progenitor cell.

LB: Luria Bertani.

LV: lateral ventricles.

NICD: notch intracellular domain.

NSC: neural stem cell.

pNSCs: proliferating neural stem cells.

qNSCs: quiescent neural stem cells.

OBs: olfactory bulbs.

P: prominin1.

PBS: phosphate buffered saline.

PI: propidium iodide

PCR: polymerase chain reaction.

qNSC: quiescent neural stem cell.

RCF: Relative Centrifugal Force.

RG: radial glia.

RNA: ribonucleic acid.

RMS: rostral migratory stream.

RT: room temperature.

SGZ: subgranular zone of hippocampus.

SVZ: subventricular zone.

TAPs: transit amplifying progenitors.

tTA: tetracycline trans activator.

TRE: tetracycline-responsive regulatory element.

WPRE: woodchuck hepatitis virus posttranscriptional regulatory element.

WT: wild type.

Acknowledgments:

First, I would like to thank my supervisor, Dr. Francesca Ciccolini, for giving me the opportunity to work in her laboratory and grow as a scientist. Also, thanks for the many scientific discussions over the years that helped me become a better scientist.

I would also want to thank my TAC members Prof. Dr. G. Elisabeth Pollerberg and Prof. Dr. Gislene Pereira for their kind advisory support over the years that has helped me very much.

I also wanted to thank Claudia Mandl and Gabrielle Hölzl- Wenig, because without them everything would have been so much more difficult. They have shown me their support not only as wonderful laboratory assistants, but also as friends, and I will always appreciate that. I want to thank the rest of lab members, Sara Monaco, Katja Baur and Yomn Abdullah for their kindness, support and good scientific discussion. Also, thanks to the many students that passed by our lab during the years, like Alba Paramio, Venkatesh Kummar, Hanna Khomyak, BurÇe Kabaoglu, Gamze Güney and Veronika Heil. They helped me becoming a better teacher and also contributed with their scientific support.

And none of this would be possible without the support of the complete neurobiology department, specially without Otto Bräunling and Irmela Meng, who were always there for me to help me in any matter. And of course, thanks to the rest of the department, for creating a nice and supportive atmosphere where I found not only colleagues but also good friends, whose support made me getting here.

More importantly, I want to thank my parents, Inmaculada Molina Cabrillana and Manuel Luque Moyano. I am what I am because of them, and this achievement is as much theirs as mine. I want to thank my sister, María Luque Molina, for her constant support and for teaching me what is like to be a strong person.

And last but not least, I want to thank my soon to be husband, Pablo Lomeña Martínez. He is my rock, and I want to thank him for being always there for me, for demonstrating me that I can always overcome the challenges, and for believing in me.